

BuBBLeS In Control

A Model-Based-Predictive-Control Strategy For Greenhouse Climate Control With Soap Bubble Cavity

Kaan Koç

Master of Science Thesis

BuBBLeS In Control

A Model-Based-Predictive-Control Strategy For Greenhouse Climate Control With Soap Bubble Cavity

MASTER OF SCIENCE THESIS

For the degree of Master of Science in Systems and Control at Delft
University of Technology

Kaan Koç

September 7, 2020

Faculty of Mechanical, Maritime and Materials Engineering (3mE) · Delft University of
Technology



The work in this thesis was supported by BBBLS Solutions. Their cooperation is hereby gratefully acknowledged.



Copyright © Delft Center for Systems and Control (DCSC)
All rights reserved.



Abstract

Advancements in knowledge and technology have led to an evolution of greenhouse operations: from simple transparent shelters to (one of) the most profitable sectors in agricultural industry. The understanding of the physiological and biological processes of the inside microclimate and crop, as well as the introduction of climate control, were critical for improving both the quality and production rate. Advanced control strategies like Model Predictive Control (MPC) involve the application of horticultural and plant physiological knowledge using mathematical models that describe the dynamical behavior of the greenhouse and crop. An on-line control method balances the benefits of crop yield and costs of the climate control equipment.

The increasing production and cultivation rate in response to the growing demand is at a point where the focus and tension is shifted to the energy input and environmental footprint of greenhouse operations. This stimulates the agricultural industry to provide sustainable solutions. An innovative greenhouse is developed by BBLS Solutions, that uses a soap bubble cavity which improves the thermal properties and energy efficiency. The concept is in development phase and is acknowledged that there is potential for improved climate control and automation of the control of the soap bubble cavity.

This research introduces a MPC strategy for controlling the greenhouse climate and the soap bubble cavity. The greenhouse processes are described by a mechanistic model, which simulates the inside climate variables as a function of the greenhouse structure, outside environmental conditions and climate control equipment. The dynamics of the soap bubble cavity and the corresponding thermal varying properties were then augmented in the climate model. The augmented model is used as a predictor for the future dynamics of the greenhouse climate, for which the optimizer generates a control input sequence for the climate control equipment and soap bubble generators inside the cavity.

The MPC implementation results demonstrate that the greenhouse temperature can be controlled within the pre-defined bounds and that the filling of the soap bubble cavity is with respect to outside conditions and priorities. Furthermore, the MPC strategy supports real-time control as the CPU time can be less than the time between control instances. The proposed methodology is an initial attempt but proves to be a promising concept for further development.

Table of Contents

1	Introduction	1
1-1	Motivation	1
1-2	Problem statement	3
1-3	Outline	4
2	Theoretical background and literature review	5
2-1	Modelling the greenhouse climate	5
2-1-1	Mechanistic models: Preliminaries	6
2-1-2	Selection of greenhouse climate models	6
2-2	Controlling the greenhouse climate: optimal control vs model predictive control	7
2-2-1	Model predictive control	8
2-3	Concept of dynamic insulation technologies	12
2-3-1	A RC-network model for building thermal performance	13
2-3-2	Static and dynamic thermal properties	14
2-4	Conclusion	14
3	Methodological approach	17
3-1	Research objectives and Aims	17
3-2	Research Questions	18
3-3	Experimental setup	19
4	An integrated model for the greenhouse climate and soap bubble cavity	21
4-1	A mechanistic model for the greenhouse climate	21
4-1-1	Heat and mass transfer of the cover	22
4-1-2	Heat transfer of the soil	23
4-1-3	Heat and mass transfer of the heating lamps	23
4-1-4	Heat and mass transfer of the air-treatment system	24

4-1-5	Heat transfer due to solar radiation	25
4-2	Modelling of the dynamic soap bubble cavity	25
4-2-1	Filling of the cavities	26
4-2-2	Simple abstraction of the soap bubble dynamics	26
4-3	Thermal performance of the soap bubble cavity	27
4-3-1	A RC-network formulation of the convective heat transfer	27
4-3-2	Thermal static and dynamic elements of the soap bubble cavity	28
4-3-3	Solar emissivity	29
5	Calibration and Validation	31
5-1	Introduction	31
5-2	Calibration and validation of the BBBS greenhouse	32
5-2-1	Calibration of the soil temperature	32
5-2-2	Calibration of greenhouse air temperature	33
5-2-3	Calibration of the heat-exchanger tube temperature	34
5-2-4	Calibration of the greenhouse air humidity	38
5-2-5	Calibration of the heating lamps	39
5-2-6	Calibration of the soap bubble cavity thermal properties	40
5-2-7	Calibration of the solar transmission	42
6	A Model Predictive Control strategy for climate control of soap bubble cavity greenhouse	45
6-1	Formulation of the prediction model	45
6-1-1	Greenhouse climate model dynamics	46
6-1-2	Predictions	46
6-1-3	Predicting future control moves using MoveBlocking MPC	46
6-2	Formulation of hard constraints for inputs	50
6-2-1	Binary control inputs	50
6-2-2	HSHE-unit	50
6-2-3	No simultaneous filling of cavities	51
6-2-4	Forced continuation of cavity filling	51
6-3	Objective function	51
6-4	Mathematical formulation and implementation	52
7	Implementation, Results and Analysis	55
7-1	Simulation study 1	55
7-1-1	Implementation	56
7-1-2	Results and Analysis	57
7-1-3	Performance	59
7-2	Simulation study 2	60
7-2-1	Implementation	61
7-2-2	Results and Analysis	62
7-2-3	Performance	65

8 Conclusion, discussion and recommendations	67
8-1 Conclusion	67
8-2 Discussion and recommendations	69
8-2-1 Greenhouse climate model Limitations	70
8-2-2 Soap bubble filling dynamics and thermal properties	70
8-2-3 Model-based-predictive control strategy	71
A Obtaining measured data	73
Bibliography	81
Glossary	85
List of Acronyms	85
List of Symbols	85

List of Figures

1-1	Visualization of the F2W2F project. From [37]	3
2-1	Multi-layer hierarchical control for greenhouse operations. From [31].	8
2-2	Schematics of the MPC algorithm: (a) control loop; (b) receding horizon control strategy. From [21]	9
2-3	Three types of constraint formulation: (a) hard; (b) soft; (c) set-point approximation. From [28]	11
2-4	Example of a RC network representation of a room. From [50].	13
4-1	RC network representation of the convective heat transfer	28
5-1	Measured and simulated data.	33
5-2	Measured and simulated data.	34
5-3	Measured and simulated data	35
5-4	Measured and simulated data	36
5-5	Measured and simulated data	37
5-6	Measured and simulated data	38
5-7	Measured and simulated data	39
5-8	Measured and simulated data	40
5-9	Measured and simulated data	41
5-10	Measured and simulated data	43
5-11	Light intensity measurement during south-roof cavity filling	43
7-1	Measured climate data used for simulation	56
7-2	Simulation results of the greenhouse air temperature (a-b), tube air temperature (c-d) and the filling levels (e-f).	58
7-3	Simulation results of the climate control utilization of the lamps (a-b), damper settings HSHE-unit (c-f) heating and cooling batteries (g-h) and soap bubble generators (i-j).	59

7-4	Measured climate data used for simulation	61
7-5	Simulation results of the greenhouse air temperature (a-b), tube air temperature (c-d) and the filling levels (e-f).	62
7-6	Simulation results of the climate control utilization of the lamps (a-b), damper settings HSHU-unit (c-f) heating and cooling batteries (g-h) and soap bubble generators (i-j).	64
A-1	Experiment 1: Measured climate data.	74
A-2	Experiment 2: Measured climate data.	75
A-3	Sketch of the air-flow in HEAT-RECOVERY mode.	76
A-4	Experiment 3: Measured climate data.	76
A-5	Experiment 4: Measured climate data.	77
A-6	Experiment 5: Measured climate data.	78
A-7	Experiment 6: Measured climate data.	79
A-8	Experiment 7: Measured climate data.	79
A-9	Experiment 8: Measured climate data.	80

List of Tables

4-1	Energy- and mass transfer and their corresponding source.	22
4-2	Cavity compartment and time to fill up	26
5-1	Original and estimated values of parameters.	32
5-2	VAF and RMSE of the calibrated response	32
5-3	Original and estimated values of parameters.	34
5-4	VAF and RMSE of the calibrated response	34
5-5	Original and estimated values of parameters.	35
5-6	VAF and RMSE of the calibrated response	35
5-7	Original and estimated values of parameters.	35
5-8	VAF and RMSE of the calibrated response	35
5-9	Original and estimated values of parameters.	36
5-10	VAF and RMSE of the calibrated response	36
5-11	Original and estimated values of parameters.	37
5-12	VAF and RMSE of the calibrated response	37
5-13	Original and estimated values of parameters.	38
5-14	VAF and RMSE of the calibrated response	38
5-15	Original and estimated values of parameters.	39
5-16	VAF and RMSE of the calibrated response	39
5-17	Original and estimated values of parameters.	41
5-18	VAF and RMSE of the calibrated response	41
5-19	Original and estimated values of parameters.	42
5-20	VAF and RMSE of the calibrated response	42
7-1	Control settings for each run.	56
7-2	Numerical results of the climate control performance for the simulations.	60

7-3	Numerical results of CPU performance	60
7-4	Control settings for each run	61
7-5	Numerical results of the climate control performance for the simulations.	65
7-6	Numerical results of the climate control performance for the simulations per time interval.	66
7-7	Numerical results of CPU performance	66

“The most sustainable way is to not make things. The second most sustainable way is to make something very useful, to solve a problem that hasn’t been solved”

— *Thomas Sigsgaard*

Chapter 1

Introduction

1-1 Motivation

A greenhouse is an enclosure that allows owners to control climatic, nutritional, biotic and cultural management variables that influence the crop growth and development. It is a transparent construction that transmits solar radiation while creating a protected micro-climate inside the enclosure. The aim is to create an optimal environment for each stage of the crop growth such that a maximum production and quality of a product is realised at minimal cost [31].

Historically, the initial motive was to use glasshouses as a protective shelter for growing plants in hostile environment conditions. It was later discovered that manipulating the indoor climate allowed growers to control the crop cultivation [47]. This triggered a horticultural and technical evolution with the purpose to improve the production and quality at a higher net outcome. Herein was the understanding of the greenhouse micro-climate and its characteristics critical for the improvement of the growth conditions. The different elements composing a greenhouse and the multiple relationships established inside make it a complex system in which energy, mass and information flows are dynamic and of different magnitudes. The crop is its main element as it is subjected to various factors, such as climate conditions, nutritional, biotic and cultural management, and interacts with a high level of complexity. At first, empirical knowledge, intuition and trial and error principle were the main driving factors for gaining insight. Later, scientific research was focused on this field describe the physical processes of the inside climate and crop in a quantitative manner. This quantitative knowledge helped create insight into and eventually led to the development of mathematical models for accurate estimation and prediction of the greenhouse micro-climate and crop growth [10].

Further improvements were made by the introduction of climate control, which involves manipulating the micro-climate to steer crop production and to cultivate and produce crops outside the growing season, hence prolonging the cultivation period [46]. At first, hand control was applied to turn climate equipment on-and-off by the growers. Later, automatic climate control replaced laborious hand control with continuous automated control. The

control algorithms however were still based on the heuristic method of the grower. Paired with the development of quantitative knowledge described earlier, a framework is developed in which horticultural and plant physiological knowledge is applied in control algorithms [7]. This is where systems and control theory has shown its potential and particularly advanced control strategies which operate in a model based framework. This framework involves the use of mathematical models that describe the dynamical behavior of the greenhouse, as usually done in the process industry [32], and an on-line control method balancing the benefits and costs of the use of the climate control equipment. The main principle of advanced control techniques relies on dynamic programming and optimization which involves an objective function, based on climatic and crop models, and optimization techniques to determine the optimal trajectories of the main variables in the greenhouse control crop problem [31][47].

The advancements in knowledge and technology has made greenhouses the most profitable sectors in the agriculture industry. Their output in terms of yield is 10 to 20 times higher than traditional outdoor horticulture. Also, the production and cultivation rate is increased. This is partly in response to the growth in population and demand. The increase in population leads to a need for higher production yield in agriculture, which in turn requires a considerable investment cost, labor, fertilizers and energy input. The increased energy demand of greenhouse operation has become a bigger problem than before since more focus and tension is applied to the fossil fuel consumption and carbon footprint [38]. Sustainable agriculture is a challenging task in countries such as the Netherlands, where 8% of the total energy use is in the agricultural industry [41]. The Dutch horticulture sector has therefore come up with a defined strategy for the Horizon 2020 research and innovation-project funding by the European Union (EU). The Horizon 2020 funding supports creating solutions for problems currently faced by farmers and foresters. It realizes that researchers and stakeholders build solutions together, sharing knowledge and producing results that are ready to be put into practice for sustainable agriculture and boosts innovation. The strategy defined by the horticulture sector contains targets in terms of reduction of emissions, improving energy efficiency and making greenhouse operation more climate neutral. Therefore, by means of stricter regulation and the urge for innovation, greenhouse sectors are pushed to come up with more sustainable and efficient greenhouse operation [3].

A novel technological approach to tackle the above mentioned problems is the Food to Waste to Food (F2W2F) project. The F2W2F project developed a closed system for processing organic waste into new food. Organic waste from urban locations and horticulture are processed to digestate and compost. The processes involved in this are vermi-composting, conditioning and mixing, substrates and nutrient solutions for vegetable growth are then applied in the greenhouse using a digeponics system. The released energy and from processing is then applied to the greenhouse which enables the production of plants.

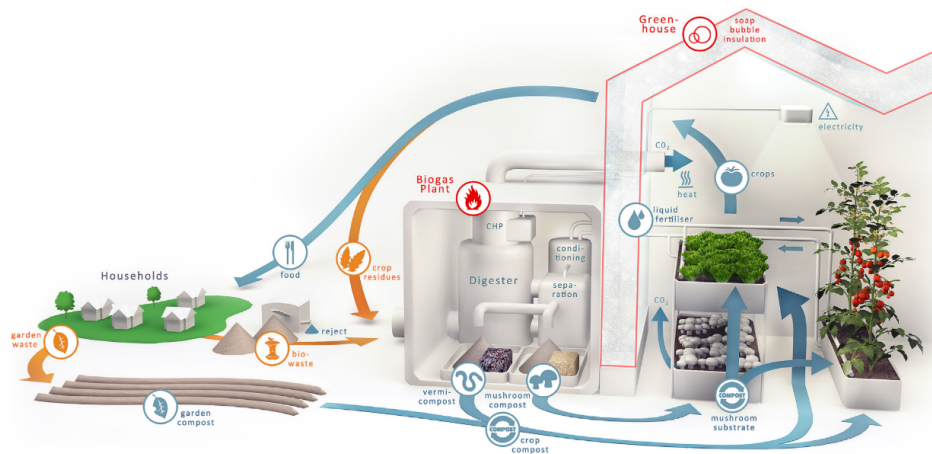


Figure 1-1: Visualization of the F2W2F project. From [37]

The novelty in the concept lies in the digestion and the greenhouse. Anaerobic digestion is used for sustainable utilization of organic waste which reduces the carbon-dioxide (CO_2) emissions. The second element is the use of the bubble-insulated greenhouse, termed BBLS-greenhouse as commercial product, from BBLS Solutions. Unlike traditional greenhouses, the BBLS-greenhouse is constructed with a double-foil cavity enclosure. The cavities in the roof and walls are filled with soap bubbles for thermal insulation, as seen in the figure. When needed, the soap bubbles are generated, thereby increasing the thermal resistance of the heat loss to the outside environment. The bubbles are also employed as shading the greenhouse from excessive solar radiation. This dynamic switching between an insulated and conductive state is more suitable for the changing environment and demands. The greenhouse climate is controlled by an integrated greenhouse climate control system, which consists of climate equipment, sensors and algorithms. The climate equipment is capable of heating, cooling, (de)-humidifying, ventilation, CO_2 injection and wall soap generation using different type of components. Air is circulated over condensers, heaters and a cross flow heat exchanger and is then circulated through perforated tubes in the greenhouse. Energy and vapour is added or extracted using heat and cold energy storage buffers. The soap bubbles are generated using a soap generator and is capable of fully filling the wall and roof cavities or a specific side. The greenhouse climate is monitored with sensors placed in different areas, measuring relevant parameters such as temperature, humidity, (vapour) pressure, radiation and CO_2 concentration. These measurements are then used for the climate control algorithm which aims to maintain a specific range of climate conditions.

1-2 Problem statement

The problem statement is formulated based on the distinctive perspectives of both the company and TU Delft. The company's perspective is that the current climate control algorithm is not optimal in controlling the inside climate; the regulation of the temperature show unwanted behaviour and the soap bubble cavity is manually controlled. Also, there sees a waste

of potential in terms of the amount of parameters used for controlling the greenhouse climate. The lack of a quantitative description of the processes inside the greenhouse hinders this. From TU Delft's perspective is that there is a gap of knowledge in modelling and control of the soap bubble cavity. Although the technology has existed for quite some time [15], no attempt has been made for automating the control.

1-3 Outline

The structure of this report aims to resolve the above mentioned problems. First, the theoretical context of the main components is introduced by reviewing the theoretical fundamental aspects and relevant existing literature in Chapter 2. Chapter 3 outlines the methodological approach, including objectives, aims, research questions and experimental-setup. In Chapter 4, a mathematical model for the greenhouse climate and soap bubble cavity is proposed, and in Chapter 5 the proposed model is calibrated and validated. Chapter 6 and 7 propose a new control strategy for controlling the greenhouse climate, which includes formulation, simulation and result analysis. Finally, conclusions, discussions and future research are discussed in Chapter 8.

Theoretical background and literature review

The previous chapter explained the problem statement and the need for conducting this research. This chapter elaborates on the fundamental aspects by means of providing a theoretical background and the review of existing literature. This section will provide an overview of existing academic work of the relevant disciplines and topics that covers this field of research.

2-1 Modelling the greenhouse climate

The diverse elements composing a greenhouse and the multiple relationships established inside make it a complex system, in which the micro-climate is viewed as one of the (main) sub-systems. The development of dynamic climate models is done for various applications, such as modelling, simulation and control and optimization purposes. The literature classifies these models in either mechanistic or empirical (black-box) models. Mechanistic models formulate physical processes using first principle physics. The main advantages are augmenting knowledge and understanding of greenhouse environment in general and on enhancing the understanding for the underlying dynamics [23]. An alternative to mechanistic models are those obtained from data, also known as empirical (black-box) models. Rather than the formulation is based on physical processes, the dynamics are described by equations (linear or nonlinear), for which coefficients are obtained through an identification procedure, defined as the problem of building mathematical models of dynamic systems based on observed data. A main advantage is the flexibility of mathematical structure and the modifiable parameters estimated from experimental data, regardless of any consideration of the governing physical principles [31]. A disadvantage is that these models offer no possibility to examine and interpret the sub-processes of the system. For this research the focus lies on mechanistic models, as there is a need for interpretation and understanding the greenhouse climate.

2-1-1 Mechanistic models: Preliminaries

Mechanistic models are represented by a set of continuous-time equations. The first approach is given by a set of ordinary first-order differential equations which are usually nonlinear and can be described as follows:

$$\frac{d\mathbf{X}}{dt} = \mathbf{f}(\mathbf{X}, \mathbf{U}, \mathbf{D}, \mathbf{V}, \mathbf{C}, t), \quad \mathbf{X}(t_0) = \mathbf{X}_0 \quad (2-1)$$

where $\mathbf{X} \in \mathbb{R}^{n_x}$ is a vector of state variables, $\mathbf{U} \in \mathbb{R}^{n_u}$ is a vector of control input variables, $\mathbf{D} \in \mathbb{R}^{n_d}$ is a vector of measurable disturbances, $\mathbf{V} \in \mathbb{R}^{n_v}$ is a vector of system variables, $\mathbf{C} \in \mathbb{R}^{n_c}$ is a vector of constants and \mathbf{f} is a set of (non)-linear equations with \mathbf{X}_0 the known initial state value at initial time t_0 . The formulation of Equation (2-1) is the result of applying first principle physics. Here the system to be modelled is split up into a number of smaller subsystems whose properties are well known and to follow this with an appropriate interconnection[12]. In a greenhouse, the principle of conservation of mass and energy applies, so the heat and mass transfer processes are studied using mass and energy balances. In this research, the mass and energy fluxes, defined respectively as the rate of heat energy transfer per unit area [1] are considered. The energy flux is described by the following differential equation:

$$\frac{dQ_{\text{area}}}{dt} = c_{\text{h,area}} \frac{dX_{\text{T,area}}}{dt} = Q_{\text{in,area}} - Q_{\text{out,area}} + Q_{\text{gen,area}} \quad (2-2)$$

where $Q_{\text{tot,area}}$ is the total amount of energy accumulated per unit area, $Q_{\text{in,area}}$ and $Q_{\text{out,area}}$ are respectively the entering and leaving rate of energy per unit area and $Q_{\text{gen,vol}}$ is the rate of generated energy inside per unit area and time. The energy is related to the temperature $X_{\text{T,area}}$, through $c_{\text{h,area}}$, which is the heat capacity per unit area. The same considerations can be done with the mass (and concentration) balances in a volume:

$$\frac{dM_{\text{tot,area}}}{dt} = c_{\text{area}} \frac{dX_{\text{c,area}}}{dt} = M_{\text{in,area}} - M_{\text{out,area}} + M_{\text{gen,area}} \quad (2-3)$$

where $M_{\text{tot,area}}$ is the total amount of mass accumulated in the volume, $M_{\text{in,area}}$ and $M_{\text{out,area}}$ are respectively the entering and leaving rate of mass inside the volume and $M_{\text{gen,area}}$ is the rate of generated energy inside the volume per unit time. The mass is related to the concentration $X_{\text{c,area}}$, through the area c_{area} .

2-1-2 Selection of greenhouse climate models

This section provides a selection of models describing the greenhouse climate from literature. The models are classified as detailed, and control-oriented.

Detailed greenhouse climate models

The models that fall in this category are developed with the aim to increase the knowledge of the greenhouse system. Models developed by [7],[12],[40] and [48] are characterized by their large set of state variables and detailed formulation of mass and energy balances for each element. The state variables are associated to the temperature, humidity and CO₂ concentration of subsystems such as the greenhouse cover, crop, inside air, soil layers, canopy and heating pipe. The physical processes included in these models are convection, conduction, ventilation, radiation and crop transpiration.

Control-oriented greenhouse climate models

Mechanistic models for optimization and control purposes are models with the purpose to be used in control and optimization problems. Models such as [39], [44], [43], each have their control approach but show similar characteristics. First, the amount of state variables describing the inside climate is comparatively less than the models in the previous category. Second, the state variables that are present relate to the same subsystem and the interconnection with different subsystems are formulated in one equation. The state variables are associated to the temperature, humidity and CO₂ concentration of the primary subsystem of which they want to control such as the inside air. The physical processes included in these models are convection, conduction, ventilation, radiation and crop transpiration.

2-2 Controlling the greenhouse climate: optimal control vs model predictive control

Controlling the greenhouse climate is essentially controlling the relevant climate variables such as the temperature, humidity and CO₂ concentration of the inside micro-climate. However, the values of what these climate variables should be controlled to is based on the crop growth and long-term strategies set by growers. Figure 2-1 elaborates on this further. Here, the greenhouse operations is divided in three control layers and three system levels. The upper layer controls on the biggest scale and takes into account the long-term objectives such as market prices, harvesting dates and required quality. These objectives are then translated to predictions of the growth state for optimal yield and profit generation. The optimization is performed to calculate the set-point trajectories for the crop growth using various growth models. The middle layer takes into account crop growth control which receives the set-point trajectories from the upper layer to make decisions on the global production schedule of the the crop. The optimization is then performed to compute the set-point trajectories of the greenhouse climate. The lower layer receives the set-point trajectories and computes adequate control signals sent to the actuators [31].

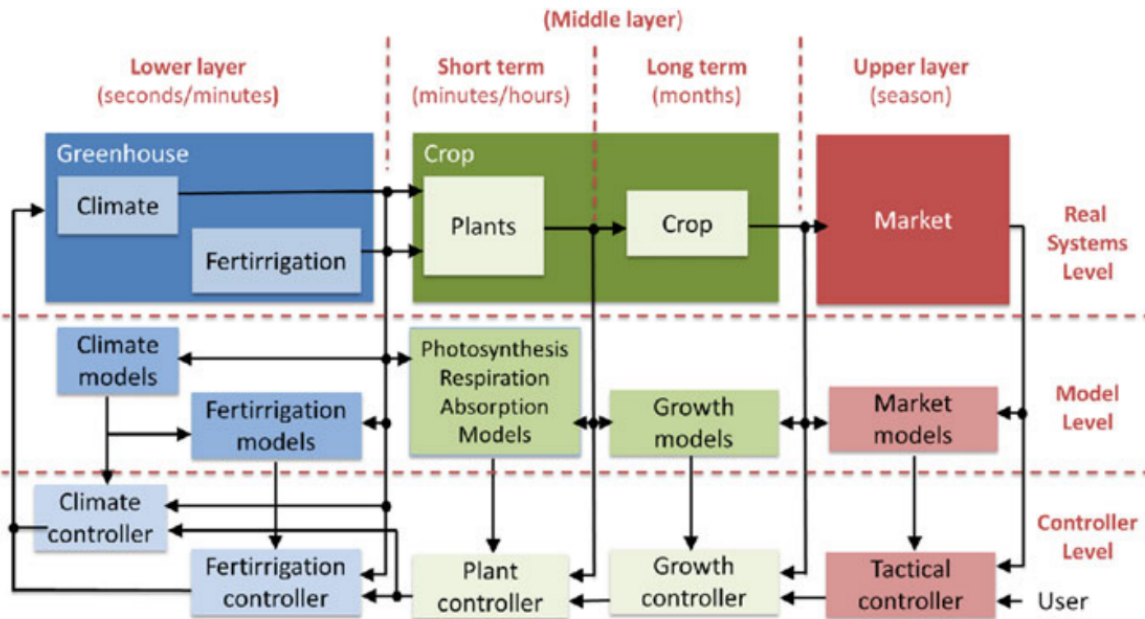


Figure 2-1: Multi-layer hierarchical control for greenhouse operations. From [31].

From the figure it is noted that by controlling the greenhouse climate is essentially taken all control layers into account. However, it is worth noting that each control layer has its own objective and time scale. One of the issues that may arise is that the difference in time scales from upper to lower layer makes it computationally intense and uncertain, as the upper layers respond relative slowly to changes in the environmental conditions compared with the relatively fast dynamic response of the greenhouse climate to changes in the control inputs and outside weather conditions [45]. This implies that the long term objectives (on the scale of months and seasons) are optimized on a minute-by-minute control strategy. Many applications have tackled these issues and considered both the climate- and crop dynamics, by a hierarchical composition of the time-scales (see e.g. [45], [17], [20]) or the formulation of multi-objective optimization problems [29]. However, in this section the review focuses solely on the control strategies designed for greenhouse climate control. Therefore for each application, a detailed description is given of the process model, objective function and set-point trajectory.

2-2-1 Model predictive control

Model Predictive Control (MPC) refers to a class of computer-controlled algorithms that uses an explicit model to obtain a control action based on a predicted plant's future response. At each control instance, an MPC algorithm computes a sequence of future manipulated variables which optimizes plant behaviour. From this sequence, only the first input is sent to the plant and the entire calculation is repeated at subsequent intervals [28]. At event (x, i) , which denotes at time i the state x [30], the first control in a finite sequence of control actions obtained by solving online a (often) constrained, discrete-time optimal control problem. MPC traded classical off-line computation of a state feedback control law $u = \kappa(x)$, such as on/off

control, proportional, integrating and differentiation control. Although these are easy to implement, they are unable to control moving processes with hard constraints [26]. A basic implementation scheme is depicted in Figure 2-2.

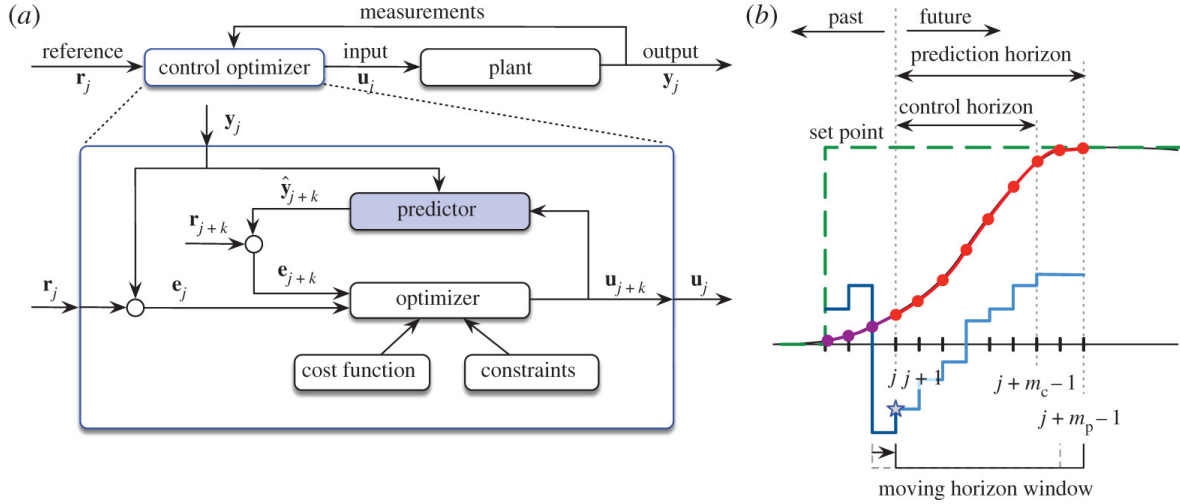


Figure 2-2: Schematics of the MPC algorithm: (a) control loop; (b) receding horizon control strategy. From [21]

The process to be controlled is represented by the plant block, which receives the input from the control optimizer and sends measurements the other way back. Within the control optimizer block, starting from the most recent measurements, the optimizer generates a control input sequence over the control horizon (represented by the solid light blue line) which optimizes the the predicted future outputs (represented by the red solid line) computed by the predictor to drive the system to the set point (represented by the green dashed line). Because it is a receding horizon control strategy, of the generated control sequences only the first is enacted to the system (represented by the blue star) [21].

The continuation of this section elaborates the necessary formulations for implementing a MPC strategy. Consider the plant be described by the following discrete time system.

$$\begin{aligned} x(k+1) &= f(x(k), u(k)) \\ y(k) &= h(x(k), u(k)) \end{aligned} \quad (2-4)$$

Let the predicted outputs be denoted as:

$$y(k+1|k), y(k+2|k), \dots, y(k+j|k), y(k+N_p-1|k), y(k+N_p|k)$$

where $y(k+j|k)$ is the predicted output variable at the sampling instant $k+m$, with given plant information $y(k)$ and N_p is the prediction horizon, which is the length of future intervals the optimization must evaluate [49]. When the states are measurable, i.e. $h(\cdot) = Cx$, with $C = I$. The the future state variables are denoted as

$$x(k+1|k), x(k+2|k), \dots, x(k+j|k), x(k+N_p-1|k), x(k+N_p|k)$$

The future control inputs are denoted by:

$$u(k|k), u(k+1|k), \dots, u(k+j|k), u(k+N_c-1|k), x(k+N_c|k)$$

where $u(k+j|k)$ is the control input at sampling instant $k+j$, which needs to be determined, and N_c is the control horizon. The control horizon dictates the number of parameters to capture the future control trajectory. If specified, $N_c < N_p$ or $N_c = N_p$ otherwise. The future states and inputs are stacked such that the following vectors are obtained:

$$\begin{aligned} \mathbf{x}^T &= [x(k+1|k) \quad x(k+2|k) \quad \dots \quad x(k+N_p|k)] \\ \mathbf{u}^T &= [u(k|k) \quad u(k+1|k) \quad \dots \quad u(k+N_c|k)] \\ \mathbf{y}^T &= [y(k+1|k) \quad y(k+2|k) \quad \dots \quad y(k+N_p|k)] \end{aligned} \quad (2-5)$$

The predicted outputs, states and inputs are then used for optimizing the plant's future behaviour. This commonly refers a cost function to be minimized at each time step. If $x(k)$ is the current state, then the optimal control problem may be posed as minimizing the cost of the future responses over the interval $[k, N_p + k]$:

$$J(x(k), u(k)) = \sum_{j=1}^{N_p} l(x(k+j|k), u(k+j|k)) \quad (2-6)$$

where $l(x, u)$ is the stage cost, which associates to a cost with respect to the value of the predicted state and control movements. Commonly, $l(x(k), (uk))$ is expressed as a quadratic function:

$$l(x(k), u(k)) = \|x(k)\|_Q^2 + \|u(k)\|_R^2 = x^T(k)Qx(k) + u^T(k)Ru(k) \quad (2-7)$$

where Q and R are positive semi-definite and positive definite weight matrices, respectively, to allow for tuning trade-offs [16]. Another variant of (2-6) includes a terminal stage cost for the terminal state $x(k+N)$ for achieving nominal stability:

$$l_N(x(k+N_p)) = x(k+N_p)^T P x(k+N_p) \quad (2-8)$$

with P a positive definite matrix. The next element in the MPC strategy is the formulation of constraints, which represents the physical limitations and control saturation of the systems. There are three types of constraints commonly used in the MPC formulation: hard, soft and set-point approximation, as shown in Figure 2-3. Hard constraints are those which should never be violated. Hard constraints for the state and input are defined by closed and compact sets, $x \in \mathbb{X} \subset \mathbb{R}^{n_x}$ and $u \in \mathbb{U} \subset \mathbb{R}^{n_u}$ and are formulated as the following inequalities:

$$\begin{aligned} x^{\min} &\leq x(k) \leq x^{\max} \\ u^{\min} &\leq u(k) \leq u^{\max} \end{aligned} \quad (2-9)$$

Soft constraints are constraints where some violation is allowed but is associated with a well-defined penalty such that the optimization problem is forced to avoid or minimize the penalty as much as possible. The implementation of these penalties are done by formulating an exact penalty function or implementing slack variables in the cost function [24]. Exact penalty functions are functions which are explicitly added in the cost function:

$$J(x(k), u(k)) + \rho \|c(x(k), u(k))\| \quad (2-10)$$

where ρ is the constraint violation penalty weight and $c(\cdot)$ contains the magnitude of the constraint violation. Another method is the implementation of slack variables, which relaxes hard constraints in (2-9) to the following:

$$\begin{aligned} x^{\min} - \epsilon &\leq x(k) \leq x^{\max} + \epsilon \\ u^{\min} - \epsilon &\leq u(k) \leq u^{\max} + \epsilon \end{aligned} \quad (2-11)$$

where ϵ are the slack variables representing the constraint violations. Similar to (2-10), the slack variables are added to the cost function as:

$$J(x(k), u(k)) + \rho \|\epsilon\| \quad (2-12)$$

Another variant of the soft constraint is the set-point approximation where set-points are defined for each soft constraint, resulting in penalty functions on both side of the constraint.

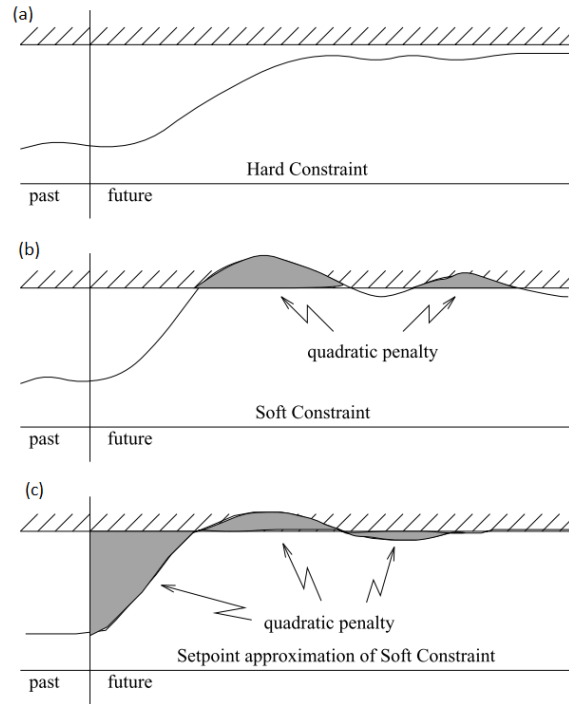


Figure 2-3: Three types of constraint formulation: (a) hard; (b) soft; (c) set-point approximation. From [28]

With the above mentioned elements in place, the MPC framework can now be formulated:

$$\min_u J(x(k), u(k)) \quad (2-13)$$

Subject to:

$$\begin{cases} x(k+1) = f(x(k), u(k), d(k)) \\ y(k) = g(x(k)) \end{cases} \quad (2-14)$$

$$u(k) \in \mathbb{U} \quad (2-15)$$

$$x(k) \in \mathbb{X} \quad (2-16)$$

The implementation is described using the following algorithm:

Algorithm 1 MPC - BBLS

Input: system in Equation (2-4), N_p

- 1: Solve Equation (2-13) - (2-15) for the optimal control sequence \mathbf{u}
 - 2: Apply first input of to system, i.e. $u(k) = \mathbf{u}(:, 0)^*$
 - 3: Set $k \leftarrow k + 1$
 - 4: Return to 1
-

2-3 Concept of dynamic insulation technologies

Controlling of inside climate variables is not only a greenhouse-specific problem. In general, buildings, regardless of designation, are also subject to the increasing tension for a more sustainable operation. Specifically, buildings are expected to meet higher requirement in terms of energy consumption and emission. Approximately, 40% of the global energy is used in buildings, whereof half of is used for indoor climate control in industrialized countries [18]. The improvement of the energy efficiency of buildings was often interpreted as minimizing the heat transmission loss by designing building envelopes with higher insulation levels and air tightness. As a consequence, the building envelope assumed the shape of massive opaque walls with relative few transparent openings [27]. This is desirable in colder climates for reducing heat losses through the building envelope to the outside environment. In periods of warmer climates however, the high insulation levels cause the building to retain undesirable heat and cause heat discomfort, for which energy is used for cooling. Such phenomenon is relevant particularly for climatized environments, where a specific range of environmental conditions must be maintained [14]. Throughout the year, it would be beneficial to have an insulating indoor conditions in periods of cold climates and heating demand and a large heat flux during warm climates with a cooling demand. Also it should take into account cool summer nights when the ambient can act as a heat sink and sunny winter days, when solar irradiance absorbed on the buildings exterior can contribute to reduce heating demand [22]. Novel technologies discussed in this section are able to modulate the energy and mass transfer between a building and its environment reversibly, in response to changing priorities. These technologies are designated in this research as dynamic insulation technologies. Dynamic insulation technologies refers to a class of building envelope technologies that are able to modulate the energy and mass transfer between the inside and outside environment. The unique feature of these technologies is the ability to adjust their thermo-optical properties reversibly in response to transient boundary conditions such as external environment and indoor requirements and changing priorities (cooling/heating). These underlying mechanics allow properties such as thermal conductivity, thermal resistance and thermal transmittance to vary, in contrast to traditional envelopes with static thermal properties.

2-3-1 A RC-network model for building thermal performance

Circuit theory is introduced for modelling the thermal performance of buildings. Here, the energy transfer between subsystems is formulated as a circuit of (temperature) nodes, resistors and capacitors. These Resistor-Capacitor (RC) enables to imitate building thermal dynamics by referring resistance and capacitances as equivalent lumped thermal parameters. RC models are often used for predicting the air temperature in a zone as well as heating and cooling load. In addition, the RC model can also be used for inferring important building thermal characteristics, such as the overall effective thermal transmittance, thermal conductance and solar gains [50]. Figure 2-4 shows the representation of the thermal dynamics in a RC model framework. Measured or prior-known values of variables are considered the system inputs and outputs, while temperature linked to thermal capacitors are system states. Here, temperature

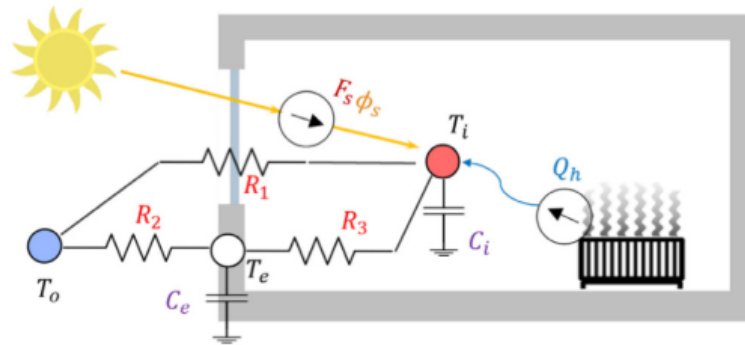


Figure 2-4: Example of a RC network representation of a room. From [50].

state variables are represented as grounded nodes with capacitances C_k while the heat transfer between two nodes is represented by a network of resistors. The thermal dynamics of each temperature node is governed by the energy-balance equations, which results in the following ordinary differential equation for a temperature node k :

$$C_k \frac{dT_k}{dt} = \sum_k \frac{T_k - T_k^*}{R_{k,k}} + \sum_j F_j Q_j \quad (2-17)$$

where T_k represents the temperature of the k^{th} node, C_k is the capacitance of the k^{th} node, T_k^* represents the temperature of a neighbor of the k^{th} node, $R_{k,k}$ is the thermal resistance between the k^{th} node and its neighbor, Q_j denotes the j^{th} heat input to the k^{th} node and F_j represents a factor that evaluates effective heat gains to the k^{th} node due to Q_j . Furthermore, the thermal resistance of the building envelope can be computed using Ohm's law. For example, the effective thermal resistance for the building in Figure 2-17 is:

$$\frac{1}{R_e} = \frac{1}{R_1} + \frac{1}{R_2 + R_3} \quad (2-18)$$

The overall thermal transmittance, or U-value, is computed by:

$$U = \frac{1}{R_e} \quad (2-19)$$

2-3-2 Static and dynamic thermal properties

The next aspect of dynamic modelling is to identify the thermally static and dynamic components in an envelope. For this the modelling framework of [11] is used. Here the thermal performance of a class of dynamic insulation technologies known as switchable thermal insulation structures are analysed. Switchable thermal insulation structures are within the envelope enclosure which are capable of reversibly alternating between an insulated state that inhibits heat flux and a conductive state that enhances the heat flux through the envelope. Within this framework an important feature is the formulations of the heat transfer coefficients of the envelopes in the insulated state and conductive state; the envelopes are composed of thermally static components and thermally dynamic components, which alternates the level of insulation while the static component remains constant. The effective heat transfer coefficient h of a switchable insulation technology is expressed as a series connection of the static component in parallel with the switchable component:

$$\bar{h} = (h_{sw}^{-1} + h_1^{-1})^{-1} + h_2 \quad (2-20)$$

where h_{sw} is the heat transfer coefficient for the switchable component and h_i ($i = 1, 2$) are the static components. For the switchable component, h_{sw} is either on or off for the conductive or insulated state, respectively.

2-4 Conclusion

In this chapter, existing academic theory was reviewed in order to provide a complete overview of the present perception and approach. In conclusion of this review, observations were drawn.

Mechanistic greenhouse climate models, compared to empirical models, provide the insight of the processes involved. The general formulation is based on the conservation of mass and energy, where each subsystem and their interconnection are formulated as mass and energy transfers. It is also found that depending on the application the modelling structure differs in terms of the set of equations and formulation of processes. For control and optimization purposes, the greenhouse climate models have relatively less state variables compared to models specifically designed for simulation only.

Controlling the greenhouse climate considers more than just the inside climate variables and crop and considers a multi-layered hierarchical control strategy. The objectives and aims of the top layers determines the set-points for the lower layers. Considering all layers in a control strategy is known as optimal control. Since the greenhouse climate is considered to be in the lower layers, the control of the climate variables can be done without considering all control layers if the set-points are already known for the climate controller. A MPC strategy could then be implemented which optimizes future behaviour of the greenhouse climate with respect to the pre-defined set-points and constraints.

Building envelopes with ability to vary their thermal properties are designated as dynamic insulation technologies. With this field, two frameworks have been introduced for modelling which transcends the underlying mechanics and focuses only on the overall thermal transmittance. It is found that circuit theory allows to model the heat loss through an envelop as a network of nodes, which represent the temperature of indoor environment, and resistors and

capacitors as lumped parameters. Within this modelling framework the thermal properties of envelopes with thermal varying properties the heat transfer coefficients are described in terms of their static and dynamic switchable components.

Methodological approach

The research context, existing challenges, relevance and theoretical background of model based predictive control of soap bubble cavity greenhouse problem have been elaborated in Chapter 2. It is evident that within the current literature, a gap of knowledge is present about integrating the novel soap bubble cavity technology in a model based predictive control problem of greenhouse climate. It is the goal of this thesis work to produce valuable contribution and an initial proposal for integrating both disciplines in one framework. The continuation of this chapter will outline the research proposal and a methodology which will explain the necessary steps to be taken throughout this thesis work, to gather the required knowledge and achieve the established objectives.

3-1 Research objectives and Aims

The primary objective of the proposed research work is to design and implement a model predictive control strategy for controlling the inside micro-climate of the BBBLS greenhouse. The control strategy must be capable of maintaining a favorable climate by finding an optimal utilization of the climate control equipment and the soap bubble cavity.

In order to achieve this objective, the following sub-objectives must be achieved first:

1. Develop a model for mechanistically describing the inside micro-climate of the BBBLS greenhouse based on physical knowledge and governed by physical laws. The model must capture all relevant processes as a function of the climate control equipment, exogenous such as the outside environment and greenhouse specifics and formulated using energy- and mass balance equations.
2. Develop a comprehensive framework for the soap bubble cavity, which reflects the dynamics of filling the cavities with soap bubbles and their corresponding influence on the thermal performance. The framework must be translated in a processable form such that it can be integrated in the greenhouse climate model developed earlier. The existing modelling frameworks of [35] and [11] could provide a valuable foundation.

3. Develop a model-based predictive control strategy for controlling the inside micro-climate of the BBLS greenhouse. The strategy must be capable of generating an optimal sequence of control inputs for maintaining a favorable climate on-line. The control sequence must be a result of optimizing over the predicted behaviour of the greenhouse climate, for which the augmented greenhouse climate model is used.

3-2 Research Questions

This section contains the research questions that need to be answered as a means to realize the project objectives. The research questions are divided in sub-questions for if answered, form the answer of the main research question. For achieving the objectives the main research question is formulated as:

Main Research Question

How can a model based predictive control strategy contribute in greenhouse climate control such that a specific condition of greenhouse climate of the BBLS greenhouse is governed by the optimized use of the climate control equipment and the bubble cavity envelope?

The underlying sub-questions are formulated as follows:

Research Questions

1. *What type of mechanistic model, based on heat- and mass balance equations, allows a representative description of the greenhouse climate of the BBLS greenhouse such that the inside climate is modelled accurately?*
 - (a) *Which heat- and mass transfer phenomena occur in the greenhouse?*
 - (b) *Which elements of the greenhouse are relevant for the micro-climate?*
 - (c) *Which set of state variables is sufficient for describing the greenhouse climate?*
2. *How can the thermal properties of the bubble cavity envelope explained in [15] be integrated in the greenhouse climate, such that it can be implemented in the modelling and control framework?*
 - (a) *Which heat- and mass transfers are affected by the thermal properties of the bubble cavity envelope during the distribution of soap bubbles?*
 - (b) *Which parts of existing frameworks by [35] and [11] enable to formulate the thermal performance of the soap bubble cavity in similar manner?*
 - (c) *How can the control signal of the utilization of the soap generator be mathematically formulated?*
3. *How can a MPC algorithm be set up for controlling the greenhouse climate of the BBLS greenhouse?*

- (a) *What type of prediction model provides an accurate prediction of the inside climate variables and soap bubble cavity filling?*
- (b) *What type of MPC strategy is the most suited?*
- (c) *What are the limitations of the greenhouse operation, in terms of climate and control bounds, and how can they be translated as constraints?*
- (d) *What sort of cost function is formulated in the optimization problem?*
- (e) *Which optimization solver allows to obtain a global solution of the optimization problem, while having ample time within each sampling instant?*

3-3 Experimental setup

The mathematical formulation and computation will be compiled using the MATLAB programming language. Within MATLAB, the SIMULINK toolbox is used for developing and validating the greenhouse climate model. The problem instances will be solved by acknowledged solvers, such as MATLAB optimization toolbox [25] and TOMLAB [2]. The experimental platform for the research work is the BBLS greenhouse in Tonsberg, Norway. Collaboration will be set up with BBLS and their engineering division to acquire specifications and set-up experiments to obtain data measurements. This is necessary to calibrate and validate the developed model for the specific greenhouse.

An integrated model for the greenhouse climate and soap bubble cavity

The purpose of this section is to present an integrated model to describe the inside micro-climate of the greenhouse and the soap bubble cavity dynamics.

4-1 A mechanistic model for the greenhouse climate

The first objective is to develop a greenhouse climate model as a function of the greenhouse specifications, climate control and exogenous inputs such as the outside environment. The initial formulation of the model does not consider the soap bubble cavity and assumes that the empty cavity has similar dynamics as a conventional glass greenhouse. To describe the indoor micro-climate of the greenhouse, energy and mass balances were set up yielding four differential equations describing the inside air temperature, soil temperature, temperature of the air out of the tube and the inside humidity, in that order:

$$\begin{aligned}\frac{dX_{T_{\text{air}}}}{dt} &= \frac{1}{c_{\text{cap,g}}} (-Q_{\text{cov}} + Q_{\text{rad}} + Q_{\text{lamp}} + Q_{\text{he}} + Q_{\text{soil}}) && (\text{K s}^{-1}) \\ \frac{dX_{T_{\text{soil}}}}{dt} &= \frac{1}{c_{\text{cap,s}}} (-Q_{\text{soil}} + Q_{\text{deep}} + Q_{\text{lamp,s}}) && (\text{K s}^{-1}) \\ \frac{dX_{T_{\text{tubes}}}}{dt} &= \frac{1}{c_{\text{cap,t}}} (-Q_{\text{bat,c}} + Q_{\text{cross}} + Q_{\text{bat,h}}) && (\text{K s}^{-1}) \\ \frac{dX_{\chi_{\text{air}}}}{dt} &= \frac{1}{h_{\text{g}}} (-\phi_{\text{cov}} + \phi_{\text{lamp}}) && (\text{g m}^{-3} \text{ s}^{-1})\end{aligned}\quad (4-1)$$

where Q and ϕ represent the energy- and mass transfers respectively, $c_{\text{cap,g}}$ the heat capacity inside the greenhouse ($\text{J m}^{-2} \text{K}^{-1}$), $c_{\text{cap,s}}$ the soil heat capacity ($\text{J m}^{-2} \text{K}^{-1}$), $c_{\text{cap,t}}$ the heat

capacity of the air flowing out of the tubes (W K^{-1}) and h_g the height of the greenhouse (m). The continuation of this section will elaborate on each energy- and mass transfer and Table 4-1 will show for each element the literature source.

Energy/Mass transfer	Section	Source
Q_{cov}	4-1-1	[42], [4] [33]
Q_{rad}	4-1-5	[42],[39]
Q_{lamp}	4-1-3	[42]
Q_{he}	4-1-4	[42],[9],[13]
Q_{soil}	4-1-2	[39]
Q_{deep}	4-1-2	[39]
$Q_{\text{lamp,s}}$	4-1-3	-
$Q_{\text{bat,c}}$	4-1-4	-
$Q_{\text{bat,h}}$	4-1-4	-
Q_{cross}	4-1-4	[42]
ϕ_{cov}	4-1-1	[42],[6],[36]
ϕ_{lamp}	4-1-3	-

Table 4-1: Energy- and mass transfer and their corresponding source.

4-1-1 Heat and mass transfer of the cover

The convective heat transfer from inside air to cover Q_{cov} involves the heat transfer from inside air through the cover to the outside air and through the cover to the education centre (EC), which is adjacent to the greenhouse:

$$Q_{\text{cov}} = c_{\text{cnv,out}} (X_{\text{Tair}}(t) - D_{\text{Tout}}(t)) + c_{\text{cnv,EC}} (X_{\text{Tair}}(t) - D_{\text{Tec}}(t)) \quad (4-2)$$

Where $c_{\text{cnv,out}}$ and $c_{\text{cnv,EC}}$ are the heat transfer coefficients, through the cover to the outside environment and EC respectively ($\text{J m}^{-2} \text{K}^{-1}$). The heat transfer coefficient combines the thermal conductivity coefficient, the convection coefficients at the inside and outside of the cover and the heat transfer by long wave radiation through the cover.

Condensation on the cover ϕ_{cov} takes place when the temperature of the cover is below the dew point temperature of the air, or similarly, when the water vapor concentration of the internal air is greater than the water concentration of the cover at saturation. This is computed as:

$$\phi_{\text{cov}} = g_c \left(a_1 e^{a_2 X_{\text{Tair}}(t)} (X_{\text{Tair}}(t) - D_{\text{Tout}}(t)) - (\chi_{\text{air}}^*(t) - X_{\chi_{\text{air}}}(t)) \right) \quad (4-3)$$

where χ_{air}^* is the saturated vapour concentration computed as:

$$\chi_{\text{air}}^*(t) = 5.5638e^{0.0572X_{\text{Tair}}(t)} \quad (\text{g m}^{-3}) \quad (4-4)$$

The mass transfer conductance g_C is computed as:

$$g_C = \max \left[0, \frac{A_{\text{cov}}}{A_{\text{soil}}} p_{\text{GC}} (X_{\text{Tair}}(t) - T_{\text{cover}}(t))^{1/3} \right] \quad (\text{g m}^{-2} \text{s}^{-1}) \quad (4-5)$$

where $\frac{A_{cov}}{A_{soil}}$ is the ratio of the cover area to soil area, p_{GC} is the parameter related to the properties of the condensation surfaces ($\text{m K}^{1/3} \text{s}^{-1}$) and T_{cover} is the cover temperature estimated by:

$$T_{cover} = \frac{2D_{T_{out}}(t) + X_{T_{air}}(t)}{3} \quad (\text{K}) \quad (4-6)$$

The terms a_1 and a_2 are considered empirical constants to be estimated.

4-1-2 Heat transfer of the soil

The soil is considered as a greenhouse thermal mass that plays an important role in greenhouse climate. During diurnal time, the soil absorbs solar radiation on its surface, heating the deep soil layers and releases (transfers) heat to the greenhouse environment. A simple formulation is considered, where the soil is divided in the upper layer (approximately 5cm thick) and a deep soil layer. The convective heat transfer from soil to inside air is computed in a similar fashion cover as convective fluxes using the following equation:

$$Q_{soil} = c_{cnv,s}(X_{T_{soil}}(t) - X_{T_{air}}(t)) \quad (4-7)$$

where $c_{cnv,s}$ is the soil convective heat transfer coefficient ($\text{J m}^{-2} \text{K}^{-1}$). The second heat transfer is the conductive flux between the soil surface and the deep soil layer computed as:

$$Q_{deep} = c_{cnd,deep}(D_{T_{deep}}(t) - X_{T_{soil}}(t)) \quad (4-8)$$

where $c_{cnd,deep}$ is the conductive soil to soil heat transfer coefficient ($\text{J m}^{-2} \text{K}^{-1}$) and $D_{T_{deep}}$ is the deep soil temperature, which is assumed to be constant.

4-1-3 Heat and mass transfer of the heating lamps

Artificial lighting by lamps produce, next to light, also heat and heats up the greenhouse air. The corresponding heat transfer is computed using the following equation:

$$Q_{lamp} = \eta_{air} P_e U_{lamp}(t) \quad (4-9)$$

where η_{air} is the efficiency factor of electrical energy transformed to heating of the greenhouse air and P_e is the rated electric power (W m^{-2}). The control signal U_{lamp} is either on or off. Translating this to a discrete logic value implies that U_{lamp} can be considered as a binary control variable:

$$U_{lamp} \in \{0, 1\} \quad (4-10)$$

Similarly, the soil is also heated up by the lamps and is computed in similar fashion:

$$Q_{lamp,s} = \eta_{soil} P_e U_{lamp}(t) \quad (4-11)$$

where η_{soil} is the part of electrical energy transformed into heat released to the soil.

The mass balance is also affected by energy released by the lamps. Condensation forms droplets on greenhouse elements. In the event that the lamps are on the heat causes the droplets to vaporise which is then circulated throughout the greenhouse by the internal circulation mode. This cause an overall increase of the humidity. We assume that this phenomenon is linear with the input of the lamps:

$$\phi_{\text{Lamp,vap}} = \epsilon_{\text{vap}} U_{\text{lamp}}(t) \quad (4-12)$$

where ϵ_{vap} is the parameter related to the vaporisation of droplets ($\text{g m}^{-2} \text{s}^{-1}$).

4-1-4 Heat and mass transfer of the air-treatment system

The BBBSL greenhouse is equipped with an air-treatment system. It circulates treated air which then goes through the perforation tubes and mixes with the greenhouse air. The air-treatment system includes a horse-shoe-heat-exchanger unit and cooling- and heating batteries. The horse-shoe heat-exchanger (HSHE)-unit exchanges thermal energy from one air-stream to another without mixing both air-streams. The air-stream inlets are on the heat-exchanger side and the horse-shoe air vent side. Both inlets are connected to two dampers, which control the source of air going through the inlet. Dependent on the damper settings the air going through the horse-shoe crosses the airflow of the heat-exchanger without mixing, exchanging only thermal energy with the air from the heat exchanger right before the air is released outside.

The corresponding heat transfer off the cross-flow exchange Q_{cross} is computed using the following equation:

$$Q_{\text{cross}} = c_{\text{cap,air}} \rho_{\text{air}} F_{\text{flow}} (T_{\text{cross-flow}}(t) - X_{T_{\text{tubes}}}(t)) \quad (4-13)$$

where F_{cross} is the flow rate of air, $c_{\text{cap,air}}$ and ρ_{air} are the specific heat capacity and density of the air respectively. T_{cross} is the temperature of the air right after the cross-flow heat exchanger, computed as the numerical average between the temperatures of the air in the heat exchanger and the horse-shoe channel:

$$T_{\text{cross-flow}} = \beta_{\text{HSHE}} T_{\text{he,in}}(t) + (1 - \beta_{\text{HSHE}}) T_{\text{hs,in}}(t) \quad (\text{K}) \quad (4-14)$$

with β_{HSHE} a numerical average to be estimated. As mentioned, the source of air-stream of both channels can be altered based on the opening of the corresponding damper. Both air channels are connected to the inside and outside environment. This implies that the temperature of air-stream inside the heat-exchanger is similar to the temperature of the outside environment or the greenhouse air, depending on the setting of the dampers. This is written as

$$T_{\text{he,in}} = \begin{bmatrix} X_{T_{\text{air}}}(t) & D_{T_{\text{out}}}(t) \end{bmatrix} \begin{bmatrix} U_{\text{he,GH}}(t) \\ U_{\text{he,out}}(t) \end{bmatrix} \quad (\text{K}) \quad (4-15)$$

with $U_{\text{he,GH}}$ and $U_{\text{he,out}}$ are the control variables of the damper of the greenhouse- and outside air respectively. The dampers have two modes: open (on) and closed (off). Translating this to a logical statement the control variables are considered as a binary value:

$$U_{\text{he,GH}}, U_{\text{he,out}} \in \{1, 0\} \quad (4-16)$$

A similar approach is done for the temperature of the air through the horse-shoe channel:

$$T_{\text{hs,in}} = \begin{bmatrix} X_{T_{\text{air}}}(t) & D_{T_{\text{out}}}(t) \end{bmatrix} \begin{bmatrix} U_{\text{hs,GH}}(t) \\ U_{\text{hs,out}}(t) \end{bmatrix} \quad (\text{K}) \quad (4-17)$$

with

$$U_{\text{hs,GH}}, U_{\text{hs,out}} \in \{1, 0\} \quad (4-18)$$

The heating and cooling batteries are connected to a thermal energy storage tank, where hot and cold water is used for controlling the outgoing flow conditions. The heat transfer of the heating and cooling batteries can be related to the temperatures of the water inside the batteries:

$$Q_{\text{bat,heat}} = c_{\text{cnd,hb}} c_{\text{cap,w}} (D_{T_{\text{hw,in}}} - X_{T_{\text{tubes}}}) \quad (4-19)$$

$$Q_{\text{bat,cool}} = c_{\text{cnd,cb}} c_{\text{cap,w}} (D_{T_{\text{cw,in}}} - X_{T_{\text{tubes}}}) \quad (4-20)$$

where c_{cnd} is the conductive heat transfer coefficient of and $c_{\text{cap,w}}$ is the specific heat capacity of the water flowing through the batteries. The batteries are controlled by applying pressure to the pumps. We assume an on/off control input for both batteries, i.e.:

$$Q_{\text{bat,heat}} = c_{\text{cnd,hb}} c_{\text{cap,w}} (D_{T_{\text{hw,in}}}(t) - X_{T_{\text{tubes}}}(t)) U_{\text{hw}}(t) \quad (4-21)$$

$$Q_{\text{bat,cool}} = c_{\text{cnd,cb}} c_{\text{cap,w}} (D_{T_{\text{cw,in}}}(t) - X_{T_{\text{tubes}}}(t)) U_{\text{cw}}(t) \quad (4-22)$$

where $U_{\text{hw}}, U_{\text{cw}} \in \{1, 0\}$. Finally, the treated air flows through the perforation tubes in the greenhouse environment. This heat transfer is computed as:

$$Q_{\text{he}} = \alpha_{\text{he}} (X_{T_{\text{tubes}}}(t) - X_{T_{\text{air}}}(t)) \quad (4-23)$$

where α_{he} is the heat transfer of air treatment system ($\text{J m}^{-2} \text{K}^{-1}$).

4-1-5 Heat transfer due to solar radiation

Energy added to the greenhouse air by incoming radiation Q_{rad} is the measured outside radiation D_{rad} multiplied by the total light transmission of the cover:

$$Q_{\text{rad}} = \tau_{\text{cov}} D_{\text{rad}}(t) \quad (4-24)$$

where τ_{cov} is the total light transmission coefficient of the cover.

4-2 Modelling of the dynamic soap bubble cavity

In previous section the greenhouse climate is modelled with the assumption that climate behaviour of the greenhouse without soap bubbles in the cavity is similar to conventional (glass) greenhouses. This section aims at a novel approach to integrate the soap bubble cavity, with its corresponding effects on the energy and mass balance, in the greenhouse climate model developed earlier.

4-2-1 Filling of the cavities

There are seven cavity compartments enclosing the cultivation area and the Education Centre. Each compartment is installed with its own soap bubble generator to use to fill up independently. However, the fillings of the cavity compartments can not be done simultaneously, as it is only possible to fill one compartment each time. Furthermore, it is found that the filling level of the cavity is not done instantaneously and requires preparation and sufficient time. Also, prior to filling the cavity the old soap bubbles are flushed, using the inside nozzles and fan and takes several minutes. Furthermore there are no sensors inside the cavity for measuring the state of the cavity filling at each time instant. A visual inspection of the cavity being "completely filled" and the time it takes approximately is only known as shown in Table 4-2.

Index	Compartment	Time to fill up [mins.]
1	Greenhouse wall south-facing	30
2	Greenhouse wall south-facing	30
3	Greenhouse roof north-facing	30
4	Greenhouse roof south-facing	30
5	Education Centre roof south-facing	60
6	Education Centre roof north-facing	30
7	Education Centre wall north-facing	60

Table 4-2: Cavity compartment and time to fill up

Furthermore the soap is subject to various factors which may break down the foam:

- Solar radiation: The solar radiation is considered to be a major factor in soap breakdown. Earlier tests have shown that the soap breaks down on various locations. The location of the breakdown is dependent on the intensity of the solar radiation on that particular part of the cavity.
- Wind: The soap is also subjected to wind, as expansion and contraction of the foil due to wind gusts causes bubble bursting .
- Time: The breakdown over time is found from visual inspections to be not significant, but the translucence of the bubbles gets affected as the soap dries out.

4-2-2 Simple abstraction of the soap bubble dynamics

For modelling the soap filling dynamics the following assumptions are made:

- Fluid dynamics: although the interconnection of bubbles creates voids which defines the porosity, it is assumed that the filling of the cavities with soap bubbles has the same properties and distribution as a mixed fluid. This is somewhat plausible as the fan and nozzle pushes the created soap to the other side of the cavity.
- No breakdown or translucency: It is assumed that once the soap bubbles enter the cavity no external factors are affecting the filling rate and the quality of the soap bubbles.

From these assumption the filling dynamics are modeled as a first order model, where the rate of change of fluid volume for each cavity i can be formulated as:

$$\frac{dV_i}{dt} = \phi_{in,i} \quad (\text{m}^3 \text{ s}^{-1}) \quad (4-25)$$

Since it is assumed that the volume is constant, the surface area of the compartment A_i is then considered to be constant:

$$A \frac{dh_i}{dt} = \phi_{in,i} \quad (4-26)$$

This implies that the bubble filling dynamics is modeled as the rate of change of fluid level (or height) of the cavity. $\phi_{in,i}$ is the flow of fluid entering the cavity. This represents the soap bubble generator on each side of cavity i . For $\phi_{in,i}$, a constant filling rate is assumed. Let $t_{fill,i}$ denote the fill up time for cavity i (s). Then the filling rate is computed as:

$$\phi_{in,i} = \frac{V_{total,i}}{t_{fill,i}} U_{fill,i}(t) \quad (4-27)$$

where $V_{total,i}$ is the total volume of compartment i (m^3). For the input, the soap bubble generator for each cavity is a binary input. Each cavity compartment is modelled using Equation 4-26. However, the main focus is the effect it has on the greenhouse area. However, the cavities enclosing the Education Centre are not considered, which implies that the cavity compartments of the south-facing wall, west-facing wall and north- and south-facing roofs of the greenhouse are considered. The filling dynamics of the selected compartments is represented with the state variable $X_{h,i}$.

$$\frac{dX_{h,i}}{dt} = \frac{1}{A_i} (\phi_{in,i}), i \quad \in 1, \dots, 4 \quad (4-28)$$

4-3 Thermal performance of the soap bubble cavity

The next step is to relate the filling level to the thermal performance of the cavity. The presence of soap bubbles in the cavity changes the thermal performance of the greenhouse. For this the frameworks of [35] and [11] are used.

4-3-1 A RC-network formulation of the convective heat transfer

From [50], the greenhouse thermal dynamics of the inside air with the outside air is reformulated as an RC network. Let $X_{T_{air}}$ be represented as a temperature node with capacitance C_{air} and $D_{T_{out}}$ be represented as a source node. By this analogy it can be deduced that $C_{air} = c_{cap,g}$ and the heat transfer between the two nodes is equivalent to the convective heat transfer through the cover, i.e.:

$$Q_{cov} = \frac{X_{T_{air}}(t) - D_{T_{out}}(t)}{R_{air,out}} + c_{cnv,EC} (X_{T_{air}}(t) - D_{T_{EC}}(t)) \quad (4-29)$$

where $R_{\text{air,out}}$ is the thermal resistance of the greenhouse cover ($\text{m}^2 \text{K}^{-1} \text{W}^{-2}$). Comparing Equation (4-29) with Equation (4-2), the following relation is deduced:

$$\frac{1}{R_{\text{air,out}}} = c_{\text{conv,out}} \quad (4-30)$$

From Equation (4-30) it is inferred that the convective energy transfer through the cover to the outside environment can be described as a network of (thermal) resistors similar to the one described in [50], where the thermal property of each element is represented by its corresponding thermal resistor R_i . The energy transfer through the cover consider the convective transfer through the west-facing wall, the south-facing wall and the roofs on top of the greenhouse. The orientation of each compartment makes it that the energy transfer directed to go through a compartment does not encounter the other compartments in that direction. For the roof however, the north-facing and south-facing are on the same plane. From circuit theory, this is analogous to the thermal resistors of each plane connected in parallel, shown in Figure 4-1:

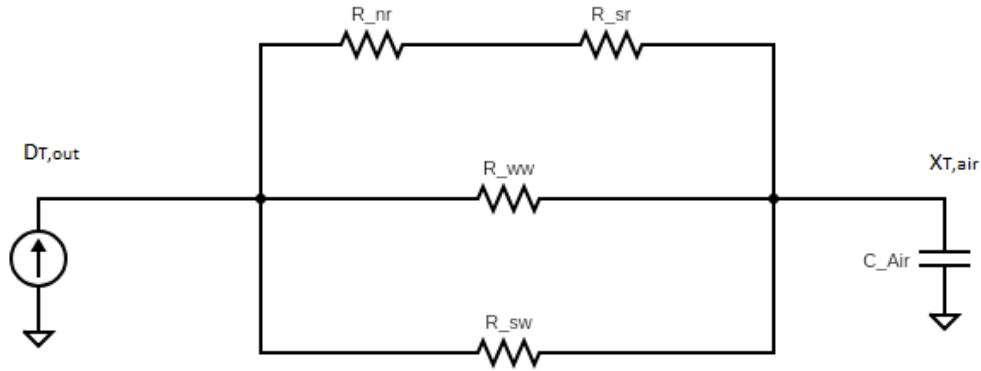


Figure 4-1: RC network representation of the convective heat transfer

Then the equivalent effective thermal resistance is computed by the following:

$$\frac{1}{R_{\text{air,out}}} = \frac{1}{R_3 + R_4} + \frac{1}{R_2} + \frac{1}{R_1} \quad (4-31)$$

4-3-2 Thermal static and dynamic elements of the soap bubble cavity

The next step is to determine the thermally static and dynamic components of the soap bubble cavity. From [11], for an envelope with switchable insulation the heat transfer coefficients is expressed as a parallel connection of the thermally static and dynamic elements. Since each cavity compartment can be switched on independently, Equation (2-20) is used to formulate the thermal resistance of each compartment in similar manner:

$$R_i = \left(R_{i,\text{sw}}^{-1} + R_{i,1}^{-1} \right)^{-1} + R_{i,2} \quad (4-32)$$

where $R_{i,\text{sw}}$ is the switchable thermal resistance and $R_{i,j}$ with $j = (1, 2)$ are the static resistance of cavity compartment i . When the cavity is empty, $R_{i,\text{sw}} = 0$, and the energy transfer through the cover is similar to the energy transfer for conventional (single glazed) greenhouses. When the soap bubble generator is initiated, the space between the membranes is filled with soap bubbles. Then the energy transfer flows through the foil and the soap bubbles. Assuming that the space between the membranes does not contribute if it is empty, the thermal resistance of the cavity compartment is then expressed as:

$$R_i = \left(R_{i,\text{sw}}^{-1} \right)^{-1} + R_{i,1} = R_{i,\text{sw}} + R_{1,2} \quad (4-33)$$

The thermally switchable component in Equation 4-33 is a function of the filling level $X_{h,i}$ and for this application only can be in two modes: off when the cavity is empty ($R_{i,\text{sw,off}} \iff X_{h,i} = 0$) and on when the cavity is filled to its maximum ($R_{i,\text{sw,on}} \iff X_{h,i} = X_{h,i}^{\text{max}}$). However, the switch from the conductive to insulated state is not done instantaneously. As shown in Table 4-2, it takes a considerable amount of time to fill up the compartments. Furthermore the overall thermal resistance varies throughout the filling process. The dynamics between the two modes must also be modeled. In this work, the thermal resistance is expressed as a linear function of the filling level:

$$R_i = \underbrace{\gamma_i X_{h,i}}_{R_{i,\text{sw}}(X_{h,i})} + R_{i,1} \quad (4-34)$$

where $\gamma_i > 0$ is the constant rate of increasing thermal resistance of the switchable component.

4-3-3 Solar emissivity

The shading of the greenhouse with the soap bubbles relates to the transmission of the cover. In Equation (4-24), the heat gain from solar radiation is reformulated similar to Equation (4-33), where the transmission coefficient is expressed in terms of the static and switchable components:

$$c_{\tau,\text{cov},i} = c_{\tau,\text{cov,sw},i} + c_{\tau,\text{cov},1,i} \quad (4-35)$$

The switchable component in Equation (4-36) is expressed similarly to Equation (4-34) as:

$$c_{\tau,\text{cov},i} = \lambda_i X_{h,i} + c_{\tau,\text{cov},1,i} \quad (4-36)$$

where $\lambda_i < 0$ is the constant rate of decreasing thermal resistance of the switchable component.

Calibration and Validation

5-1 Introduction

The model developed in Chapter 4 provides a detailed description of the climate conditions inside the greenhouse. The model is essentially used in a model-based predictive control framework if it is able to predict the relevant output of the greenhouse climate with sufficient accuracy for a wide range under varying climate conditions. The complexity here lies in the finding/adjusting of parameters related to the physical processes. Therefore, prior to validating and determining if the greenhouse model is capable to predict the inside micro-climate, the model must go through a calibration process. This section describes the calibration and validation of the greenhouse climate model. The calibration process consists of altering model parameters to get a better fit between estimated and measured data. We use the system in 4-1, where the states are directly measurable. The calibration involves the alteration of chosen parameters $\mathbf{C}' \in \mathbf{C}$ to obtain a better fit between the simulated and measured data. An appropriate method is to use a non-linear least-squares optimization problem, where it is aimed to find the set of parameters \mathbf{C}'^* which minimizes the the sum of squared errors [39][19]:

$$\min_{\mathbf{C}' \in \mathbf{C}} J(\mathbf{C}) = \sum_{h=1}^L \sum_{i=1}^M \sum_{j=1}^N w_h (\bar{y}_h(t_i, \mathbf{C}) - y_{hj}(t_i))^2 \quad (5-1)$$

where w_h is the relative weight of each output, $\bar{y}_h(t_i, p)$ is the simulated output y_h in time t_i , y_{hj} is the j th repetition of the measurement y_h in time t_i , L is the number of outputs, M is the number of real measurements (time), N is the number of repetitions in each real measurement (time) and p is the parameter set of calibration . The weights determine the relative importance of the different outputs and explicitly the parameters. The model is fit is evaluated using the variance accounted for (VAF) and root mean squared error (RMSE).

5-2 Calibration and validation of the BBLS greenhouse

The calibration of the greenhouse climate model is performed in a sequential manner. It is aimed to isolate parts of the system such that the influence of the different sub-models is partly taken into account in the calibration process. Doing so results in a more accurate description of the overall system behaviour. This implies that the greenhouse is set-up experimentally such that the measured data can be related to certain processes and phenomena. The experiments conducted are found in Appendix A.

5-2-1 Calibration of the soil temperature

The heat capacity of the soil is computed using the following equation:

$$c_{\text{cap},s} = \rho_{\text{soil}} c_{\text{th},s} c_{\text{sph},s} \quad (5-2)$$

which is a product of the density $c_{\text{den},s}$ (kg m^{-3}), thickness $c_{\text{th},s}$ (m) and the specific heat capacity $c_{\text{sph},s}$ ($\text{J kg}^{-1} \text{K}^{-1}$). The density of the soil is assumed to be $c_{\text{sph},s} = 1.25 \times 10^3 \text{ kg m}^{-3}$ and the specific heat capacity $c_{\text{sph},s} = 1.48 \times 10^3 \text{ J m}^{-2} \text{K}^{-1}$. The thickness of the soil is equivalent to the depth of the ground sensor, which is $c_{\text{th},s} = 0.05 \text{ m}$. From [39], $c_{\text{cnv},s} = 5.75$ and $c_{\text{cnd},\text{deep}} = 2 \text{ J m}^{-2} \text{K}^{-1}$. For the deep soil layer temperature it is not possible to measure its value. It is assumed that it is similar to the yearly average temperature, which is around $7 - 10^\circ\text{C}$. The calibration is done using the measured soil temperature from **Experiment 1** of Appendix A as no other elements affects the soil temperature. Results of the calibration are shown in Figure 5-1, with the estimated values and evaluation in Table 5-1 and 5-2.

Parameter	Original value	Estimated value
$c_{\text{cap},s}$	$92.5 \cdot 10^3$	$1.93 \cdot 10^5$
$c_{\text{cnv},s-a}$	5.75	2.56
$c_{\text{cnd},ss-d}$	2.00	1.94

Table 5-1: Original and estimated values of parameters.

Evaluation	Value
VAF [%]	79.016
RMSE	0.42433

Table 5-2: VAF and RMSE of the calibrated response

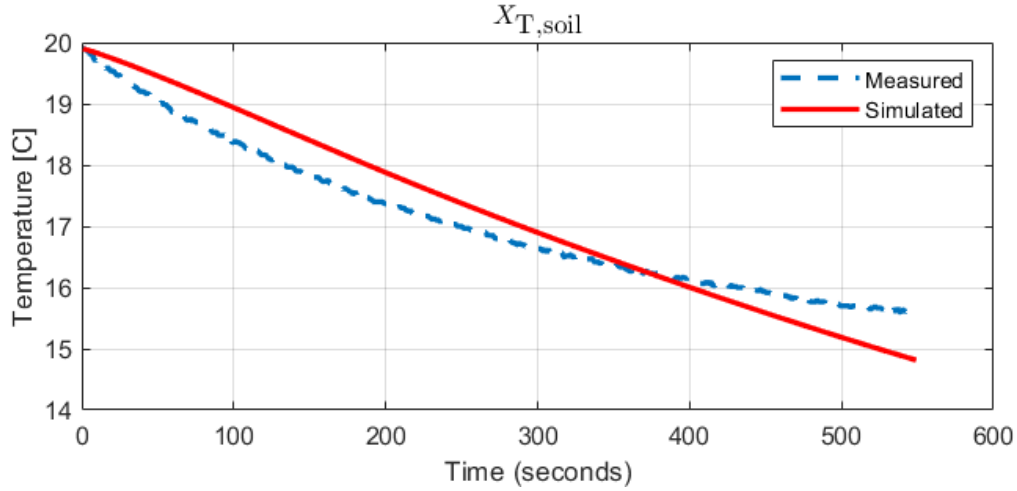


Figure 5-1: Measured and simulated data.

5-2-2 Calibration of greenhouse air temperature

For the heat capacity of the greenhouse $c_{cap,g}$, various components make up for the heat capacity besides the greenhouse air. The greenhouse heat capacity is the sum of the heat capacity of the elements inside the greenhouse. It is assumed that the greenhouse air medium and substrate tanks has the biggest contribution. Therefore the heat capacity of the greenhouse is built up with the following elements. For the greenhouse air, the heat capacity is computed as follows:

$$c_{cap,air} = \rho_{air} c_{sph,air} h_g \quad (5-3)$$

The specific heat capacity of the greenhouse air $c_{p,air}$ is taken from REF, which is $c_{p,air} = 1.0 \times 10^3 \text{ J kg}^{-1} \text{ K}^{-1}$. For the density, $\rho_{air} = 1.25 \text{ kg m}^{-3}$ and the height of the greenhouse is $c_h = 7 \text{ m}$. This results in $c_{cap,air} = 8.75 \times 10^3 \text{ J m}^{-2} \text{ K}^{-1}$. The next element is the substrate tank. It is assumed that the average temperature of the water inside the tank is 15°C , which corresponds to a specific heat capacity of $4.19 \times 10^3 \text{ J kg}^{-1} \text{ K}^{-1}$. On average, the tank contains 2.6 m^3 of water. The heat capacity of the tank is then $c_{cap,tank} = 1.09 \times 10^4 \text{ J m}^{-2} \text{ K}^{-1}$. The remaining elements inside is estimated using the following expression:

$$c_{cap,a} = c_{cap,air} + c_{cap,tank} + c_{cap,remainder} \quad (5-4)$$

For $c_{cnv,out}$ and $c_{cnv,EC}$, the initial values are taken from [34], where it is assumed to be similar to double glazing greenhouses with air between the glass membranes. The parameters are estimated using the measured greenhouse air temperature from **Experiment 1**, as this isolates the heat loss through the cover. Results of the calibration are shown in Figure 5-2, with the estimated values and evaluation in Table 5-3 and 5-4.

Parameter	Original value	Estimated value
$c_{cap,a}$	$1.96 \cdot 10^4$	$2.737 \cdot 10^4$
$c_{cnv,out}$	3	2.96
$c_{cnv,EC}$	3	4.04

Table 5-3: Original and estimated values of parameters.

Evaluation	Value
VAF [%]	95.525
RMSE	0.33154

Table 5-4: VAF and RMSE of the calibrated response

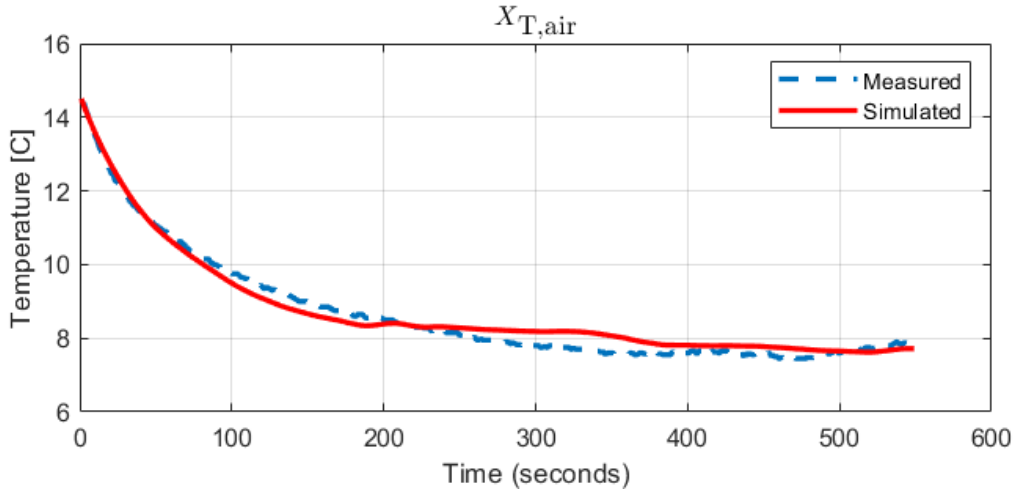


Figure 5-2: Measured and simulated data.

5-2-3 Calibration of the heat-exchanger tube temperature

The calibration of the tube temperature starts with the heat capacity of the air flowing out of the tubes. The heat capacity is computed as:

$$c_{cap,t} = \rho_{air} c_{sph,air} c_{vol,he} F_{he} \quad (5-5)$$

The average velocity of the air-stream inside the HSHE-unit is $F_{he} = 2.1 \times 10^{-3} \text{ m}^3 \text{ s}^{-1}$. The volume of the air assumed to be equal to the displacement of the air over an finite step. The finite step is equal to the sampling time of the model, which is 60 s. Therefore, $c_{vol,he} = 0.166 \text{ m}^3$. For β_{he} , an initial value of 0.5 is taken. For estimating β_{he} , the data from **Experiment 3** of Appendix A, as during this experiment the heating and cooling batteries were switched off. Results of the calibration are shown in Figure 5-3, with the estimated values and evaluation in Table 5-5 and 5-6.

Parameter	Original value	Estimated value
β_{he}	0.5	0.4466

Table 5-5: Original and estimated values of parameters.

Evaluation	Value
VAF [%]	95.525
RMSE	0.33154

Table 5-6: VAF and RMSE of the calibrated response

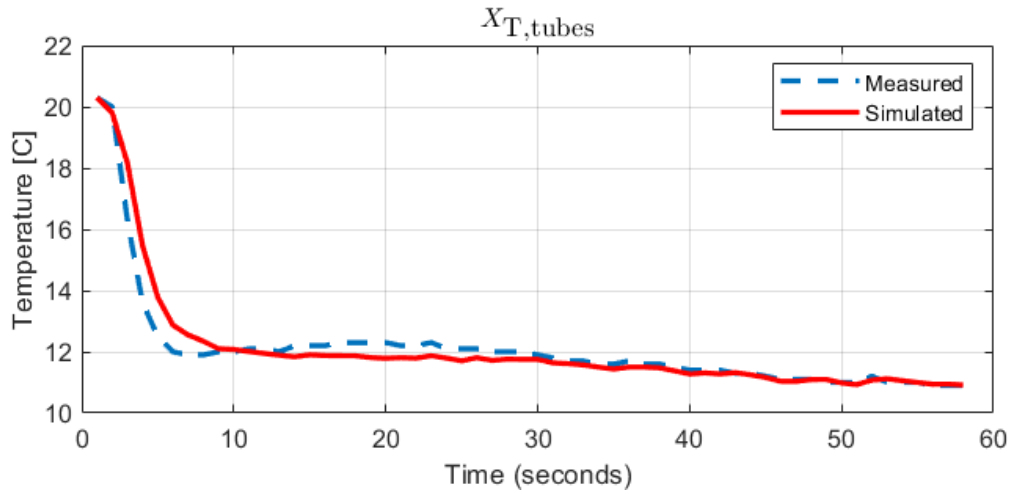


Figure 5-3: Measured and simulated data

The next part of the calibration involves the heat transfer of the cooling battery. The measured tube air temperature from **Experiment 4** of Appendix A is used, as during this experiment only the cooling battery was switched on. Results of the calibration are shown in Figure 5-4. The estimated value and evaluation are shown in Table 5-7 and 5-8.

Parameter	Original value	Estimated value
$c_{cnd,cb}$	1×10^3	1.61×10^3

Table 5-7: Original and estimated values of parameters.

Evaluation	Value
VAF [%]	77.01
RMSE	0.44263

Table 5-8: VAF and RMSE of the calibrated response

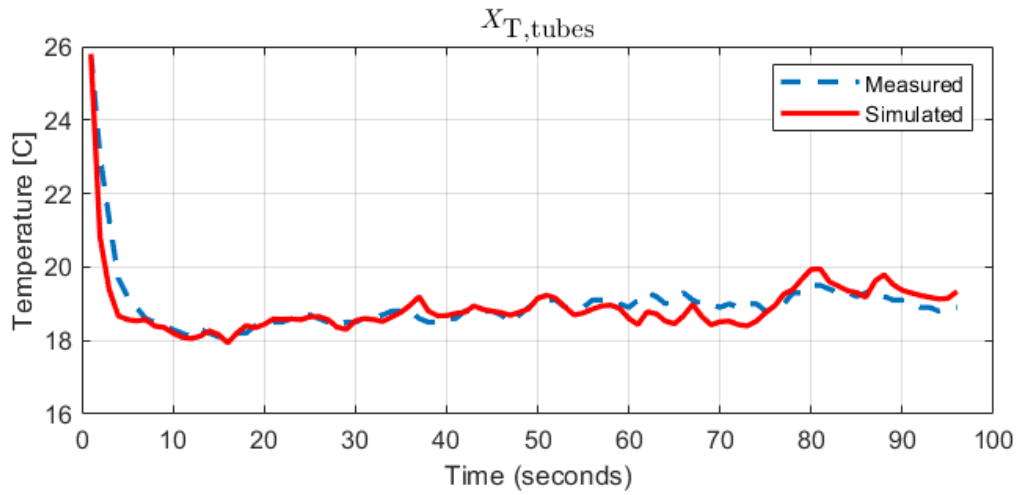


Figure 5-4: Measured and simulated data

Similarly, the heat transfer of heating battery is estimated using the measure tube air data from **Experiment 5**. Results of the calibration are shown in Figure 5-5. The estimated value and evaluation are shown in Table 5-9 and 5-10.

Parameter	Original value	Estimated value
$c_{\text{cnd,hb}}$	1×10^3	1.29×10^3

Table 5-9: Original and estimated values of parameters.

Evaluation	Value
VAF [%]	29.3
RMSE	0.799

Table 5-10: VAF and RMSE of the calibrated response

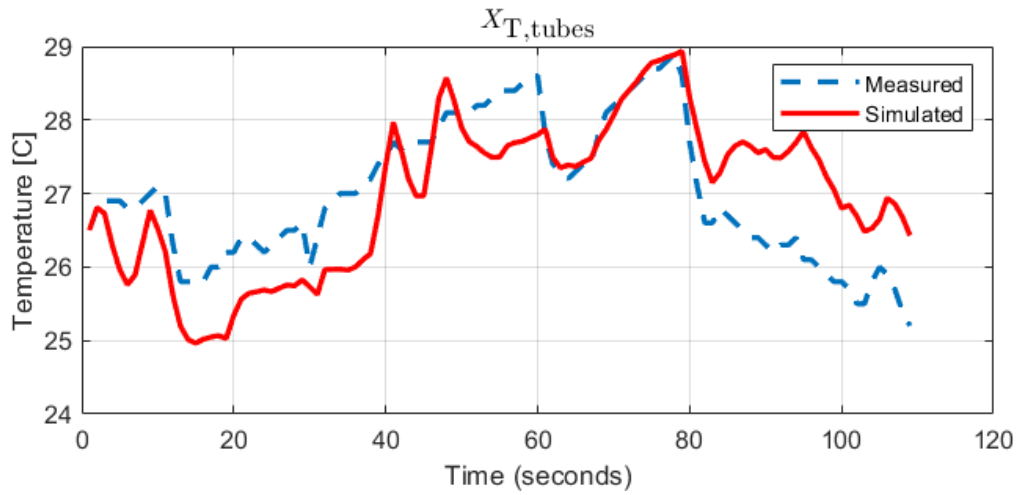


Figure 5-5: Measured and simulated data

Finally, the heat transfer of the air treatment system to the greenhouse air is estimated. From [43] an initial value of $10 \text{ J m}^{-2} \text{ K}^{-1}$ is taken. The heat transfer is estimated using the measured greenhouse air temperature of **Experiment 4**. Results of the calibration are shown in Figure 5-6. The estimated value and evaluation are shown in Table 5-11 and 5-12.

Parameter	Original value	Estimated value
α_{he}	10	15.2

Table 5-11: Original and estimated values of parameters.

Evaluation	Value
VAF [%]	96.957
RMSE	0.34307

Table 5-12: VAF and RMSE of the calibrated response

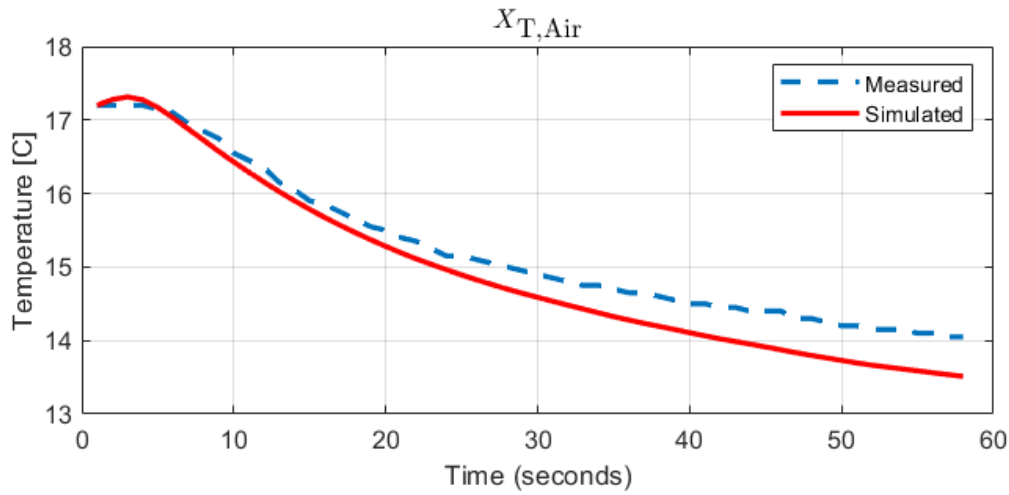


Figure 5-6: Measured and simulated data

5-2-4 Calibration of the greenhouse air humidity

Based on the greenhouse dimension, $\frac{A_{cover}}{A_{ground}} = 0.62$. The remaining parameters are estimated. The measured greenhouse humidity from **Experiment 1** of Appendix A is used as the only mass transfer process occurring is the condensation. Results of the calibration are shown in Figure 5-7. The estimated value and evaluation are shown in Table 5-13 and 5-14.

Parameter	Original value	Estimated value
a_1	0.2522	0.0729
a_2	0.0485	0.015
p_{GC}	1.8×10^3	0.1872

Table 5-13: Original and estimated values of parameters.

Evaluation	Value
VAF [%]	96.053
RMSE	0.0801

Table 5-14: VAF and RMSE of the calibrated response

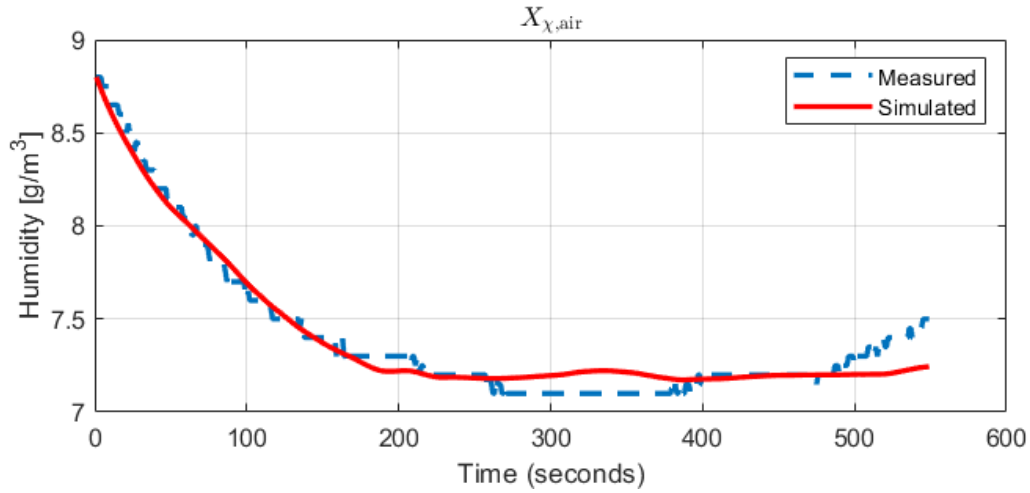


Figure 5-7: Measured and simulated data

5-2-5 Calibration of the heating lamps

The parameter related to the energy and mass transfer of the lamps are estimated using the data in **Experiment 2**. Initial values are taken from [42]. Results of the calibration are shown in Figure 5-8. The estimated value and evaluation are shown in Table 5-15 and 5-16.

Parameter	Original value	Estimated value
η_{air}	0.75	0.7473
η_{soil}	0.75	0.5276
ϵ_{air}	0.1	6.494×10^{-04}

Table 5-15: Original and estimated values of parameters.

Evaluation	$X_{T_{\text{air}}}$	$X_{T_{\text{soil}}}$	$X_{\chi_{\text{air}}}$
VAF [%]	92.0	62.5	38.4
RMSE	0.424	0.2401	0.401

Table 5-16: VAF and RMSE of the calibrated response

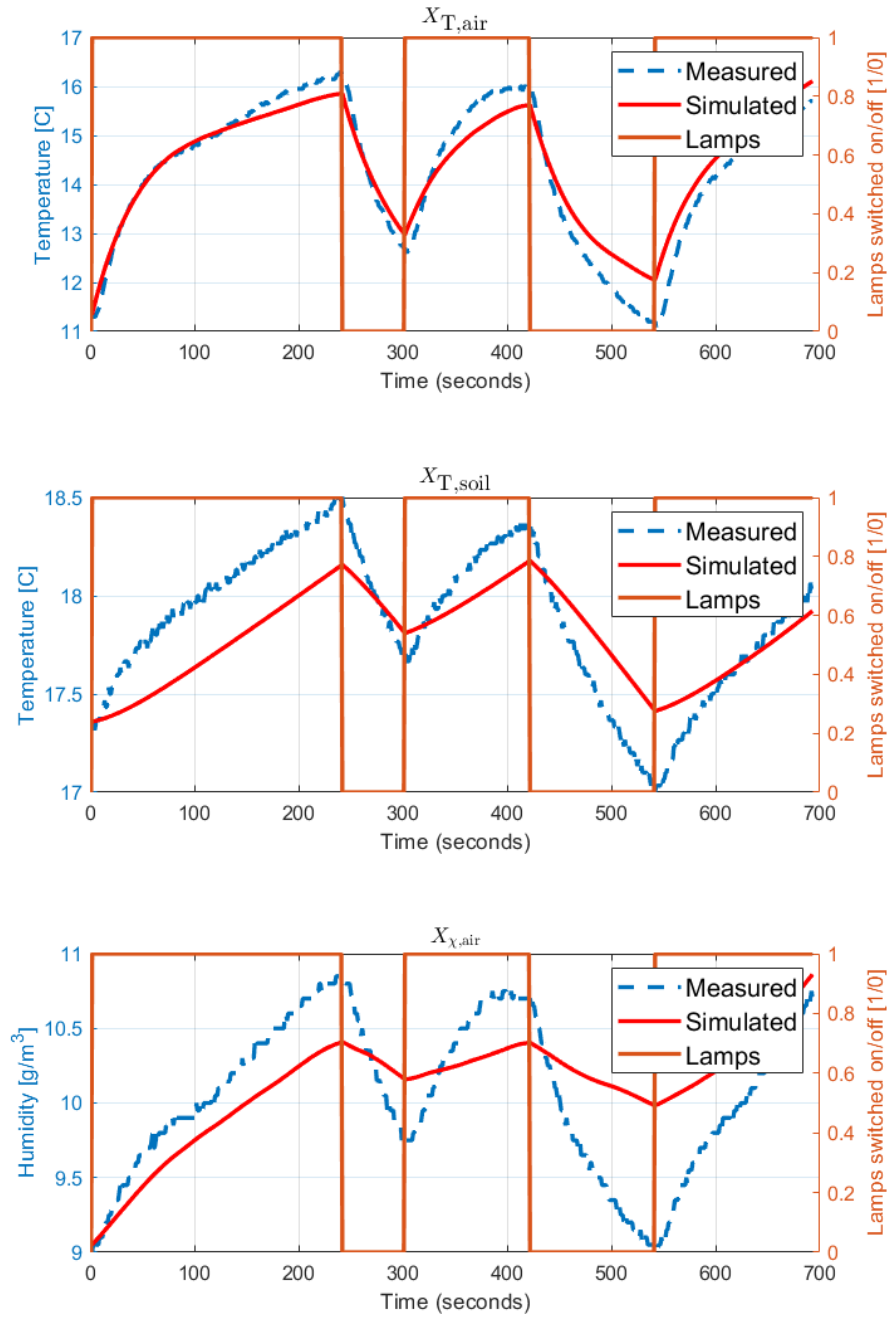


Figure 5-8: Measured and simulated data

5-2-6 Calibration of the soap bubble cavity thermal properties

From Equation (4-34), the thermal resistance of the soap bubble cavity comprises of a static component and a (linear) varying component. It is assumed that the static component along each parallel connection is equal to each other, i.e.:

$$R_{1,1} = R_{2,1} = R_{3,1} + R_{4,1} \quad (5-6)$$

This implies that the energy transfer through the cover to the outside environment is equivalent to the energy transfer through the empty soap bubble cavity:

$$c_{\text{cnv,out}} = \frac{1}{R_1(0)} + \frac{1}{R_2(0)} + \frac{1}{R_3(0) + R_4(0)} \quad (5-7)$$

The convective heat transfer coefficient for an empty cavity was estimated in Section 5-2-2 at $2.96 \text{ J m}^{-2} \text{ K}^{-1}$. From Equation 5-8 this results in $R_{i,1} = 0.84 \text{ m}^2 \text{ K J}^{-1}$. Next is estimating the thermal varying component. The data in **Experiment 6** represents the natural heat loss through the cover with fully filled cavities. The same methodology is applied as in Equation (4-34), but now the heat transfer coefficient is equivalent to the heat transfer through the fully filled soap bubble cavity:

$$\tilde{c}_{\text{cnv,out}} = \frac{1}{R_1(X_{h,1}^{\text{max}})} + \frac{1}{R_2(X_{h,2}^{\text{max}})} + \frac{1}{R_3(X_{h,3}^{\text{max}}) + R_4(X_{h,4}^{\text{max}})} \quad (5-8)$$

where $\tilde{c}_{\text{cnv,out}}$ is the heat transfer coefficient through the cover when the compartment are filled. $\tilde{c}_{\text{cnv,out}}$ is then estimated from the air temperature measurement of **Experiment 6**. Results of the calibration are shown in Figure 5-9. The estimated value and evaluation are shown in Table 5-17 and 5-18.

Parameter	Original value	Estimated value
$\tilde{c}_{\text{cnv,out}}$	2.97	1.644

Table 5-17: Original and estimated values of parameters.

Evaluation	Value
VAF [%]	95.5
RMSE	0.3321

Table 5-18: VAF and RMSE of the calibrated response

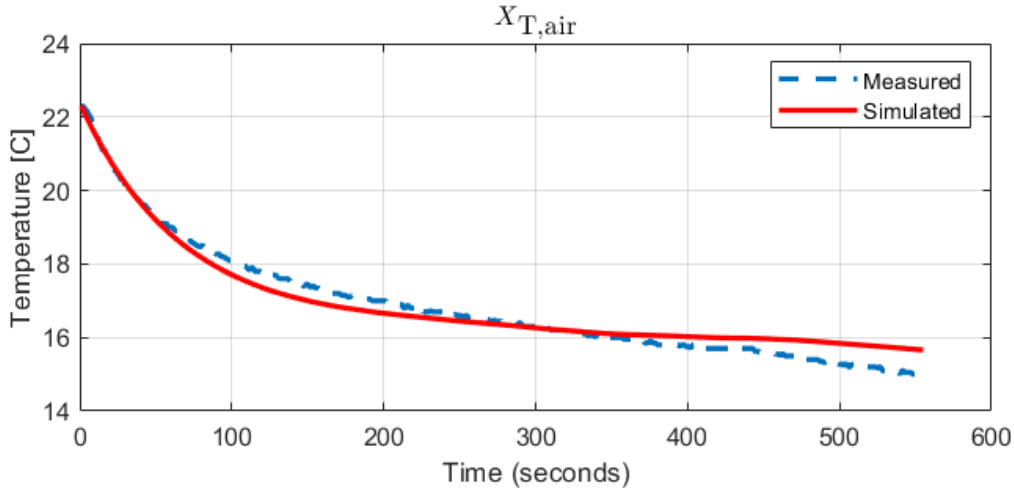


Figure 5-9: Measured and simulated data

Assuming that the thermal resistance along each parallel connection are equal:

$$R_1(X_{h,1}^{\max}) = R_2(X_{h,2}^{\max}) = R_3(X_{h,3}^{\max}) + R_4(X_{h,4}^{\max}) \quad (5-9)$$

The thermal resistance of each compartment in insulated state is $R_{i,\text{ins}} = 1.52 \text{ m}^2 \text{ K J}^{-1}$. From the greenhouse dimensions, $X_{h,1}^{\max} = 18.5 \text{ m}$, $X_{h,2}^{\max} = 29.1 \text{ m}$, $X_{h,3}^{\max} = 49 \text{ m}$ and $X_{h,4}^{\max} = 49 \text{ m}$. Interpolating between the empty and full cavity results in the following values for the thermal rates:

$$\begin{aligned} \gamma_1 &= 0.0368 \\ \gamma_2 &= 0.0234 \\ \gamma_3 &= 0.0139 \\ \gamma_4 &= 0.0139 \end{aligned} \quad (5-10)$$

5-2-7 Calibration of the solar transmission

The calibration for the solar transmission coefficient is firstly done for the case when the soap bubble cavities are empty. For this the data in **Experiment 7** is used. Results of the calibration are shown in Figure 5-10. The estimated value and evaluation are shown in Table 5-19 and 5-20.

Parameter	Original value	Estimated value
τ_{cov}	1	0.83324

Table 5-19: Original and estimated values of parameters.

Evaluation	Value
VAF [%]	87.6
RMSE	48.55

Table 5-20: VAF and RMSE of the calibrated response

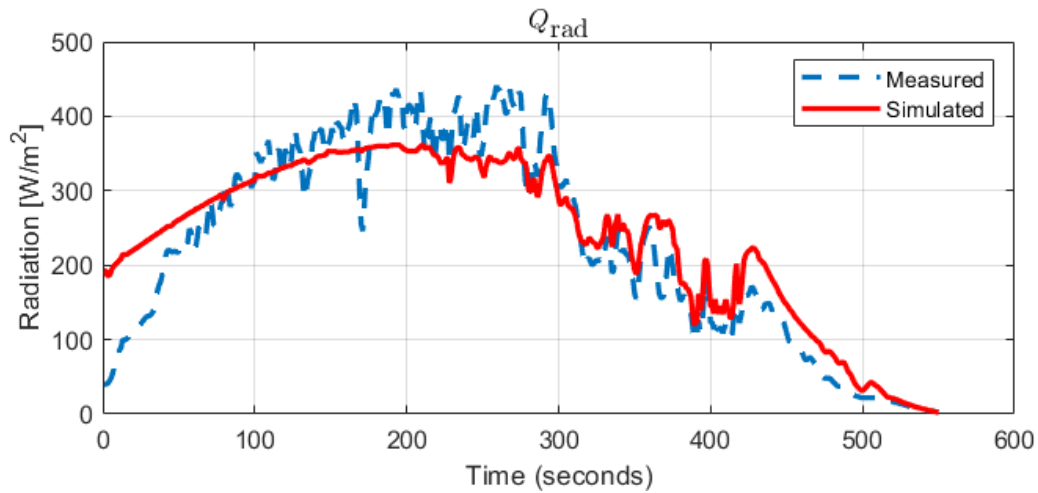


Figure 5-10: Measured and simulated data

The next calibration is the case when the soap bubble cavities are filled. Here the data in **Experiment 8** is used. However the interpretation of the measurements must be discussed first. Figure 5-11 aids in the interpretation. At approximately 11:55, indicated by the vertical dashed line, the light intensity inside the greenhouses decreases radically while the outside light intensity still remains relatively high. The interpretation of this drop is as follows; the sensor measuring the light intensity of the inside greenhouse is directed towards the south-facing roof of the greenhouse. As the south-roof cavity is being filled, the soap bubble medium reaches the point where the light intensity sensor is placed, hence it measures the light intensity through the soap bubble medium.

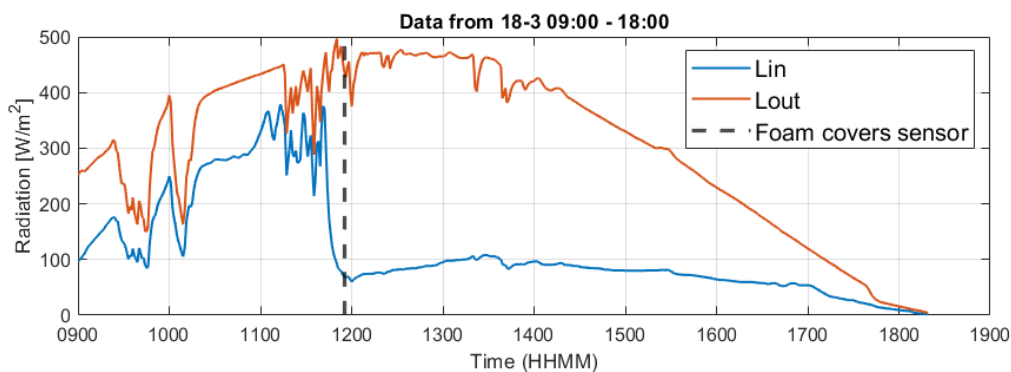


Figure 5-11: Light intensity measurement during south-roof cavity filling

It is therefore assumed that the light transmission of the cover is only affected by the south-facing roof of the greenhouse. Furthermore, the transmission coefficient of the greenhouse in insulated state is assumed to be the value related to the point where the soap bubble medium covers the sensor. From the data, $\tilde{\tau}_{cov} = 0.1576$. The static and varying components are formulated in similar fashion to the thermal resistance. The static component of the transmission is then equal to the previous estimated transmission coefficient, i.e. $\tau_{cov,1,3} =$

0.833. Then the varying component of the transmission coefficient is:

$$\lambda_3 = -0.1576 \quad (5-11)$$

This implies that the heat transfer due to solar radiation is now also a function of the filling level of the south-roof compartment:

$$Q_{\text{rad}} = (\tau_{\text{cov}} - \lambda_3 X_{\text{h},3}) D_{\text{rad}} \quad (5-12)$$

A Model Predictive Control strategy for climate control of soap bubble cavity greenhouse

6-1 Formulation of the prediction model

The augmented greenhouse climate mode is described as:

$$\begin{aligned}\frac{dX_{T_{\text{air}}}}{dt} &= \frac{1}{c_{\text{cap,g}}} (-Q_{\text{cov}} + Q_{\text{rad}} + Q_{\text{lamp}} + Q_{\text{he}} + Q_{\text{soil}}) && (\text{K s}^{-1}) \\ \frac{dX_{T_{\text{soil}}}}{dt} &= \frac{1}{c_{\text{cap,s}}} (-Q_{\text{soil}} + Q_{\text{deep}} + Q_{\text{lamp,s}}) && (\text{K s}^{-1}) \\ \frac{dX_{T_{\text{tubes}}}}{dt} &= \frac{1}{c_{\text{cap,t}}} (-Q_{\text{bat,c}} + Q_{\text{cross}} + Q_{\text{bat,h}}) && (\text{K s}^{-1}) \\ \frac{dX_{\chi_{\text{air}}}}{dt} &= \frac{1}{h_{\text{g}}} (-\phi_{\text{cov}} + \phi_{\text{lamp}}) && (\text{g m}^{-3} \text{ s}^{-1}) \\ \frac{dX_{h,1}}{dt} &= \frac{1}{A_1} (\phi_{\text{in},1}) && (\text{m}^3 \text{ s}^{-1}) \\ \frac{dX_{h,2}}{dt} &= \frac{1}{A_2} (\phi_{\text{in},2}) && (\text{m}^3 \text{ s}^{-1}) \\ \frac{dX_{h,3}}{dt} &= \frac{1}{A_3} (\phi_{\text{in},3}) && (\text{m}^3 \text{ s}^{-1}) \\ \frac{dX_{h,4}}{dt} &= \frac{1}{A_4} (\phi_{\text{in},4}) && (\text{m}^3 \text{ s}^{-1})\end{aligned}\quad (6-1)$$

The model is referred to during this section for formulating the predictor.

6-1-1 Greenhouse climate model dynamics

For predicting the future dynamics of the greenhouse climate a control oriented model is used to predict the future state variables and outputs. Let the augmented model in Equation (6-1) be represented as:

$$\frac{d\mathbf{X}}{dt} = \mathbf{f}(\mathbf{X}, \mathbf{U}, \mathbf{D}, t), \quad \mathbf{X}(t_0) = \mathbf{X}_0 \quad (6-2)$$

Here, the explicit system variables and constant dependencies are omitted. The discrete time version is obtained using Euler approximation:

$$x(k+1) = f(x(k), u(k), d(k)) \quad (6-3)$$

where k is the discrete sample and :

$$f(x(k), u(k), d(k)) = x(k) + h \cdot \mathbf{f}(\mathbf{X}(k), \mathbf{U}(k), \mathbf{D}(k)) \quad (6-4)$$

here, the continuous time dynamics are discretised with the sampling time h .

$$\begin{aligned} x(k) &= \left[X_{T_{\text{air}}}(k) \quad X_{T_{\text{soil}}}(k) \quad X_{T_{\text{tubes}}}(k) \quad X_{\chi_{\text{air}}}(k) \quad X_{h,\text{sw}}(k) \quad X_{h,\text{ww}}(k) \quad X_{h,\text{sr}}(k) \quad X_{h,\text{nr}}(k) \right]^T \\ u(k) &= \\ &= \left[U_{\text{lamp}}(k) \quad U_{\text{HE,GH}}(k) \quad U_{\text{HE,out}}(k) \quad U_{\text{HS,GH}}(k) \quad U_{\text{HS,out}}(k) \quad U_{\text{hb}}(k) \quad U_{\text{cb}}(k) \quad U_{\text{in},1}(k) \quad U_{\text{in},2}(k) \quad U_{\text{in},3}(k) \quad U_{\text{in},4}(k) \right]^T \\ d(k) &= \left[D_{T_{\text{out}}}(k) \quad D_{T_{\text{EC}}}(k) \quad D_{T_{\text{deep}}}(k) \quad D_{\chi_{\text{out}}}(k) \quad D_{\text{rad}}(k) \quad D_{T_{\text{cw}}}(k) \quad D_{T_{\text{hw}}}(k) \right]^T \end{aligned} \quad (6-5)$$

6-1-2 Predictions

The model in Equation (6-3) is used to predict the future behaviour of the greenhouse climate up till a defined horizon N_p . The predicted states and outputs at time step k are defined as:

$$\begin{aligned} \mathbf{x} &:= \left[x(k+1|k)^T \quad x(k+2|k)^T \quad \dots \quad x(k+j|k)^T \quad x(k+N_p-1|k)^T \quad x(k+N_p|k)^T \right]^T \\ \mathbf{y} &:= \left[y(k+1|k)^T \quad y(k+2|k)^T \quad \dots \quad y(k+j|k)^T \quad y(k+N_p-1|k)^T \quad y(k+N_p|k)^T \right]^T \end{aligned} \quad (6-6)$$

A similar formulation is used for predicting the exogenous inputs:

$$\mathbf{d} := \left[d(k|k)^T \quad d(k+1|k)^T \quad \dots \quad d(k+N_p-1|k)^T \right]^T \quad (6-7)$$

6-1-3 Predicting future control moves using MoveBlocking MPC

In general, the formulation of the future control inputs is done similarly as for the exogenous inputs and disturbances in Equation (6-7):

$$\mathbf{u} := \left[u(k|k)^T \quad u(k+1|k)^T \quad \dots \quad u(k+N_p-1|k)^T \right]^T \quad (6-8)$$

An essential element of MPC is that the calculation of the control input is carried out online in real-time as a function of the current state, reference and measured disturbances. However, the dimension of the inputs of the greenhouse model together with the prediction horizon associates to a high computational burden. This results in that the computation time exceeds the time between two sampling instants and (in case of a forced stop) sub-optimal or infeasible results.

Another factor is from a practical point of view; since the greenhouse climate is (comparatively) a slow process with large time constants, it is impractical that the climate should be maintained by frequent switching between the different modes of the equipment, as all control inputs are binary values. This makes the part of the degrees of freedom redundant. This also concerns the soap bubble generators, as stated in Section 4-2-1 that only one cavity compartment can be filled simultaneously and, once started, must finish the cavity without interruption. It is therefore essential that the future outputs consider this restrictive control of the soap bubble generators.

The above mentioned factors motivates to restrict the control inputs of the greenhouse climate control and decrease the degrees of freedom. For this the input is parameterized using a move blocking scheme [8]. Here, the control input determined by the optimisation is not allowed to vary freely at each sampling step of the prediction horizon but only in predefined patterns. Therefore, rather than solving for the optimal control input \mathbf{u} , the move blocking scheme parameterizes the inputs as:

$$\mathbf{u} = (T \otimes I_M) \hat{\mathbf{u}} \quad (6-9)$$

where $\hat{\mathbf{u}} := [\hat{u}_0^T \ \hat{u}_1^T \ \dots \ \hat{u}_{k+M-1}^T]^T \in \mathbb{R}^{n_{\hat{u}} \times M}$ is a vector with future blocked inputs with decreased degree of freedom with $n_{\hat{u}} < n_u$ and $M < N_p$. The blocking matrix $T \in \mathbb{R}^{N_p \times M}$ is assumed to be a matrix of ones and zeros only, with each row containing exactly one non zero element and I_M is a identity vector with M ones on the diagonal. An example of a input move blocking scheme and the corresponding blocking matrix is shown in Equation (6-10), where the input of a SISO system with $N_p = 4$ is blocked for the first, second and third predicted time step:

$$\mathbf{u} = \begin{bmatrix} u(k|k) \\ u(k+1|k) \\ u(k+2|k) \\ u(k+3|k) \end{bmatrix} = \underbrace{\begin{bmatrix} 1 & 0 \\ 1 & 0 \\ 1 & 0 \\ 0 & 1 \end{bmatrix}}_T \underbrace{\begin{bmatrix} \hat{u}_0 \\ \hat{u}_1 \end{bmatrix}}_{\hat{\mathbf{u}}} \quad (6-10)$$

Here, the degrees of freedom problem has thus been reduced from $N_p = 4$ to $M = 2$.

The parameterisation of the control inputs of the BBLS greenhouse is formulated for the climate control equipment and the soap bubble generators in a separate manner. Let u_{cc} represent a vector of the control inputs of the climate control equipment:

$$u_{cc}(k) = \left[U_{\text{lamp}}(k) \ U_{\text{HE,GH}}(k) \ U_{\text{HE,out}}(k) \ U_{\text{HS,GH}}(k) \ U_{\text{HS,out}}(k) \ U_{\text{hb}}(k) \ U_{\text{cb}}(k) \right]^T \quad (6-11)$$

For the future control inputs of the climate control equipment, denoted as \mathbf{u}_{cc} , it is assumed that they are not subject to operational restrictions. For the climate control, a constant

blocking matrix is defined where the future control inputs are equally blocked throughout the prediction horizon N_p :

$$\mathbf{u}_{cc} = (T_{cc} \otimes I_M) \hat{\mathbf{u}}_{cc} \quad (6-12)$$

where T_{cc} is the blocking matrix defined as:

$$T_{cc} = \begin{bmatrix} \mathbf{1}_{N_p/M} & \mathbf{0} & \dots & \mathbf{0} \\ \mathbf{0} & \mathbf{1}_{N_p/M} & \dots & \mathbf{0} \\ \vdots & \vdots & \ddots & \vdots \\ \mathbf{0}_{N_p/M} & \mathbf{0}_{N_p/M} & \mathbf{0}_{N_p/M} & \mathbf{1}_{N_p/M} \end{bmatrix} \quad (6-13)$$

where $T_{cc} \in \mathbb{R}^{N_p \times N_p/M}$ is the blocking matrix and $\mathbf{1}_{N_p/M}$ and $\mathbf{0}_{N_p/M}$ are vectors of length N_p/M with ones and zeros respectively, on the condition that N_p and M are integer values and the modulus of $(N_p \bmod M) = 0$.

The next step is to formulate a move-blocking scheme for the soap bubble generators. Let u_{bbbls} denote the vector of the soap bubble generator control inputs:

$$u_{bbbls}(k) = [U_{h,1}(k) \quad U_{h,2}(k) \quad U_{h,3}(k) \quad U_{h,4}(k)]^T \quad (6-14)$$

Let $N_{fill,i}$ denote the number of time instants needed to fully fill an empty cavity compartment i , computed as follows:

$$N_{fill,i} = \frac{t_{fill,i}}{h}, \quad N_{fill,i} \in \mathbb{Z} \quad (6-15)$$

On the condition that:

$$N_{fill,i} \leq N_p \quad (6-16)$$

$$t_{fill,i} \bmod h = 0 \quad (6-17)$$

Here, Equation (6-16) ensures that the prediction horizon captures the entire filling dynamics and Equation (6-17) guarantees no loss of information due to rounding. Based on Equations (6-15 - 6-17), a blocking matrix is formulated for each cavity. For cavities where $N_{fill,i} = N$, the blocking matrix is formulated as:

$$\begin{bmatrix} u_{bbbls}(k|k) \\ u_{bbbls}(k+1|k) \\ \vdots \\ u_{bbbls}(k+N_{fill,i}-1|k) \end{bmatrix} = \mathbf{1}_{N_{fill,i}} \hat{u}_0 \quad (6-18)$$

From Equation (6-18) it is noted that the degrees of freedom is reduced to $M = 1$. When the prediction horizon is longer than the time needed for filling the cavity, the blocking matrix is then defined as:

$$\begin{bmatrix} u_{bbbls}(k|k) \\ u_{bbbls}(k+1|k) \\ \vdots \\ u_{bbbls}(k+N_{fill,i}-1|k) \\ \vdots \\ u_{bbbls}(k+N_p-1|k) \end{bmatrix} = \begin{bmatrix} \mathbf{1}_{N_{fill,i}} & \mathbf{0} \\ \vdots & \vdots \\ \mathbf{0}_{N_p-N_{fill,i}} & \mathbf{1}_{N_p-N_{fill,i}} \end{bmatrix} \begin{bmatrix} \hat{u}_0 \\ \hat{u}_1 \end{bmatrix} \quad (6-19)$$

From Equation (6-19) it is noted that the degrees of freedom is reduced to $M = 2$. Both blocking matrices fix the input to be constant over the time needed to fill up the cavity and initially, when all cavities are empty, captures the entire filling dynamics and their corresponding thermal performance. However, the proposed formulation of the blocking matrices in Equation (6-18) and (6-19) pose a problem for real-time optimization. For example, at time instant k the optimization problem is solved and one of the soap bubble generators is set to 1. The optimization problem only considers the blocked inputs \hat{u} , which implies that the predicted future behaviour of the system is optimised by letting the particular cavity be completely filled. However a MPC strategy is used in a RHOC approach which implies that, although the inputs of the soap bubble generators are blocked up till $N_{\text{fill},i}$, only the first control signal is sent to the system. Then at the next time instant $k + 1$ the algorithm encounters the problem that the blocked inputs still consider an empty cavity while at the previous time instant the soap bubble generator is started to fill the cavity (initial value of the filling level of the cavity is nonzero). To encounter this problem the move blocking scheme must also take into account the control values of past signals and block the inputs accordingly. The move blocking matrices in Equation (6-18) and (6-19) are reformulated and made a function of the past inputs $\mathbf{u}_{\text{bbbls}}^- := [u_{\text{bbbls}}(k-1)^T \quad u_{\text{bbbls}}(k-2)^T \quad \dots \quad u_{\text{bbbls}}(-1)^T]^T$:

$$\begin{bmatrix} u_{\text{bbbls}}(k|k) \\ u_{\text{bbbls}}(k+1|k) \\ \vdots \\ u_{\text{bbbls}}(k+N_{\text{fill},i}-1|k) \end{bmatrix} = T_{\text{bbbls}}(\mathbf{u}_{\text{bbbls}}^-) \begin{bmatrix} \hat{u}_0 \\ \hat{u}_1 \end{bmatrix} \quad (6-20)$$

where T_{bbbls} is the move blocking matrix computed using the following algorithm.

Algorithm 2 Compute T_{bbbls}

Input: \mathbf{u}^- , N_p , $N_{\text{fill},i}$

Ensure: $N_{nz} = \text{nnz}(\mathbf{u}^-)$

$N_{nz} \leftarrow$ number of nonzero elements

$N_{nz} \leftarrow \text{nnz}(\mathbf{u}^-)$

if $N_{nz} = 0 \vee N_p = N_{\text{fill},i}$ **then**

$T_{\text{bbbls}} \leftarrow [\mathbf{1}_{N_p}]$

else if $N_{nz} = 0 \vee N \geq N_{\text{fill},i}$ **then**

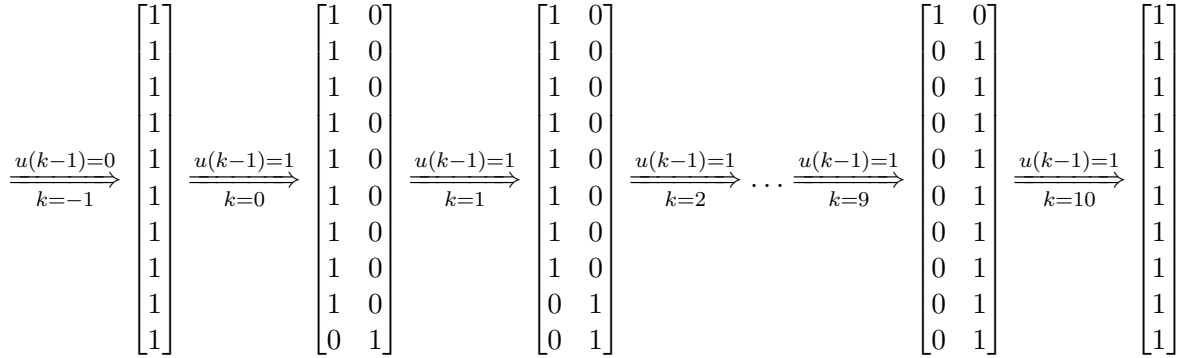
$T_{\text{bbbls}} \leftarrow \begin{bmatrix} \mathbf{1}_{N_{\text{fill},i}} & \mathbf{0}_{N_{\text{fill},i}} \\ \mathbf{0}_{N_p - N_{\text{fill},i}} & \mathbf{1}_{N - N_{\text{fill},i}} \end{bmatrix}$

else if $N_{nz} \geq 0$ **then**

$T_{\text{bbbls}} \leftarrow \begin{bmatrix} \mathbf{1}_{N_{\text{fill},i} - N_{nz}} & \mathbf{0}_{N_{\text{fill},i} - N_{nz}} \\ \mathbf{0}_{N_{nz}} & \mathbf{1}_{N_{nz}} \end{bmatrix}$

end if

Algorithm 1 implies that the number of blocked inputs (ones in the left column) recedes for each sequential time instant as the cavity is filling up. An example of the evolution of T_{bbbls} and its receding iterative process is schematically given in the following (with $N_p = N_{\text{fill},i} = 10$):



From the scheme above it is noted that the number of blocked inputs in each column vary as the cavity is filled. Although the number of blocked inputs corresponds to the real system behaviour, restrictions are still needed to be imposed for ensuring that the soap bubble generators stays on. These restrictions are explained in the next section.

6-2 Formulation of hard constraints for inputs

This section describes the formulation of the constraints. The formulation of constraints could be done in three ways: hard constraints, soft constraints and set-point approximation. Constraints for the control inputs are according to [28] implemented as hard constraints, which are formulated as inequality functions. The continuation of this section first explains the limitations and restrictions in descriptive manner which is then processed and translated as a hard constraint. Also, this section covers the constraints implemented for the actual inputs (not the blocked ones).

6-2-1 Binary control inputs

As mentioned earlier, the control inputs of the greenhouse climate control and soap bubble generators are either in one of the states: on, indexed by the integer value 1, or off, indexed by the integer value 0. Therefore, for all future inputs the following constraint is applied:

$$\mathbf{0}_{n_u} \leq u(k+j) \leq \mathbf{1}_{n_u}, \quad \forall k+j \quad (6-21)$$

6-2-2 HSHE-unit

The HSHE-unit lets air from the greenhouse or outside through the heat-exchanger and horse-shoe depending on the damper settings. Since both elements have two dampers, it is restricted that both dampers on each component are simultaneously open and closed. This translates to the following inequality constraints:

$$\begin{aligned}
U_{\text{HE,GH}}(k+j) + U_{\text{HE,out}}(k+j) &\leq 1, \quad \forall k+j \\
U_{\text{HS,GH}}(k+j) + U_{\text{HS,out}}(k+j) &\leq 1, \quad \forall k+j
\end{aligned} \quad (6-22)$$

The additional heating and cooling of the air is done by the heating and cooling batteries, respectively. From an operational standpoint it is impractical to heat and cool the air simultaneously and makes it redundant to consider this in the optimization problem. Therefore the following constraint forces to either use one of the elements:

$$U_{cb}(k+j) + U_{hb}(k+j) \leq 1, \forall k+j$$

6-2-3 No simultaneous filling of cavities

The current configuration makes it not possible for multiple soap bubble generators to be on simultaneously. The following inequality constraint is formulated:

$$U_{in,sw}(k+j) + U_{in,ww}(k+j) + U_{in,sr}(k+j) + U_{in,nr}(k+j) \leq 1 \quad (6-23)$$

6-2-4 Forced continuation of cavity filling

As mentioned earlier it is not only important to fix the control inputs of the soap bubble generator over the filling time span but also ensure that, once initiated, the soap bubble generator must stay on. For this, the blocked input corresponding to the left most column of T_{bbbls} must be constrained such that it stays on and the blocked input corresponding to the right most column must be constrained to stay off throughout the time to fill up the cavity. This is realized by the following algorithm:

Algorithm 3 Set inequality constraints

Input: \mathbf{u}^-

$nnz \leftarrow$ nonzero element

$N_{nz} \leftarrow nnz(\mathbf{u}^-)$

if $N_{nz} \neq 0$ **then**

$1 \leq \hat{u}_0 \leq 1$

$0 \leq \hat{u}_1 \leq 0$

else

$0 \leq \hat{u}_0 \leq 1$

$0 \leq \hat{u}_1 \leq 1$

end if

Here, **Algorithm 3** redefines the lower and upper bounds of the decision variable corresponding to the left-most column.

6-3 Objective function

The research reported in this paper on optimal greenhouse climate management for a predefined climate zone. The objective is to minimize to minimize the

In previous sections the future model dynamics and constraints have been described. This section describes the formulation of the objective function. The objective function must be designed such that the future outputs of the system are optimized towards a desired state which correspond to a minimal cost. In Section 2-2-1 a objective function is described for optimizing the states for tracking a reference set-point $r(k)$. However, an argument is made against this particular objective function for controlling the greenhouse climate as stated in [5]: It is very important to maintain a favorable climate condition while optimizing the utilization of climate control equipment. Maintaining a favorable climate does not explicitly refer to following a specific set-point, but rather maintaining the climate variables into a range of values that are considered to be optimal. This is related to the zone-control cost implementation. An important property of zone control is that the strictness of the bounds are considered "soft", which implies that the bounds are violable but at the expense of an increased cost.

The objective function for the BBLS greenhouse consists of two element: a cost associated function with maintaining a pre-defined air temperature and a cost associated function for the utilization of the various control equipment:

$$J(y(k), u(k)) = \phi_{T_{\text{air}}}(k) + \phi_h(k) + l(u(k)) \quad (6-24)$$

Penalty functions in the cost function are used as soft constraints for the predicted outputs and states. First, soft constraints for T_{air} and χ_{air} are implemented as penalty function, which incurs a penalty when a constraint violation is occurring:

$$\phi_{T_{\text{air}}}(k) = Q_1 \sum_{j=1}^{N_p} \max\{0, (T_{\text{air}}(k+j|k) - T_{\text{max}})\} + \max\{0, (T_{\text{min}} - T_{\text{air}}(k+j|k))\} \quad (6-25)$$

where ϕ is a penalty function associated with constraint violation of upper and lower bounds for each state and Q a weighting matrix. A similar formulation of penalty function is done for the cavity filling levels, which enables to not exceed the maximum filling level:

$$\phi_h(k) = Q_2 \sum_{i=1}^4 \sum_{j=1}^{N_p} \max\{0, (h_i(k+j|k) - h_{\text{max},i})\} + \max\{0, (h_{\text{min},i} - h_i(k+j|k))\} \quad (6-26)$$

The second element is designed for the control inputs. A quadratic function is defined as:

$$l(u(k)) = \sum_{j=0}^{N_p-1} u^T(k+j|k) R u(k+j|k) \quad (6-27)$$

where $R \in \mathbb{R}^{n_u}$ is a squared positive definite matrix with (only) non-zero values (weights) on the diagonal.

6-4 Mathematical formulation and implementation

Now that all elements are defined, the mathematical formulation of the optimization problem can be presented. At each time instant k , the following optimization problem is solved:

Algorithm 4 MPC - BBLS

Input: nonlinear system in Equation (6-3), $\mathbf{u}_{\text{bbbls}}^-, N_p, Q_1, Q_2, R, T_{\text{cc}}, T_{\text{max}}, T_{\text{min}}$

- 1: Compute $T_{\text{bbbls}}(\mathbf{u}_{\text{bbbls}}^-)$ using **Algorithm 2**
 - 2: Define new constraints set for u_{bbbls} using **Algorithm 3**
 - 3: Solve for $\hat{\mathbf{u}}_{\text{cc}}^*, \hat{\mathbf{u}}_{\text{bbbls}}^*$ which minimizes 6-28 subject to 6-29 - 6-36
 - 4: Apply first input of $\hat{\mathbf{u}}_{\text{cc}}^*, \hat{\mathbf{u}}_{\text{bbbls}}^*$ to system
 - 5: Append $\mathbf{u}_{\text{bbbls}}^-$ with $\hat{\mathbf{u}}_{\text{bbbls}}^*$
 - 6: set $k \leftarrow k + 1$
-

$$\min_{\hat{\mathbf{u}}_{cc}, \hat{\mathbf{u}}_{bbbls}} J(y(k), u(k)) \quad (6-28)$$

Subject to:

$$\begin{cases} x(k+1) = f(x(k), u(k), d(k)) \\ y(k) = g(x(k)) \end{cases} \quad (6-29)$$

$$\mathbf{0}_{n_u} \leq u(k+j) \leq \mathbf{1}_{n_u}, \quad \forall k+j \quad (6-30)$$

$$\mathbf{u}_{cc} = (T_{cc} \otimes I_M) \hat{\mathbf{u}}_{cc} \quad (6-31)$$

$$\mathbf{u}_{bbbls} = T_{bbbls}(\mathbf{u}_{bbbls}^-) \hat{\mathbf{u}}_{bbbls} \quad (6-32)$$

$$U_{HE,GH}(k+j) + U_{HE,out}(k+j) \leq 1, \quad \forall k+j \quad (6-33)$$

$$U_{HS,GH}(k+j) + U_{HS,out}(k+j) \leq 1, \quad \forall k+j \quad (6-34)$$

$$U_{hb}(k+j) + U_{cb}(k+j) \leq 1, \quad \forall k+j \quad (6-35)$$

$$U_{in,sw}(k+j) + U_{in,ww}(k+j) + U_{in,sr}(k+j) + U_{in,nr}(k+j) \leq 1, \quad \forall k+j \quad (6-36)$$

Implementation, Results and Analysis

This chapter contains the implementation and testing of the MPC algorithm for real problem instances. In order to obtain a valid assessment of the performance of the controller, separate runs will be executed on earlier logged data. The implementation of the MPC algorithm is done for two cases. Since there are also different parameters to be defined, multiple runs for each climate log is performed.

7-1 Simulation study 1

The MPC algorithm will be implemented in an open loop manner using the discrete time system for controlling the greenhouse climate on 31-01-2020. The climate data used on that day is from 15:38 - 21:06, as in this particular time span the climate is controlled using the equipment which are formulated in the model. This day resembles a typical usage of the soap bubble generator; it is desired to maintain a high temperature as the solar radiation decreases.

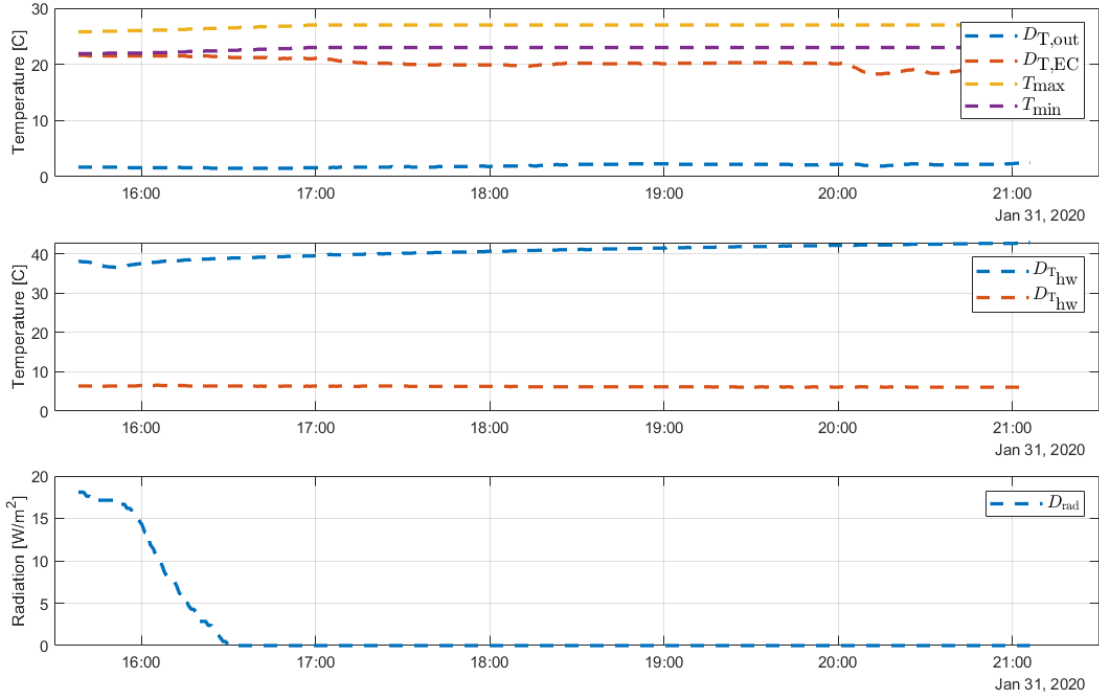


Figure 7-1: Measured climate data used for simulation

7-1-1 Implementation

In order to analyse the MPC algorithm performance several runs were performed. Each simulation run is different in terms of the parameters and settings. Table 7-1 shows the specifications for each simulation run.

Parameter	Run 1	Run 2	Run 3	Run 4
h	180	180	300	300
N_p	20	20	12	12
M	{2,2,2,2,2,2,2,1,2,2,2}	{2,2,2,2,2,2,2,1,2,2,2}	{2,2,2,2,2,2,2,1,2,2,2}	{2,2,2,2,2,2,2,1,2,2,2}
Q_1	10^5	10^5	10^5	10^5
Q_2	10^5	10^5	10^5	10^5
R	Equation (7-2)	Equation (7-2)	Equation (7-2)	Equation (7-2)
Previous solutions as initial	no	yes	no	yes

Table 7-1: Control settings for each run.

Run 1 and **Run 2** are simulated with a sampling time of three minutes. The corresponding prediction horizon is set to be $N_p = 20$. Equivalently, the prediction horizon for **Run 3** and **Run 4** are obtained in the same manner, where a sampling time of five minutes correspond to $N_p = 12$. M is an array of integer values, where each integer represents the number of decision variables (blocked inputs) for each control variable in the following order:

$$M := \{M_{U_{\text{lamp}}}, M_{U_{\text{HE,GH}}}, M_{U_{\text{HE,out}}}, M_{U_{\text{HS,GH}}}, M_{U_{\text{HS,out}}}, M_{U_{\text{hb}}}, M_{U_{\text{cb}}}, M_{U_{\text{in},1}}, M_{U_{\text{in},2}}, M_{U_{\text{in},3}}, M_{U_{\text{in},4}}\} \quad (7-1)$$

The weights of the states Q_1 and Q_2 are set relatively higher than the weights in R to enforce that the MPC algorithm to stay within the bounds. The inputs weight matrix defined as the following diagonal matrix:

$$R = \text{diag}(2000, 25, 25, 25, 25, 2000, 2000, 100, 100, 100, 100) \quad (7-2)$$

Within the R matrix, the values for the heating and cooling equipment associate with a certain scarcity. The weights for the soap bubble generators are relatively lower than for the heating and cooling equipment to enforce the MPC algorithm to insulate the greenhouse rather than use heating sources. The final setting is the use of the previous solution as an initial solution for the optimization problem in Equation 6-28, which is considered as a MINP problem. If not, a vector with only zeros is used as initial solution.

7-1-2 Results and Analysis

Each model run was simulated once. The results of the simulation for the states are shown in Figure 7-2 and their corresponding control action is shown in Figure 7-3. Analyzing Figure 7-2 (a-b), it is found that simulations maintained the greenhouse air temperature within the maximum and minimum bounds without violation. A notable difference is between the simulations with and without the use of an initial point; the greenhouse air temperature for the simulations with the use of an initial point appears to be smoother than the simulations runs without. The tube air temperature in 7-2 (c-d) yields the same finding. In 7-2 (e-f), the cavity fillings of the compartment is shown. In general, the simulations attempted insulating the greenhouse for minimizing the heat loss. However, the simulation runs with the use of an initial point have only filled three out of the four compartments, whilst the other runs filled all compartments. Another finding is the point of filling the south roof compartment. The transmission coefficient of the augmented model is assumed to be only a function of $X_{h,3}$, which is the south roof bubble generator. The solar radiation was until 16:30. Run 1 and Run 3 filled the south roof compartment after 16:30, when the solar radiation decreased to zero. The simulation runs predicted the potential heat gain and decided not to decrease the transmission by filling the south roof compartment. This in contrast to the other simulation, where in Run 2 the south roof compartment was not filled and in Run 4 the south roof compartment was filled during the presence of solar radiation.

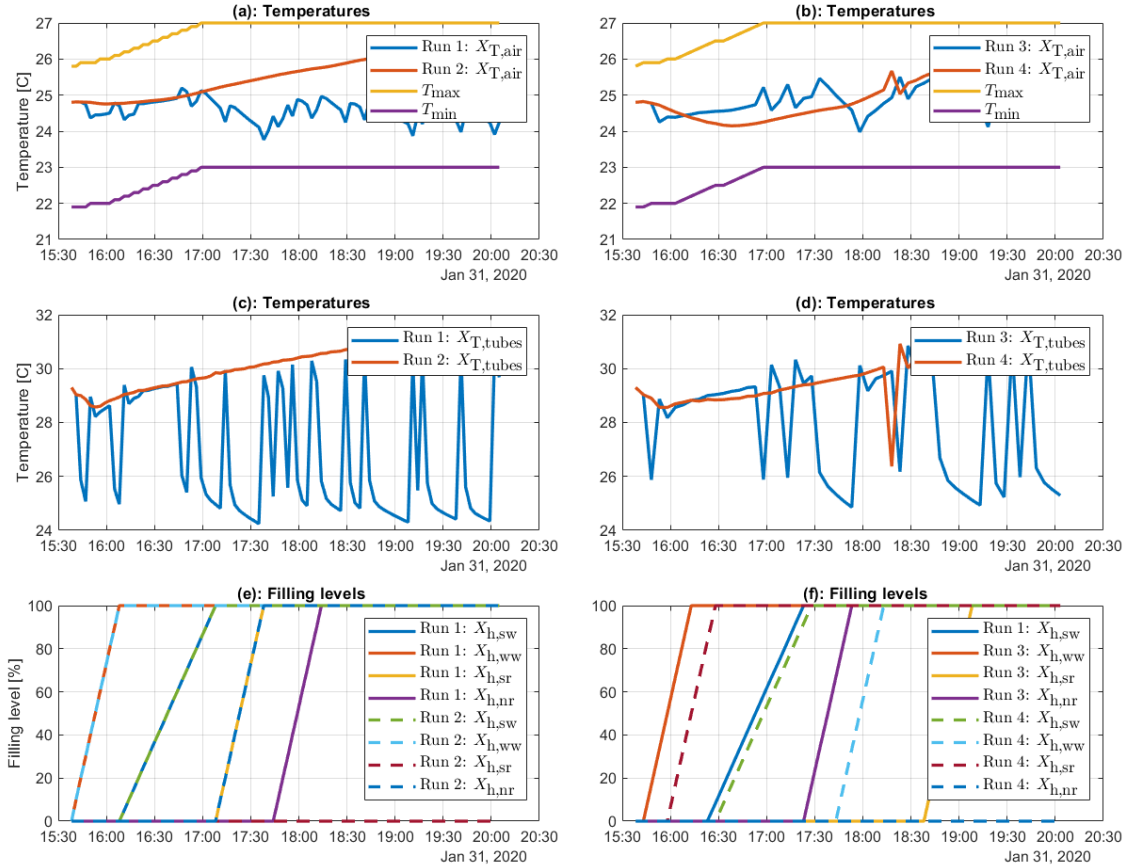


Figure 7-2: Simulation results of the greenhouse air temperature (a-b), tube air temperature (c-d) and the filling levels (e-f).

The control action for all simulations are analyzed using Figure 7-3. A general finding is that only the heating equipment was used throughout the simulation. Furthermore, the dampers for the outside air of the HSHE-unit were closed. This control action seems sensible as there is no need for mixing the warmer inside air with the colder outside air for maintaining a higher inside air temperature. A notable difference is the control action for the heating equipment. In (a-b) and (g-h), the control of the lamps and heating batteries for Run 1 and Run 3 involved more on-off switching, compared to Run 2 and Run 4. The utilization of the heating equipment correspond to the inside air and tube air temperatures in Figure 7-2; the on-off switching of the heating equipment induces a fluctuation in the temperatures. A possible explanation lies in the use an initial point. For Run 1 and Run 3, no initial point was defined. The solver then uses a default vector of zeros. Because this vector lies outside the feasible solution space, the optimization problem searches a new solution. For Run 2 and Run 4, the optimal control sequence of the previous time-step is used as an initial point. This poses the possibility that the optimal solution of the previous time step is also an optimal solution for the next, as the dynamics of the greenhouse and the outside environment is static; the temperature zone for which the air temperature must stay within is constant as the outside environment conditions, such as temperature of the outside air and EC and solar radiation, is static with little fluctuation enough for the optimization problem to come up with a different

solution. The control action of the soap bubble generators in (i-j) meets the requirements earlier described: only one soap bubble generator can be on at each time instant, and once initiated the cavity must be filled without impediment.

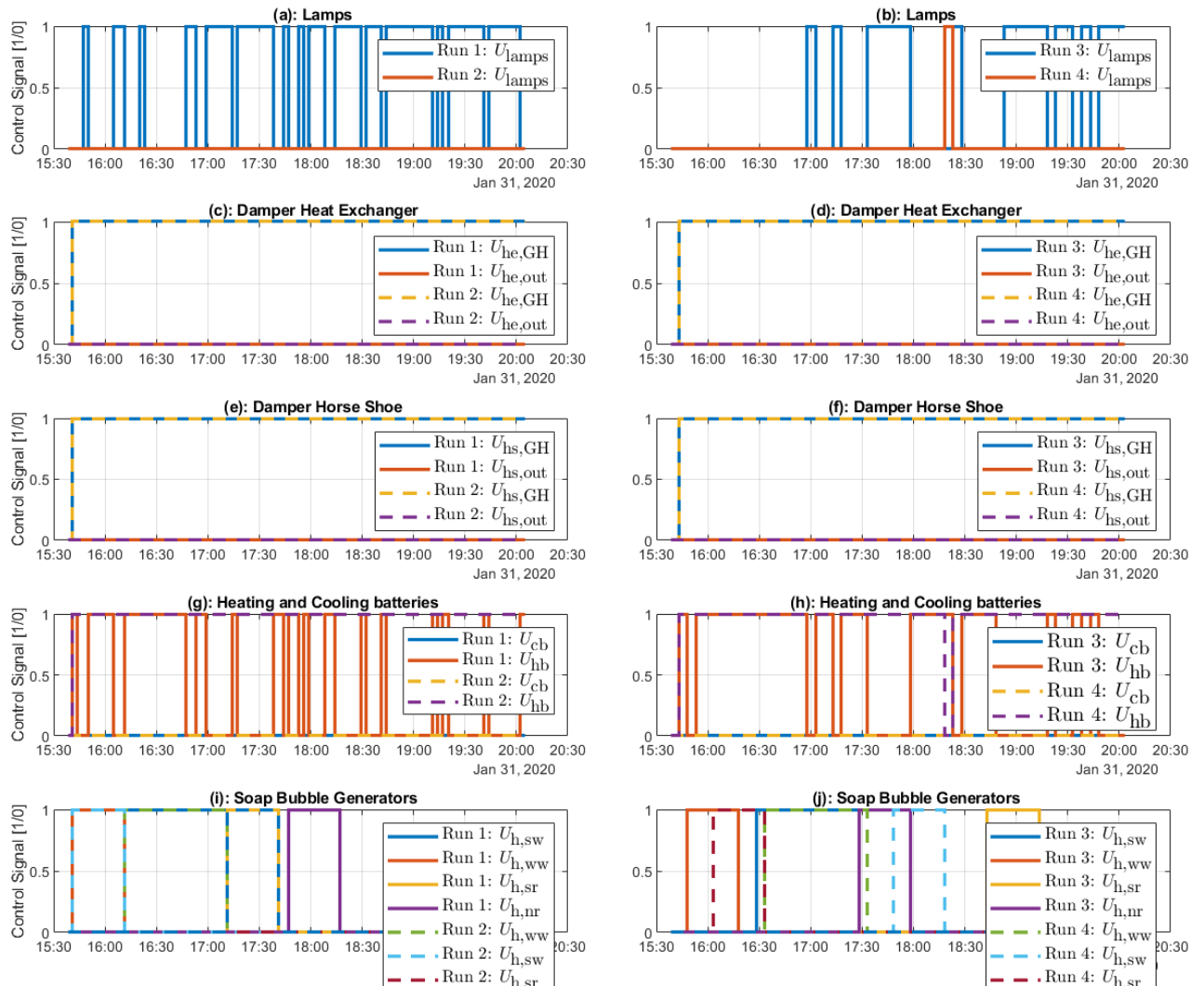


Figure 7-3: Simulation results of the climate control utilization of the lamps (a-b), damper settings HSHE-unit (c-f) heating and cooling batteries (g-h) and soap bubble generators (i-j).

7-1-3 Performance

The numerical results of the climate control utilization and performance for all simulations is shown in Table 7-2. As presented in the table, the performance of each simulation is with respect to the total hours of utilization (on), the corresponding wattage and the number of initialization (switching from off to on). The power usage of the lamps is 85 kW h^1 and the heating battery 18 kW h^1 . Note that the energy consumption of the fans inside the HSHE-unit is not within the scope of the analysis, as it is assumed that the fans are always on. From the table, a general finding is that the total hours of the climate control equipment

of the simulations are not far from each other. An important finding is the distribution of the climate control; for the simulation without the use of an initial point the control action switches between different equipment. Another finding concerns the energy consumption. Analyzing the energy consumption it is found that the energy consumption of Run 1 and Run 3 is much higher compared to Run 2 and Run 4. The use of the lamps have a major contribution in the total energy consumption, and Run 1 and Run 2 have used it for a considerable amount of time. It is also found that the switching for the simulations with a smaller sampling time is more frequent than for the simulations with larger sampling time. However, only Run 4 was able to compute all solutions within the sampling time.

Parameter	Run 1			Run 2			Run 3			Run 4		
	Lamps	H. bat	Total	Lamps	H. bat	Total	Lamps	H. bat	Total	Lamps	H. bat	Total
Hours of use	2.7 hrs.	1.75 hrs.	4.45 hrs.	0	4.45 hrs.	4.45 hrs.	1.667 hrs.	2.583 hrs.	4.25 hrs.	0.0833 hrs.	4.333 hrs.	4.4167 hrs.
Power	229.5 kW	31.5 kW	261 kW	0	80.1 kW	80.1 kW	141.7 kW	46.45 kW	188.15 kW	7.06 kW	80 kW	87.6 kW
Switches	15	1	16	15	15	30	8	9	17	1	2	3

Table 7-2: Numerical results of the climate control performance for the simulations.

Another performance indicator is the time for each model run. The focus for this thesis is the CPU time, which is the amount of time for which a central processing unit (CPU) was used for processing instructions. In this case, the amount of time for initiating **Algorithm 3** at each time step. The CPU time is a crucial aspect for RHOC problems as there must be ample time between consecutive sampling times for using an on-line control strategy. As shown in the Table it is found that the model runs with the use of previous optimal solutions have a higher percentage of CPU time less than the sampling time.

Description	Run 1	Run 2	Run 3	Run 4
Sampling time	180 s	180 s	300 s	300 s
# Computations	89	89	53	53
% Computations with CPU time < h	95.5056%	98.8764%	92.4528 %	100%

Table 7-3: Numerical results of CPU performance

7-2 Simulation study 2

The previous simulation study simulated the greenhouse climate control for steady outside environment conditions and bounds. This study is aims to control the climate using the data in Figure 7-4. The climate data represents a cold day from 21-02-2020 - 22-02-2020. At first, the inside air temperature must be controlled similar to the previous study. At 18:00, the bounds make an instantaneous drop for which the temperature must be controlled to. Then at 01:00 the temperature bounds are slowly increased again.

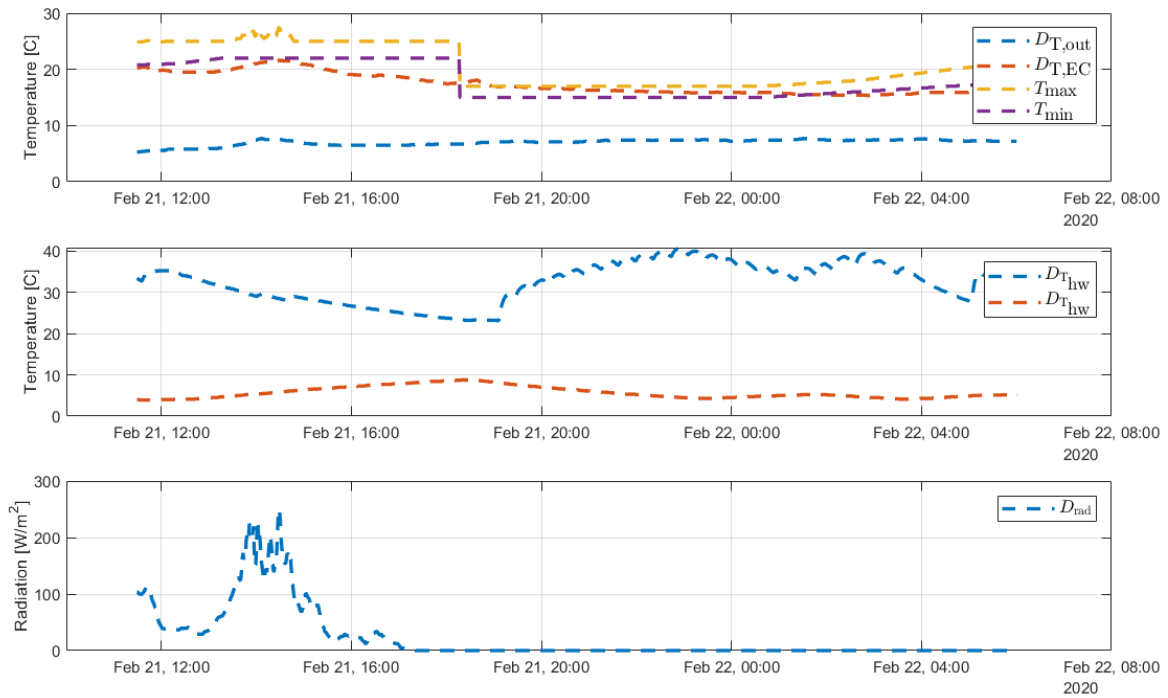


Figure 7-4: Measured climate data used for simulation

7-2-1 Implementation

In this study it is important that the MPC algorithm must be able to do real-time changes, as the temperature bounds vary significantly throughout the simulation. Previous section showed that the simulation run with sampling time of 300 s and the use of an initial point yield the best CPU time performance. These settings are the baseline for all simulation runs. Table 7-4 shows the specification for each run.

Parameters	Run 1	Run 2	Run 3	Run 4
h	300	300	300	300
N_p	12	12	12	12
M	2,2,2,2,2,2,2,1,2,2,2	4,2,2,2,2,4,4,1,2,2,2	2,2,2,2,2,2,2,1,2,2,2	4,2,2,2,2,4,4,1,2,2,2
Q_1	10^5	10^5	10^5	10^5
Q_2	10^5	10^5	10^5	10^5
R	Equation 7-2	Equation 7-2	Equation 7-3	Equation 7-3
Previous solutions as initial	yes	yes	yes	yes

Table 7-4: Control settings for each run

Run 1 is similar to Run 4 in previous simulation study. For Run 2, the number of decision variables for the heating and cooling equipment is increased from 2 to 4, to determine if the increase of decision variables yields better performance. Run 3 and Run 4 are similar to Run 1 and Run 2 respectively, with the difference that the penalty of the soap bubble generators

is increased such that the climate control is done without it:

$$R = \text{diag} \left(2000, 25, 25, 25, 25, 2000, 2000, 10^6, 10^6, 10^6, 10^6 \right) \quad (7-3)$$

7-2-2 Results and Analysis

Each model run was simulated once. The results of the simulation for the states are shown in Figure 7-5 and their corresponding control action is shown in Figure 7-6. The analysis is discussed for certain time-intervals where the temperature bounds change.

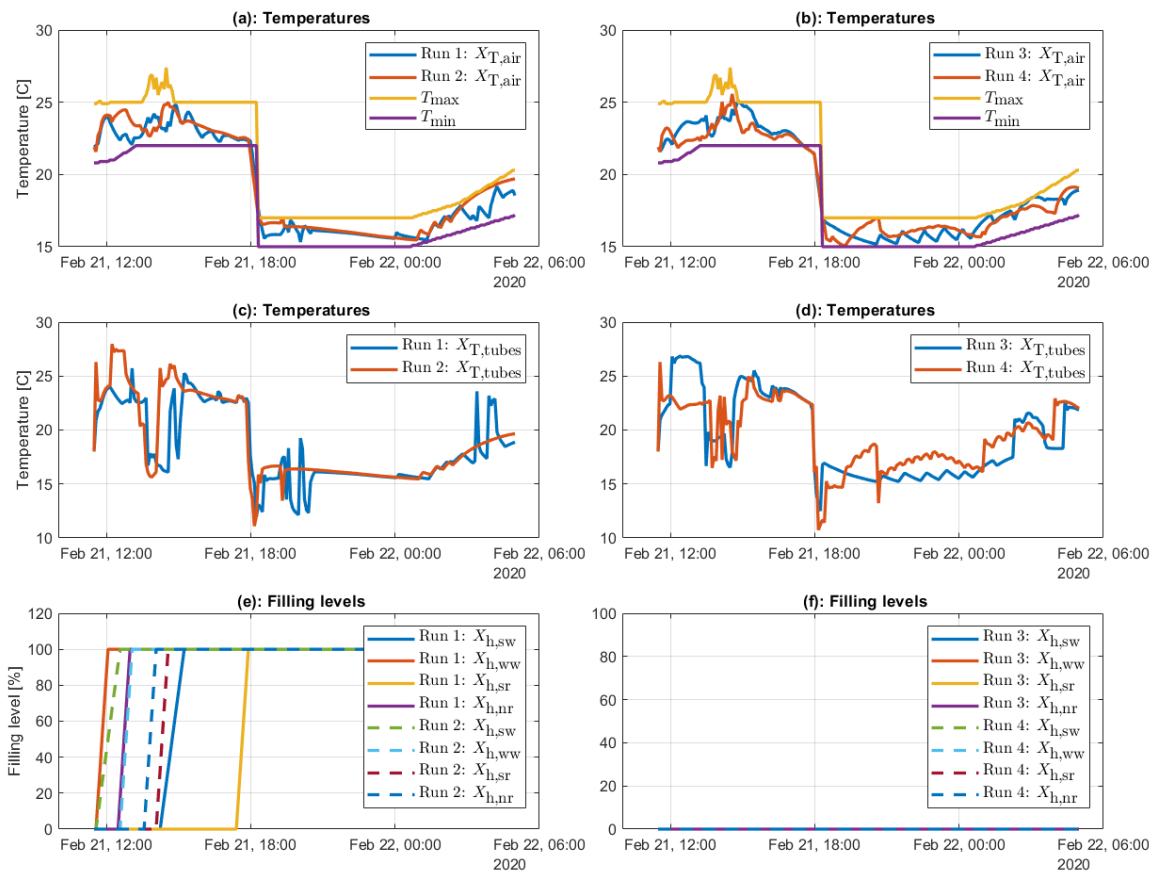


Figure 7-5: Simulation results of the greenhouse air temperature (a-b), tube air temperature (c-d) and the filling levels (e-f).

11:30 - 17:45

Throughout this time interval the dynamics of the greenhouse resembles with the previous simulation shown in 7-5; for the greenhouse air temperature (a-b), it is maintained within the bounds. Even though the maximum temperature bound varied for a moment, the inside air temperature maintained a steady temperature. The second point is the use of the soap bubble cavity (e-f). It is noted that all soap cavities are being filled throughout this time period. This in response to the low outside air temperature to prevent the heat loss through

the cover as the inside air must maintain a higher temperature. The order of the cavity filling is influenced by the outside solar radiation. The algorithm optimizes over minimizing the heat loss while receiving potential heat gain from the solar radiance by filling the south roof cavity as last. Run 1 decided to fill the south roof cavity after sunset, while Run 2 initiated the south roof cavity filling during the moment of high solar radiation. Run 3 and Run 4 did not filled the cavity compartments.

17:45 - 20:30

Throughout this time interval the greenhouse climate is subjected to the following tasks: a steep drop-off of the temperature and then maintaining it at a lower range of values. The drop-off is initiated at 18:15. However it is found that the temperature drops before this moment. As shown in the Figure 7-5 (a-b), the MPC algorithm allows the temperature to already drop below the lower bound before the bounds changes. The reason is that the prediction model and the cost function takes the future minimum and maximum bounds on the temperature into consideration. The penalty functions now consider the new minimum and maximum temperature values for which it should be minimized. The steep drop off resembles a reference trajectory for which the greenhouse climate is not able to track properly and violation of the bounds is inevitable. Since the decrease is of short notice it can be argued for letting the inside air temperature drop before the change in bounds yields the least amount of violation. Comparing Run 1 with Run 2, from (a) it is arguable if the extra dimension in the decision variables yielded any improvement in minimizing the bond violation. The control action during this interval is shown in Figure 7-5. In (c-e), all simulations opened the dampers of the outside air dampers for cooling the inside air and remained open throughout this interval. Throughout this period additional cooling is supplied by the cooling batteries. However, it is also found that the lamps and heating batteries were occasionally used.

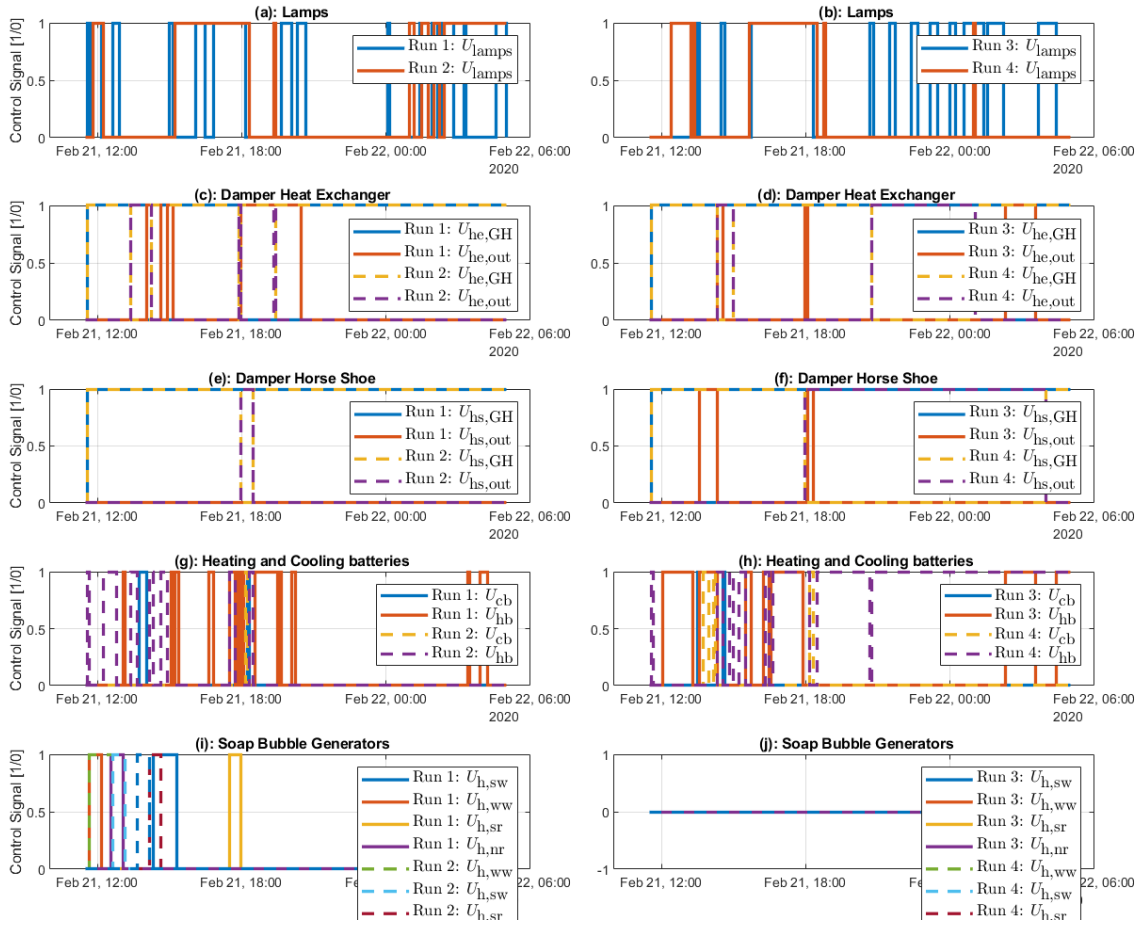


Figure 7-6: Simulation results of the climate control utilization of the lamps (a-b), damper settings HSHU-unit (c-f) heating and cooling batteries (g-h) and soap bubble generators (i-j).

20:30 - 01:00

Throughout this time interval the temperature is still be maintained around 15 – 17 °C. During this interval the control utilization of Run 1 and Run 2 was comparatively lower than for Run 3 and Run 4. Even with the low involvement of the climate control equipment, the temperature was maintained within the bounds. This can be explained by analysing the cavity fillings and the tube temperature. First the cavities of Run 1 and Run 2 were filled prior to this time interval. This implies that the heat loss through the cover is minimized. Another factor is the temperature of the tube air. The temperature is higher than the inside air temperature throughout this period. The dampers for the greenhouse air were open throughout this period. This internal circulation of the warmer tube air was sufficient for maintaining the inside greenhouse air within the bounds. For Run 3 and Run, additional heat was required for maintaining the temperature within the bounds.

00:45 - 05:00

Throughout this time interval the greenhouse should heat up gradually. The minimum and maximum temperatures gradually increases for which the greenhouse air must be controlled to stay within these increasing bounds. Both model runs did that without violation of the bounds. The increase of the temperature was through the use of both the heating battery and lamps. All simulation were able to control the greenhouse temperature in response to the increasing temperature bounds.

7-2-3 Performance

The climate control utilization for each model run shown in Table 7-5, excluding the dampers. It is found that the total hours of climate control utilization for Run 1 and Run 2 (average of 8.38 hrs.) is 44% lower than the climate control utilization of Run 3 and Run 4 (average of 14.8 hrs.). Furthermore the total climate control utilization of Run 2 (7.7 hrs.) is 15% less than Run 1 (9.1 hrs.). This implies that the simulation with more degrees of freedom yields less climate control utilization. However, this comes at a cost of more frequent switching. Analyzing the energy consumption it is found that the average total energy consumption of the climate control utilization for simulation with the use of soap bubble generators (552.2 kW) is 10% less than the simulations without the use of the soap bubble generators (609 kW). This implies that the energy consumption with the use of soap bubble generators is less than without.

Parameter	Run 1			Run 2			Run 3			Run 4		
	Lamps	H. bat	C. bat	Lamps	H. bat	C. bat	Lamps	H. bat	C. bat	Lamps	H. bat	C. bat
Hours of use	6.92 hrs.	1.75 hrs.	0.42 hrs.	5.08 hrs.	2.5 hrs.	0.08 hrs.	6.33 hrs.	5.75 hrs.	0.17 hrs.	3.92 hrs.	12.92 hrs.	0.5 hrs.
Power	588.2 kW	31.5 kW	7.56 kW	431 kW	45 kW	1.44 kW	538 kW	103.5 kW	3.1 kW	333.2 kW	232.6 kW	9 kW
Switches	7	7	2	15	12	1	11	7	2	5	8	3

Table 7-5: Numerical results of the climate control performance for the simulations.

More insight is provided if the performance in response to the changing dynamics is analysed. Table 7-6 presents the total hours and energy consumption for each of the above mentioned time intervals. For the first time interval, it is found that the average total hours of the climate control utilization for the simulation with soap bubbles (4.0 hrs) is 33% less than the simulations without soap bubbles (5.9 hrs.). The explanation can be found in Figure 7-5 (e-f). The soap bubble cavities for Run 1 and Run 2 were filled in this interval, hence decreasing the heat loss through the cover and eventually less involvement of the heating equipment. For the next time interval, it is found that during the drop-off the heating equipment was more involved than the cooling battery for all simulations. This may struck as an odd finding, and the reasoning behind it is found in Figure 7-6. For all simulations, one damper of the HSHE-unit for the outside air was opened, thus letting cold outside air flow through the greenhouse. The heat exchange with the outside air causes a steep drop in the tube air temperature and decreases the greenhouse air temperature. With the aid of the heating equipment, the greenhouse temperature decreases with a rate which kept the violation of the bounds minimal. For the next time interval, it is found that the average total hours of climate control utilization for Run 1 and Run 2 (0.13 hrs.) is 96% lower than the average climate control utilization for Run 3 and Run 4 (3.13 hrs.). This is due to two factors: the fully filled soap bubble cavities

and the tube air temperature. The tube air temperature was higher than the greenhouse air temperature. From 7-6 (c-d), the dampers of the HSHE-unit were opened for the greenhouse air. This implies that re-circulation of the greenhouse air through the HSHE-unit produced sufficient heat for the heating equipment not to get involved, as the heat loss through the cover is minimized. For the last time-interval, no significant difference is found.

Time interval	Parameter	Run 1			Run 2			Run 3			Run 4		
		Lamps	H. Bat	C. Bat									
11:30 - 17:45	[hrs.]	3	1.58	0	2.33	0.75	0.33	2.33	3.75	0.17	3.08	2.08	0.33
	[kW]	255	28.4	0	198.1	13.5	5.94	198.1	67.5	3.1	261.8	37.4	5.94
17:45 - 20:30	[hrs.]	0.58	0.17	0.08	1	1.33	0.08	0.5	0.08	0	0.75	2.42	0.17
	[kW]	49.3	3.1	1.44	85	23.9	1.44	42.5	1.44	0	63.8	43.6	3.1
20:30 - 01:00	[hrs.]	0.08	0	0	0.17	0	0	1.75	0	0	0.08	4.42	0
	[kW]	6.8	0	0	14.5	0	0	148.8	0	0	6.8	79.6	0
01:00 - 05:00	[hrs.]	3.25	0	0	1.58	0.42	0	1.75	1.92	0	0	4	0
	[kW]	276.3	0	0	134.3	7.6	0	148.8	34.56	0	0	340	0

Table 7-6: Numerical results of the climate control performance for the simulations per time interval.

Another performance indicator concerns the real-time optimization. Table 7-7 shows the percentage of computations that were within the sampling time. Only the simulation runs with the use of soap bubble generators are analysed. From the table it is found that the simulation with more degrees of freedom is not always able to compute within each sampling instance.

Description	Run 1	Run 2
Sampling time	300 s	300 s
# Computations	210	210
% Computations with CPU time < h	100%	97.1%

Table 7-7: Numerical results of CPU performance

Conclusion, discussion and recommendations

In this final chapter a condensed review of the work reported under the present thesis is provided. Apart from conclusions and discussing the interpretation of the results, recommendations for continued research are also formulated.

8-1 Conclusion

The primary objective of this thesis was to design and implement a model predictive control strategy for controlling the inside micro-climate of the bubble insulated greenhouse of BBBL Solutions. Sub-objectives were formulated which then were translated in research questions which answered upon would give answer to the main research question and realizing the primary objective.

Main Research Question

How can a model based predictive control strategy contribute in greenhouse climate control such that a specific condition of greenhouse climate of the BBBL greenhouse is governed by the optimized use of the climate control equipment and the bubble cavity envelope?

First the research questions are stated again, for which the answer is given below.

1. *What type of mechanistic model, based on heat- and mass balance equations, allows a representative description of the greenhouse climate of the BBBL greenhouse such that the inside climate is modelled accurately?*

The greenhouse climate results from a combination of physical processes and their interaction. This leads to the identification of the separate processes and thereupon to

their integration into a dynamic model. The identified processes in the BBLS greenhouse are formulated as heat- and mass transfer phenomena as shown in Table 4-1. The greenhouse cover, soil, heating lamps and air treatment system were considered the main elements influencing the greenhouse climate. The greenhouse climate is described by a four-state differential equation for the greenhouse air temperature, greenhouse soil temperature, temperature of the air from the perforated tubes and the greenhouse air humidity. From the calibration and validation process the VAF and RMSE values indicate that the model provides an accurate representation of the physical properties the interrelation between the various greenhouse climate quantities.

2. *How can the thermal properties of the bubble cavity envelope explained in [15] be integrated in the greenhouse climate, such that it is can be implemented in the modelling and control framework?*

The soap bubble cavity was compartmentalized into various cavity areas, enclosing the cultivation area and education centre. Only the cavity compartments which enclosing the cultivation area were considered. The dynamics of the filling of each cavity compartment was described by a first order model, where it is assumed that the filling of the cavity with the porous medium behaved as a liquid. As the level of filling was not measured, the greenhouse climate model is then augmented with four auxiliary states, which represent the filling level of the south-wall facing, west-wall facing and roof cavities.

For the thermal performance, the heat loss through the cover and the transmission of the cover for solar radiation were considered as the main heat transfer influenced by the soap bubbles inside the cavities. First the heat transfer of the cover is viewed as a network of (temperature) nodes and an interconnection of (thermal) resistors. Based on network theory, the convective heat transfer coefficient formulated as a connection of the thermal resistors. Within each resistor, based on the framework in [11], the thermal resistance is divided in a static (constant) component and a dynamic (varying) component. The dynamic component of each thermal resistance was assumed to be linear with the filling level of that particular cavity. The effect on the transmission of the cover for solar radiation was assumed to be only affected by the south-facing roof of the cavity, for which a linear function of filling level is formulated.

The greenhouse climate model is then augmented by adding the filling levels of the cavities as auxiliary states which can not be measured, the heat transfer coefficient is then substituted for the thermal resistance above and the transmission coefficient is now a function of the filling level of the south-facing roof. The model is then validated with only calibrating the newly introduced parameters and based on the VAF and RMSE has shown a representative description.

3. *How can a MPC algorithm be set up for controlling the greenhouse climate of the BBLS greenhouse?*

For implementing a MPC controller the predictor and optimizer must be developed first.

The predictor is a essentially a model used for predicting the greenhouse climate variables up till a defined horizon. A discretised version of the augmented model described above is used with sampling time h . By setting the prediction horizon equal to the number of time instances needed to fill the (slowest filling) cavities, the predictor is then

able to capture the dynamics of the soap bubble cavities where the future behaviour is then based on the entire filling dynamics.

The future control inputs for the climate control equipment and soap bubble generators are also predicted up till N_p , which comes at the cost of computational effort and complexity. By applying a MoveBlocking MPC strategy, which essentially decreases the degrees of freedom and the decision variables the MPC algorithm optimizes for, as the control inputs over the horizon are not allowed to vary. The use of move-blocking MPC benefits both control inputs. The control inputs of the climate control equipment are blocked to reduce the overall computational effort by a constant blocking matrix. For the soap bubble generators, the number of blocked inputs are equal to the number of time instances needed to fill the corresponding cavity. This enforces the MPC algorithm to consider only two states, either an empty cavity or a full cavity throughout over the prediction horizon, as it is required to fill the cavity without interruption. For this a blocking matrix as function of the past inputs is designed to change the structure of the blocked inputs as the cavity is filled up.

The control signals are formulated as binary signals and the limitations of the control inputs are formulated as hard constraints. Furthermore hard constraints are formulated for the soap bubble generators to for two reasons: The control inputs of the soap bubble generators is constrained such that only one at each time step is allowed to be initiated. Second a constraint is introduced such that the control signal of the soap bubble generator which was initiated in the previous step is constrained such that it remains initiated until the cavity is filled completely.

The cost function is designed for an optimized use of the climate control equipment and soap bubble generators while maintaining a favorable climate within the greenhouse. The cost function consists of three elements. The first element associates to maintaining the temperature within a predefined zone. This is implemented using penalty functions, where a penalty incurs if the inside air temperature violates the minimum or maximum temperature bounds. The second element is associated with the filling level of the cavities, where a penalty incurs if the filling level exceeds the maximum level. The third element associates the utilization of the control inputs, which is a squared sum.

The optimization problem within the optimizer of the MPC algorithm is classified as a mixed integer nonlinear programming (MINP) problem. From the first simulation study, it is concluded that the MPC algorithm is able to control the greenhouse using the climate control equipment and soap bubble generators and an on-line control method is applicable if the sampling time is 300 s and an initial solution is used. From the second simulation study it is concluded that greenhouse climate with full soap bubble cavities is controlled with 44% less use of the heating- and cooling equipment than without soap bubble cavities. It is also concluded that the overall energy consumption is 10% lower when the cavities are filled. Finally, the second simulation study also concluded the possibility for on-line control using the same setting as in the previous simulation.

8-2 Discussion and recommendations

In spite of concluding the work in this thesis, the interpretation and relevance is still something to be discussed. This section evaluates the findings and provides recommendation for better

understanding.

8-2-1 Greenhouse climate model Limitations

The greenhouse climate model of the BBLS greenhouse was a first attempt of mechanistically describing the greenhouse climate. However, the model only considers an empty greenhouse, without cultivation and crop-physiological processes. From several publications it is found that the crop related processes such as transpiration and evapo-transpiration affect the overall energy- and mass balance of the greenhouse. The air-treatment system was only considered to be affecting the energy-balance of the greenhouse. However, another function of the air-treatment system is humidity control. The humidity of the air flowing out of the tubes is a function of the damper settings and condensation within the units. The cooling battery is also used for de-humidification. Furthermore, the opening of the windows are not considered in the model. The windows are used for temperature and humidity control.

Based on the above mentioned limitations it is recommended to augment the greenhouse climate model with the missing mass- and energy transfers. The formulation of these missing processes are possibly available in recent publications, but a recommendation is to do future research in obtaining the formulation from greenhouse climate models which were developed for control and optimization purposes, as these make a suitable trade-off between accuracy and computational effort for real-time optimization. When certain processes are identified, it is recommended to apply the same methodology of conducting experiments which target and possibly isolate subsystems for better estimation properties.

8-2-2 Soap bubble filling dynamics and thermal properties

This research proposed an initial abstraction to develop a framework for the soap bubble cavity and thermal varying properties in a control-oriented setting. However simplification and assumptions limit the application of the framework for certain situations. The solar radiation was considered to be the most prominent factor of soap breakdown. However, within this framework the cavity fillings were not subjected to solar radiation. This is due to the fact that the dynamics of the cavity filling are modeled as a first-order model where the soap bubble medium was assumed to have similar behaviour as a fluid. This breakdown of soap would analogically correspond to outflow of the fluid. However it is not possible to measure any out-flowing processes, as the only known quantity of the soap cavity is the (fixed) amount of time to fill the cavity. Furthermore, the removal of soap bubbles is not considered. From a practical point of view the removal of soap bubbles occur for instance when the soap bubbles are become translucent and dry or when climate priorities and settings change.

The conductive and insulated states of the greenhouse is determined by estimating the heat transfer coefficient of the cover when the cavities were empty and filled, respectively. Based on this it is assumed that the static and dynamic thermal resistances were equal. However it can be argued that each cavity contribute to the overall thermal resistance differently. A similar limitation is the transmission of the greenhouse. The measurements of inside solar radiation is from a sensor placed at the south-facing roof of the greenhouse. The model therefore, only considered the decrease of the transmission as a function of the filling level of the south-facing

roof. However, it can be argued that it should be a function of all the cavity compartments, as the solar radiation goes through multiple cavity compartments.

Based on the above mentioned limitations it is recommended to augment the soap bubble cavity model with the missing elements and processes. For this, future research should focus on possible methods and instrumentation setup to quantitatively measure the actual filling and breakdown/outflow of the cavity filling level. For the thermal properties, future research should focus on estimating the thermal performance of each cavity individually. A recommendation for this is to conduct several experiments similar to **Experiment 6**, but filling one cavity compartment each experiment and then estimating the corresponding heat transfer coefficient. A similar recommendation also pertains to the transmission of the greenhouse.

8-2-3 Model-based-predictive control strategy

The final outcome of this thesis is the integration of the above mentioned models in a model-based-predictive control framework for optimizing the climate control equipment and soap bubble cavity while maintaining the greenhouse climate. The prediction model used exogenous variables which were already measured, such the outside environment conditions. For real-time applications, these variables are not known a priori and have to be estimated using proper forecasting methods. An unreliable forecast could have adverse effects on the performance of the control strategy. The objective function was formulated for controlling the greenhouse temperature within pre-defined bounds. However, controlling the greenhouse climate involves more than just temperature control, as the humidity is an equally important variable to consider in the control strategy. Due to the missing element of processes regarding the mass transfer, the prediction of the greenhouse air humidity would not be representative and correct.

Based on the mentioned limitations, future research should focus on the possibility of accurate forecasting of the exogenous variables for the prediction model. Second, it is recommended that the control of the humidity inside the greenhouse is only possible if the prediction model also considers the missing elements. Finally, a real-time application of the MPC algorithm for controlling the greenhouse is of most importance.

Appendix A

Obtaining measured data

Experiment 1: A night-time greenhouse experiment without climate control

The most simple experiment setup is for the unforced greenhouse. Here the experiment is set-up at night-time and the climate control equipment is shut off throughout the experiment. This experiment simulates the 'natural' heat-gain and -loss without the influence of the climate control and the solar radiation which induces the greenhouse-effect. The measured climate data is shown in Figure A-1.

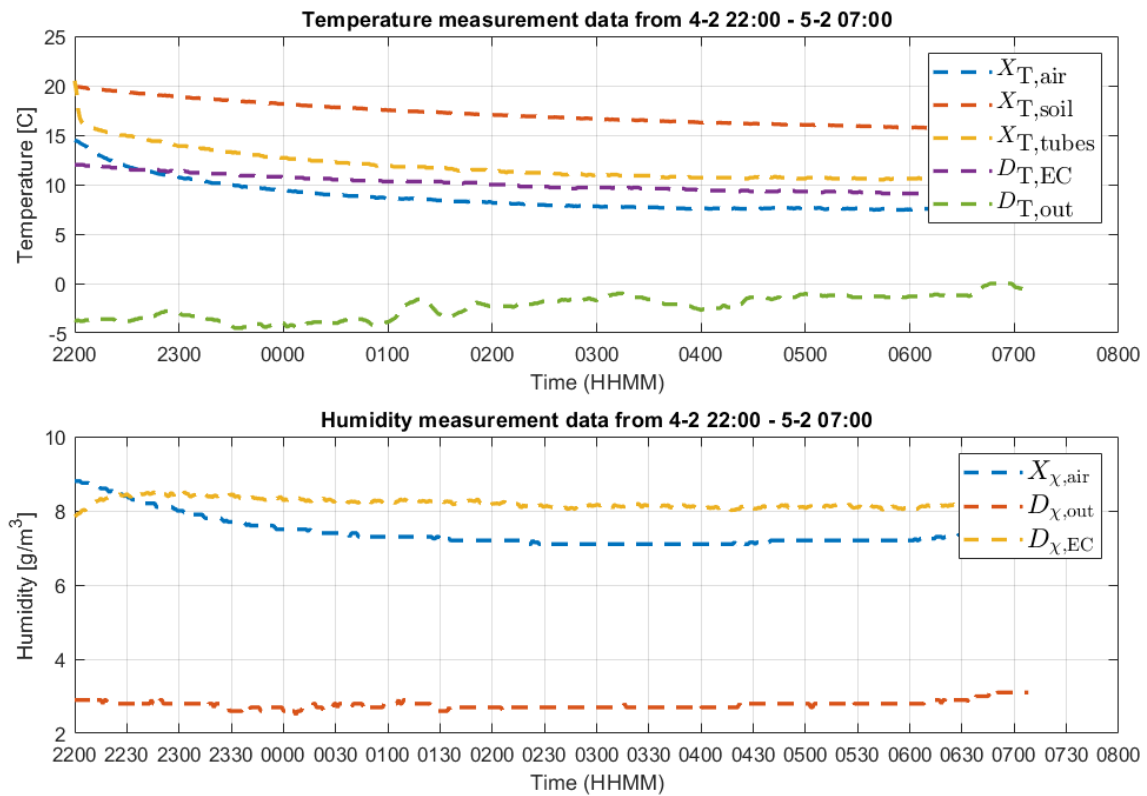


Figure A-1: Experiment 1: Measured climate data.

Experiment 2: A night-time greenhouse setting with artificial lighting

The second experiment is conducted in similar fashion with the exception that the experiment now concerns the artificial lighting of the indoor lamps. This experiment gives insight in the added heat gain and latent heat of the greenhouse when the lamps are switched on and off at certain intervals throughout the experiment. The measured climate data is shown in Figure A-2.

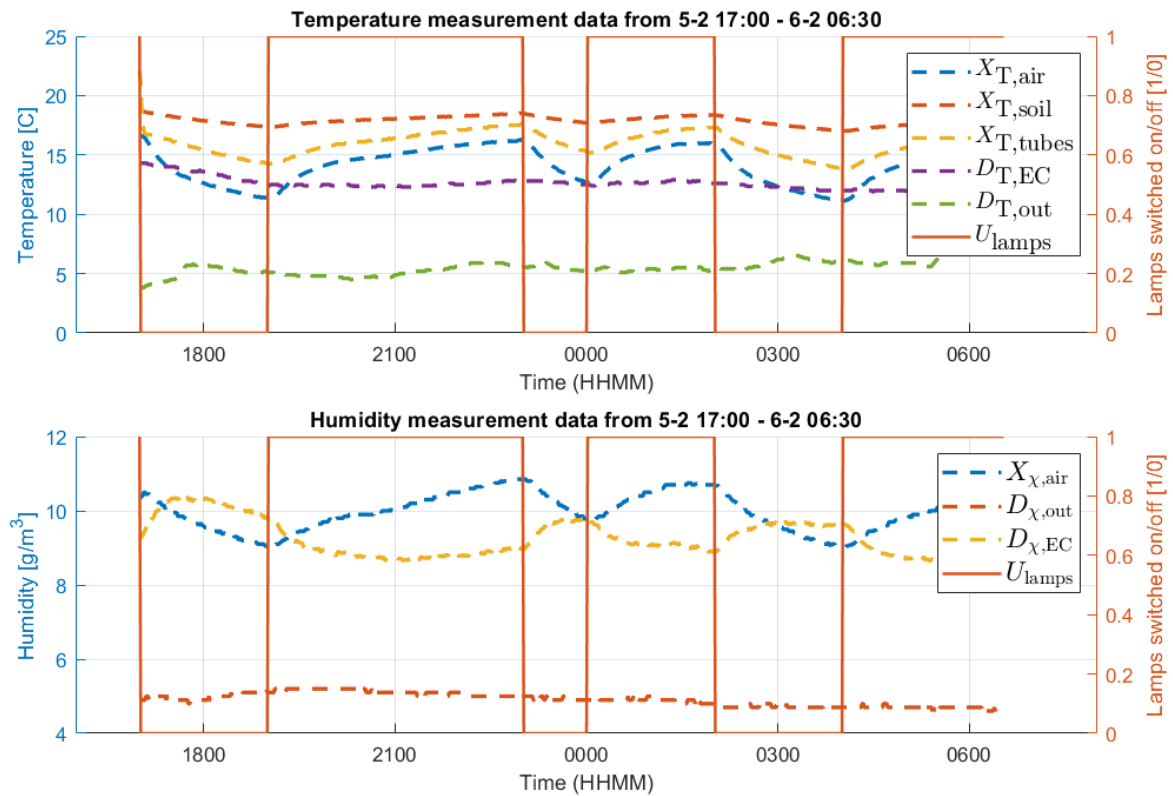


Figure A-2: Experiment 2: Measured climate data.

Experiment 3: A cross-flow heat-exchanger experiment in HEAT-RECOVERY mode

The third experiment is conducted for obtaining data of the heat-exchange system. There are different types of mode settings for the heat-exchange system, which translates to the settings of the dampers and pressure valves. One of the operator modes is the HEAT-RECOVERY mode, shown in Figure A-3. Here, the damper of the horse-shoe is opened for the greenhouse air to go through (red) while the damper of the outside air of the heat-exchanger is open (blue). This allows an increase in temperature of the air inside the heat-exchanger. The heating and cooling batteries are bypassed so there is no exchange between them.

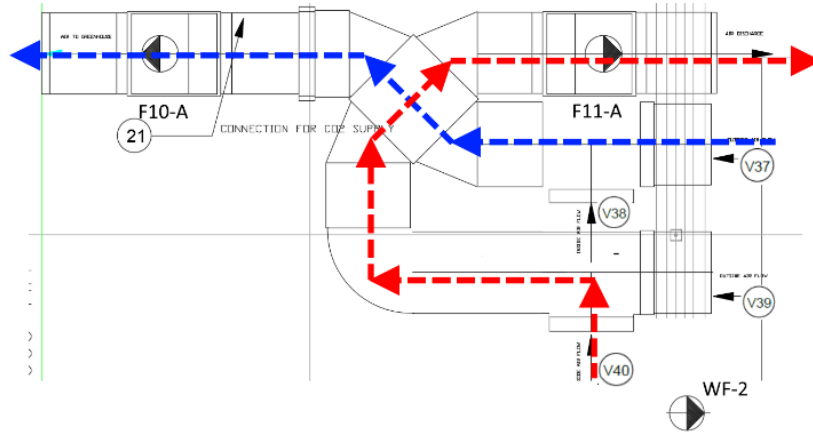


Figure A-3: Sketch of the air-flow in HEAT-RECOVERY mode.

Measured data is shown in Figure A-4. In addition, the temperature of the air before the heating and cooling batteries, T_{intocond} is also shown.

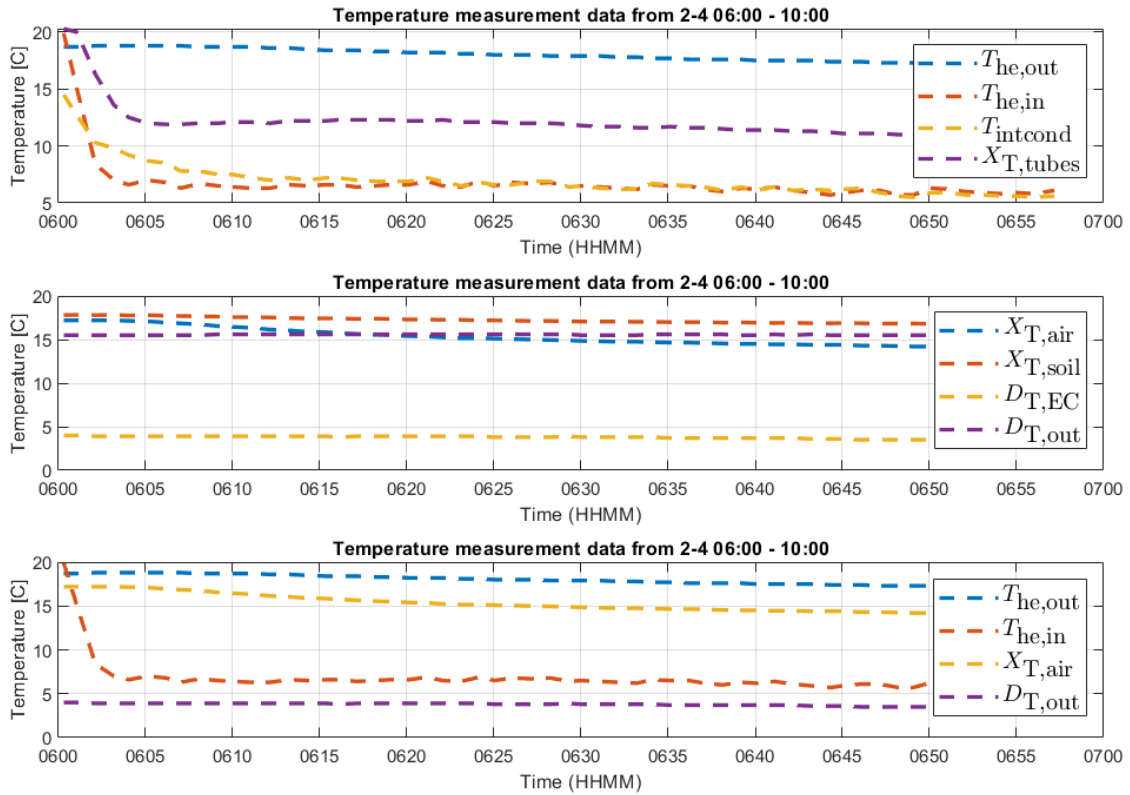


Figure A-4: Experiment 3: Measured climate data.

Experiment 4: Heat-exchange with the cooling-battery

The addition of the cooling battery further decreases the temperature of the air out of the HSHE-unit. A similar figure with the measured data is shown in Figure A-5. The energy balance of the cooling battery is extracted by analyzing the measured temperature of the cold water before ($T_{cw,T}$) and after ($T_{cw,R}$) the exchange with the air.

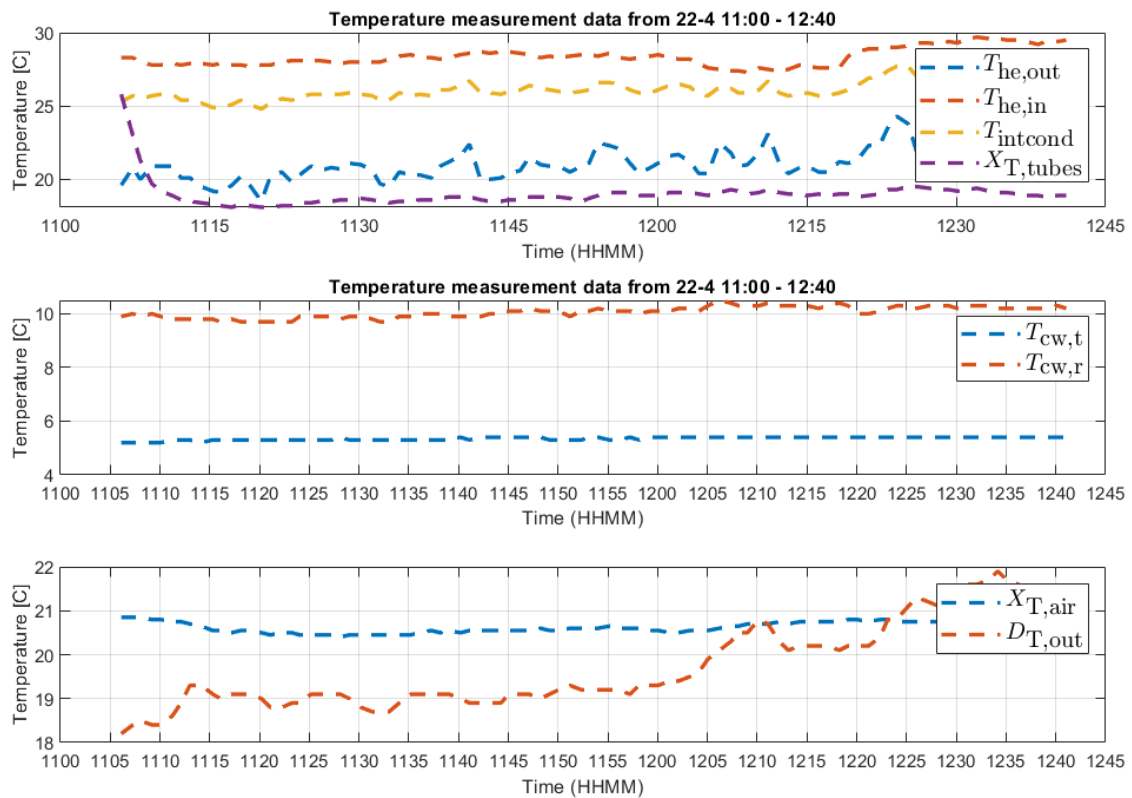


Figure A-5: Experiment 4: Measured climate data.

Experiment 5: Air treatment with heating battery

The addition of the heating battery increases the temperature of the air out of the HSHE-unit. A similar figure with the measured data is shown in Figure A-6. The energy balance of the cooling battery is extracted by analyzing the measured temperature of the hot water before ($T_{hw,T}$) and after ($T_{hw,R}$) the exchange with the air.

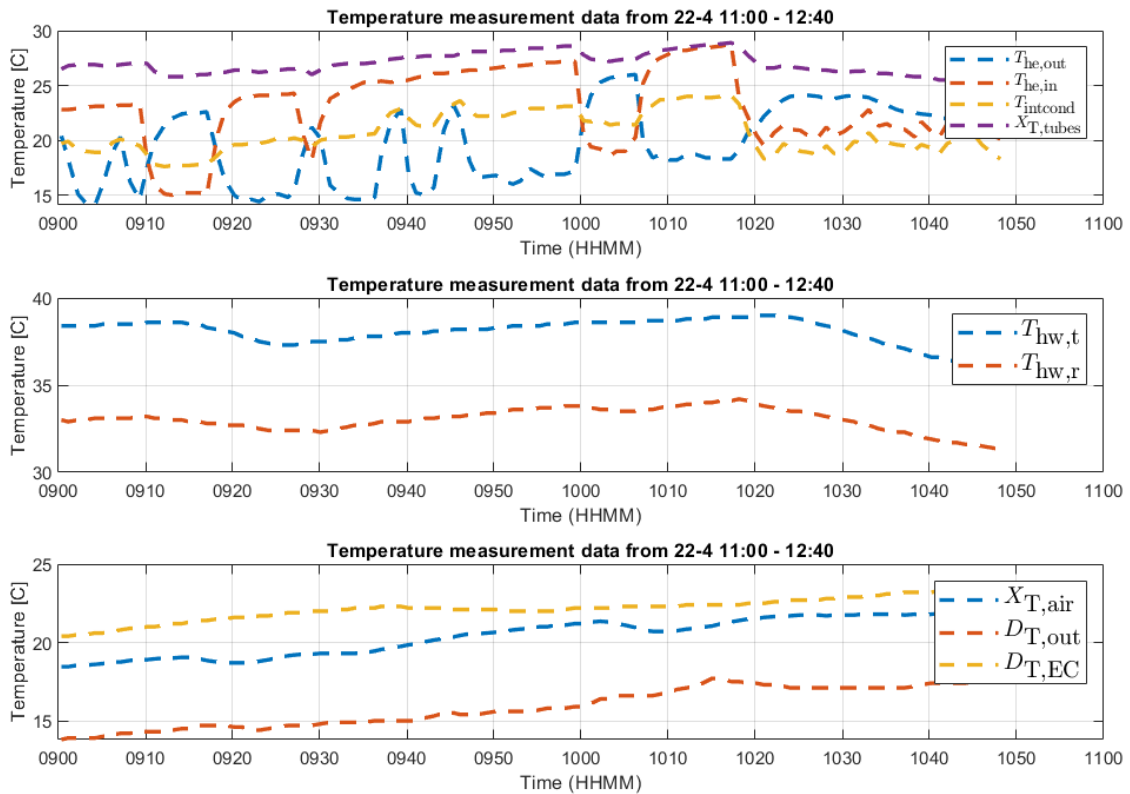


Figure A-6: Experiment 5: Measured climate data.

Experiment 6: A night-time greenhouse setting with full soap cavity

The next experiment is conducted in a similar setting to **Experiment 1**, with the addition that all soap bubbles in the cavities. As mentioned in the previous chapter it is aimed to find the specifics of the greenhouse in "insulated" state, which implies that all cavity compartment enclosing the greenhouse are fully filled with soap bubbles. The measured climate data is shown in Figure A-7.

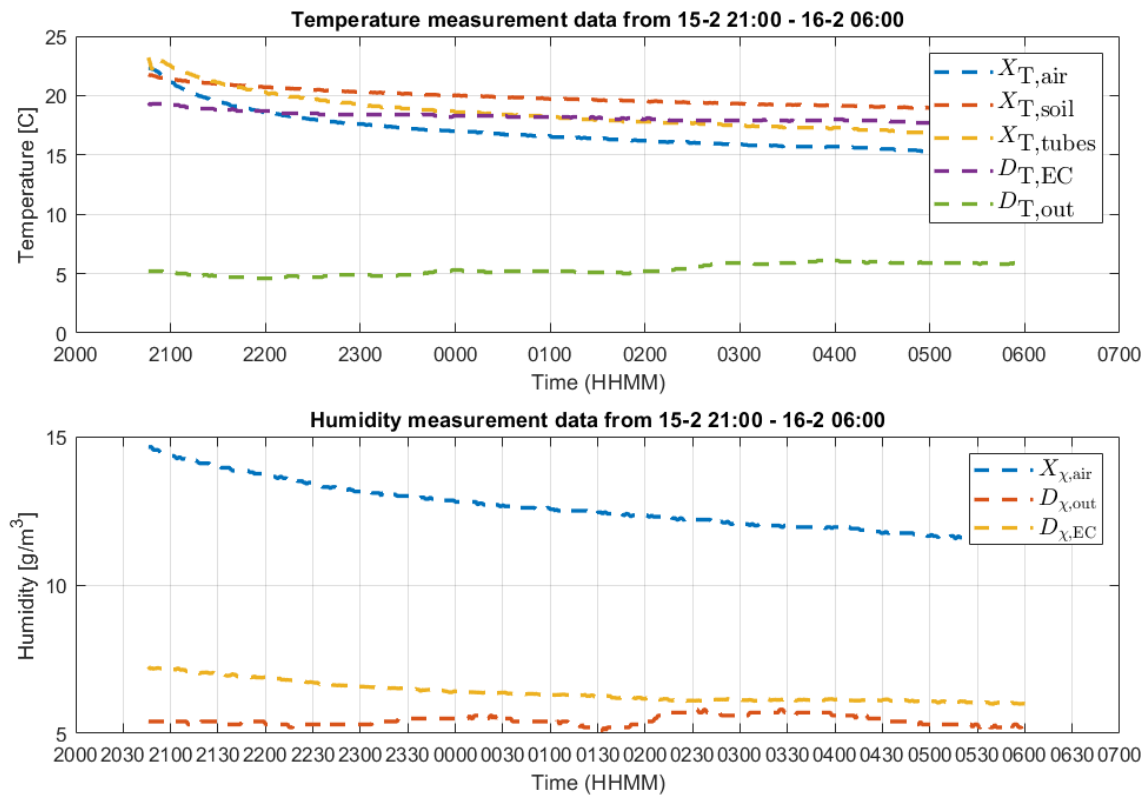


Figure A-7: Experiment 6: Measured climate data.

Experiment 7: A light-intensity experiment with no soap bubbles

The next experiment is conducted for measuring the inside and outside light intensity, shown in Figure A-8.

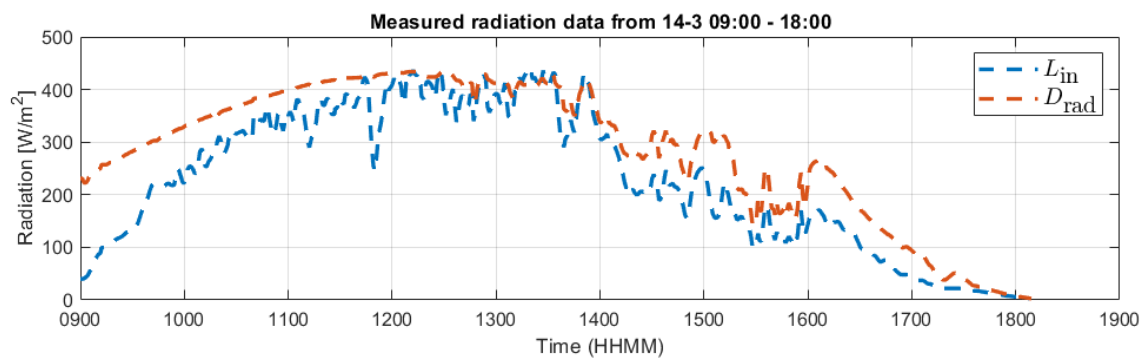


Figure A-8: Experiment 7: Measured climate data.

Experiment 8: A light-intensity experiment with the south roof filled with soap bubbles

The next experiment is conducted for measuring the inside and outside light intensity, with the south-facing room covered with soap bubbles, shown in Figure A-9

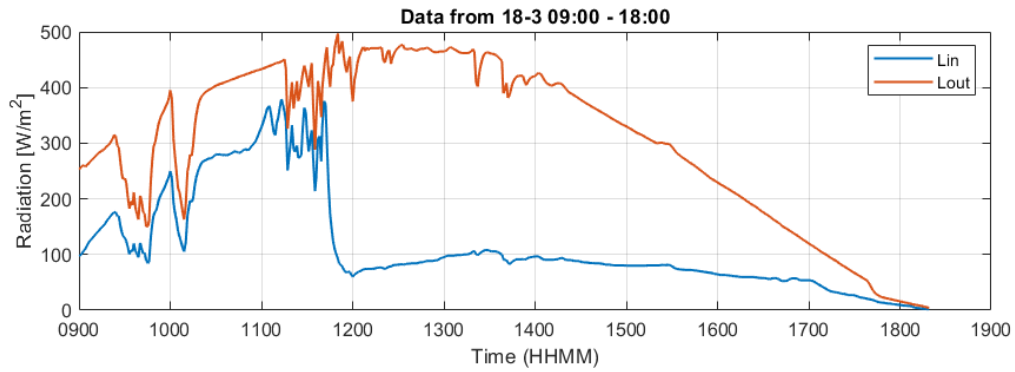


Figure A-9: Experiment 8: Measured climate data.

Bibliography

- [1] Heat Flux - an overview | ScienceDirect Topics.
- [2] MATLAB® Optimization Software | TOMLAB Optimization.
- [3] Horizon 2020: EU framework programme for research and innovation, 2014.
- [4] Ahmed M. Abdel-Ghany and Toyoki Kozai. On the determination of the overall heat transmission coefficient and soil heat flux for a fog cooled, naturally ventilated greenhouse: Analysis of radiation and convection heat transfer. *Energy Conversion and Management*, 47(15-16):2612–2628, sep 2006.
- [5] X. Blasco, M. Martínez, J. M. Herrero, C. Ramos, and J. Sanchis. Model-based predictive control of greenhouse climate for reducing energy and water consumption. *Computers and Electronics in Agriculture*, 55(1):49–70, 2007.
- [6] J Bontsema, J Hemming, C Stanghellini, P de Visser, Ej van Henten, J Budding, T Rieswijk, S Nieboer, and De Lier. On-line estimation of the transpiration in greenhouse horticulture. *Proceedings Agricontrol*, (September):3–5, 2007.
- [7] G.P.A. Bot. *Greenhouse climate: from physical processes to a dynamic model*. PhD thesis, Wageningen University, 1983.
- [8] R Cagienard, P Grieder, E C Kerrigan, and M Morari. Move blocking strategies in receding horizon control. *Journal of Process Control*, 17(6):563–570, 2007.
- [9] J B Campen, G. P.A. Bot, and H. F. De Zwart. Dehumidification of Greenhouses at Northern Latitudes. *Biosystems Engineering*, 86(4):487–493, 2003.
- [10] Nouredine Choab, Amine Allouhi, Anas El Maakoul, Tarik Kousksou, Said Saadeddine, and Abdelmajid Jamil. Review on greenhouse microclimate and application: Design parameters, thermal modeling and simulation, climate controlling technologies. *Solar Energy*, 191(August):109–137, 2019.

- [11] Hanxiao Cui and Mauro Overend. A review of heat transfer characteristics of switchable insulation technologies for thermally adaptive building envelopes. *Energy and Buildings*, 199:427–444, 2019.
- [12] H.F. de Zwart. *Analyzing energy-saving options in greenhouse cultivation using a simulation model*. PhD thesis, Wageningen University, 1996.
- [13] P.L. Dhar. Modeling of Thermal Equipment. In *Thermal System Design and Simulation*, pages 147–296. 2017.
- [14] Fabio Favoino, Mauro Overend, and Qian Jin. The optimal thermo-optical properties and energy saving potential of adaptive glazing technologies. *Applied Energy*, 156:1–15, 2015.
- [15] Guohui Gan. CFD modelling of transparent bubble cavity envelopes for energy efficient greenhouses. *Building and Environment*, 44(12):2486–2500, 2009.
- [16] Jorge L. Garriga and Masoud Soroush. Model predictive control tuning methods: A review. *Industrial and Engineering Chemistry Research*, 49(8):3505–3515, 2010.
- [17] Ramón González, Francisco Rodríguez, José Luis Guzmán, and Manuel Berenguel. Robust constrained economic receding horizon control applied to the two time-scale dynamics problem of a greenhouse. *Optimal Control Applications and Methods*, 35(4):435–453, jul 2014.
- [18] Mattias Gruber, Anders Trüschel, and Jan Olof Dalenbäck. Model-based controllers for indoor climate control in office buildings - Complexity and performance evaluation. *Energy and Buildings*, 68(PARTA):213–222, 2014.
- [19] R. Guzmán-Cruz, R. Castañeda-Miranda, J. J. García-Escalante, I. L. López-Cruz, A. Lara-Herrera, and J. I. de la Rosa. Calibration of a greenhouse climate model using evolutionary algorithms. *Biosystems Engineering*, 104(1):135–142, 2009.
- [20] Ilya Ioslovich, Per Olof Gutman, and Raphael Linker. Hamilton-Jacobi-Bellman formalism for optimal climate control of greenhouse crop. *Automatica*, 45(5):1227–1231, 2009.
- [21] E Kaiser, J N Kutz, and S L Brunton. Sparse identification of nonlinear dynamics for model predictive control in the low-data limit. *Proceedings of the Royal Society A: Mathematical, Physical and Engineering Sciences*, 474(2219), 2018.
- [22] S. J.M. Koenders, R. C.G.M. Loonen, and J. L.M. Hensen. Investigating the potential of a closed-loop dynamic insulation system for opaque building elements. *Energy and Buildings*, 173:409–427, 2018.
- [23] I. L. López-Cruz, E. Fitz-Rodríguez, R. Salazar-Moreno, A. Rojano-Aguilar, and M. Kacira. Development and analysis of dynamical mathematical models of greenhouse climate: A review. *European Journal of Horticultural Science*, 83(5):269–279, 2018.
- [24] Jan Maciejowski and Eric Kerrigan. Soft constraints and exact penalty functions in Model Predictive Control. *Predictive Control*, (January):1–290, 2000.

-
- [25] Mathworks. Optimization Toolbox . *R2011b*, pages 1–663, 2012.
- [26] David Q. Mayne. Model predictive control: Recent developments and future promise. *Automatica*, 50(12):2967–2986, 2014.
- [27] Marco Perino and Valentina Serra. Switching from static to adaptable and dynamic building envelopes: A paradigm shift for the energy efficiency in buildings. *Journal of Facade Design and Engineering*, 3(2):143–163, 2015.
- [28] S. Joe Qin and Thomas A. Badgwell. A survey of industrial model predictive control technology. *Control Engineering Practice*, 11(7):733–764, 2003.
- [29] A. Ramírez-Arias, F. Rodríguez, J. L. Guzmán, and M. Berenguel. Multiobjective hierarchical control architecture for greenhouse crop growth. *Automatica*, 48(3):490–498, 2012.
- [30] James B. Rawlings, David Q. Mayne, and Moritz M. Diehl. *Model predictive control: theory, computation, and design*. Nob Hill Publishing, 2nd edition, 2017.
- [31] Francisco Rodríguez, Manuel Berenguel, José Luis Guzmán, and Armando Ramírez-arias. *Modeling and Control of Greenhouse Crop Growth*. Springer International Publishing Switzerland, Glasgow, 2014.
- [32] I. Seginer. Optimal control of the greenhouse environment: An overview. In *Acta Horticulturae*, volume 406, pages 191–201, 1996.
- [33] V. P. Sethi, K. Sumathy, Chiwon Lee, and D. S. Pal. Thermal modeling aspects of solar greenhouse microclimate control: A review on heating technologies. *Solar Energy*, 96:56–82, oct 2013.
- [34] V. P. Sethi, K. Sumathy, Chiwon Lee, and D. S. Pal. Thermal modeling aspects of solar greenhouse microclimate control: A review on heating technologies. *Solar Energy*, 96:56–82, 2013.
- [35] Vinay Shekar and Moncef Krarti. Control strategies for dynamic insulation materials applied to commercial buildings. *Energy and Buildings*, 154:305–320, 2017.
- [36] Cecilia Stanghellini and Taeke de Jong. A model of humidity and its applications in a greenhouse. *Agricultural and Forest Meteorology*, 76(2):129–148, 1995.
- [37] K. Stoknes, F. Scholwin, W. Krzesiński, E. Wojciechowska, and A. Jasińska. Efficiency of a novel Food to waste to food system including anaerobic digestion of food waste and cultivation of vegetables on digestate in a bubble-insulated greenhouse. *Waste Management*, 56:466–476, 2016.
- [38] Morteza Taki, Abbas Rohani, and Mostafa Rahmati-Joneidabad. Solar thermal simulation and applications in greenhouse. *Information Processing in Agriculture*, 5(1):83–113, 2018.
- [39] F. Tap. *Economics-based optimal control of greenhouse tomato crop production*. PhD thesis, 2000.

- [40] Amir Vadiée. *Energy Analysis of the Closed Greenhouse Concept-Toward one Sustainable Energy Pathway-*. PhD thesis, KTH School of Industrial Engineering and Management, 2011.
- [41] Amir Vadiée and Viktoria Martin. Energy management in horticultural applications through the closed greenhouse concept, state of the art, sep 2012.
- [42] P. J.M. Van Beveren, J. Bontsema, G. Van Straten, and E. J. Van Henten. Minimal heating and cooling in a modern rose greenhouse. *Applied Energy*, 137:97–109, jan 2015.
- [43] P. J.M. van Beveren, J. Bontsema, G. van Straten, and E. J. van Henten. Optimal control of greenhouse climate using minimal energy and grower defined bounds. *Applied Energy*, 159:509–519, dec 2015.
- [44] E. J. Van Henten. Sensitivity analysis of an optimal control problem in greenhouse climate management. *Biosystems Engineering*, 85(3):355–364, jul 2003.
- [45] E. J. Van Henten and J. Bontsema. Time-scale decomposition of an optimal control problem in greenhouse climate management. *Control Engineering Practice*, 17(1):88–96, jan 2009.
- [46] G. Van Straten and E. J. Van Henten. Optimal greenhouse cultivation control: Survey and perspectives. *IFAC Proceedings Volumes (IFAC-PapersOnline)*, 3(PART 1), 2010.
- [47] Gerrit Van Straten. *Optimal greenhouse cultivation control: Quo vadis?*, volume 1. IFAC, 2013.
- [48] B. H.E. Vanthoor, C. Stanghellini, E. J. Van Henten, and P. H.B. De Visser. A methodology for model-based greenhouse design: Part 1, a greenhouse climate model for a broad range of designs and climates. *Biosystems Engineering*, 110(4):363–377, 2011.
- [49] Liuping Wang. *Control system design and implementation using MATLAB*. 2009.
- [50] Zequn Wang and Yuxiang Chen. Data-driven modeling of building thermal dynamics: Methodology and state of the art, nov 2019.

Glossary

List of Acronyms

CO₂	carbon-dioxide
EU	European Union
F2W2F	Food to Waste to Food
MPC	Model Predictive Control
RHOC	Receding Horizon Optimal Control
RC	Resistor-Capacitor
HSHE	horse-shoe heat-exchanger
VAF	variance accounted for
RMSE	root mean squared error
MINP	mixed integer nonlinear programming
EC	education centre
CPU	central processing unit

